Universidade de Lisboa

Faculdade de Farmácia

Departamento de Microbiologia e Imunologia

U

LISBOA

UNIVERSIDADE
DE LISBOA

Human factors required for *Mycobacterium tuberculosis* macrophage infection

Nuno Baltazar do Carmo

Doutoramento em Farmácia

(Biologia Celular e Molecular)

2014

Universidade de Lisboa

Faculdade de Farmácia

Departamento de Microbiologia e Imunologia

U

LISBOA

UNIVERSIDADE
DE LISBOA

Human factors required for *Mycobacterium tuberculosis* macrophage infection

Nuno Baltazar do Carmo

Doutoramento em Farmácia

(Biologia Celular e Molecular)

Tese orientada pela Professora Doutora Elsa Maria Ribeiro dos Santos Anes, especialmente elaborada para a obtenção do grau de doutor no ramo de Farmácia, especialidade de Biologia Celular e Molecular.

Dissertação de candidatura ao Grau de Doutor em Farmácia, apresentada à Faculdade de Farmácia, Universidade de Lisboa.

De acordo com o disposto no ponto 1 do artigo nº40 do regulamento de Estudos Pós-Graduados da Universidade de Lisboa, deliberação nº 93/2006, publicado em Diário da República – II série nº 153 – 5 de Julho de 2003, o autor desta dissertação declara que participou na concepção e execução do trabalho experimental, interpretação dos resultados obtidos e redacção dos manuscritos.

Preface

The purpose of his work is to dissect the host factors involved in *Mycobacterium tuberculosis* infection. *Mycobacterium tuberculosis* is a facultative intracellular pathogen that subverts host pathways to establish its replication niche. Once the infection is established, the use of current anti-tuberculosis drugs have proven limited efficacy due to the long treatment time that led to low patient compliance and to *M. tuberculosis* drug resistance.

Here we developed several methodologies, based in fluorescent proteins using fluorimetry to test the susceptibility of *M. tuberculosis* to host factors and new drugs during their intracellular life style within macrophages. These techniques enable and to study the effect of host vesicular traffic proteins and micro RNA 142-3-p during macrophage internalization and on macrophage intracellular survival. Additionally we studied and dissect the role of Rab GTPases in exosome secretion.

The results of this thesis are published in international scientific journals with referees, in international chapter books, in patents and in scientific meetings proceedings.

A.   International Publications with referees:

1.   Paulo Bettencourt, David Pires, **Nuno Carmo** and Elsa Anes. 2010. Application of Confocal Microscopy for Quantification of Intracellular Mycobacteria in Macrophages. Microscopy: Science, Technology, Applications and Education A. Méndez-Vilas and J. Díaz (Eds.). pg 614-621, ISNN(13):978-84-614-6189-9

2.   Paulo Bettencourt, Sabrina Marion, Leonor Freire Santos, David Pires, **Nuno Carmo**, Jonathon Blake, Vladimir Benes, Gareth Griffiths, and Elsa Anes. Actin-binding protein regulation by microRNAs as a novel microbial strategy to avoid

phagocytosis by host cells: the case of N-Wasp and miR-142-3p. Front Cell Infect Microbiol. 2013 Jun 5;3:19. doi: 10.3389/fcimb.2013.00019. eCollection 2013.

3. Matias Ostrowski, **Nuno Carmo**, Sophie Krumeich, Isabelle Fanget, Graça Raposo, Ariel Savina, Catarina Moita, Kristine Schauer, Alistair Hume, Rui Freitas, Bruno Goud, Philippe Benaroch, Miguel Seabra, Nir Hacohen, Mitsunori Fukuda, Claire Desnos, François Darchen, Sebastian Amigorena, Luis F. Moita and Clotilde Thery. Rab27a and Rab27b control different steps of the exosome secretion pathway Nat Cell Biol. 2010 12(1):19-30; sup pp 1-13.

3. David Pires, Paulo Bettencourt, **Nuno Carmo**, Tina Bergant, Luísa Jordão and Elsa Anes. Interference of *Mycobacterium tuberculosis* with the endocytic pathways on macrophages and dendritic cells from healthy donnors: role of Cathepsins. Drug Discovery Today 2010.Volume 15 issue 23-24 pg 1112.

4. David Pires, Paulo Bettencourt, **Nuno Carmo**, Michael Niederweis and Elsa Anes, E. Role of *Mycobacterium tuberculosis* outer-membrane porins in bacterial survival within macrophages . Drug Discovery Today 2010. Volume 15 issue 23-24 pg 1112-1113.

5. **Nuno Carmo**, David Pires, Pedro Timóteo, Joana Bugalhão, Joana Marques, Paulo Bettencourt, Elsa Anes. Development of dual fluorescent reporter assays to assess mycobacteria intracellular survival within macrophages: applications for Hight through put assays for Host factors involved in vesicle trafficking. submitted

6. **Nuno Carmo**, David Pires, Pedro Timóteo, Joana Bugalhão, Joana Marques, Paulo Bettencourt, Elsa Anes Hight through put assay for Host factors involved in *Mycobacterium tuberculosis* internalization within macrophages. In prep

B.   Patents:

1. Luis Constantino , Elsa Anes, Emilia Valente, Teresa Almeida, **Nuno Carmo** Esteres do ácido pirazinóico ramificados com acção antimicobacteriana e boa estabilidade em plasma. Pt patent 2012/106051 W

2. Luis Constantino, Elsa Anes, Emilia Valente, Teresa Almeida, **Nuno Carmo**. Patent Number: WO2013084214. Pyrazinoic Acid Prodrugs activated by Esterases of Mycobacteria.(2013) Universidade de Lisboa, Lisboa, Portugal.

C.   Publications in scientific meetings:

1. **Nuno Carmo,** David Pires, Joana Bugalhão, Joana Marques, Paulo Bettencourt, Pedro Timóteo, and Elsa Anes. Host factors affecting *Mycobacterium tuberculosis* macrophage infection. Presented at the EMBO Conference – Tuberculosis 2012. Biology, Pathogenesis, Intervention and Strategies. Institute Pasteur, Paris, France. (Poster).

2. David Pires, Nuno Carmo, Joana Marques, Joana Bugalhão, Paulo Bettencourt and Elsa Anes. 2012 To control or to be controlled during M. tuberculosis infection? Cathepsins   and   their   inhibitors   within   host   dendritic   cells   or macrophages.Tuberculosis 2012, Biology, Pathogenesis, Intervention strategies, Inst. Pasteur, France, Sep.11-15

3. **Nuno Carmo**, David Pires, Joana Bugalhão, Joana Marques, Paulo Bettencourt, Pedro Timóteo and Elsa Anes. 2013 Host Factors Affecting Mycobacterium tuberculosis Macrophage Infection. pg112 5th iMed.UL Postgraduate Students Meeting July18th, Lisbon, Portugal.

4.   David Pires, **Nuno Carmo**, Joana Marques, João Pombo, Pedro Timóteo, Paulo Bettencourt and Elssa Anes Cut or be Cut: Cathepsins and their Inhibitors During Mycobacterial Infection of Macrophages and Dendritic Cells. pg103 5th iMed.UL Postgraduate Students Meeting July18th 2013, Lisbon, Portugal.

5.   David Pires, Paulo Bettencourt, **Nuno Carmo**, Tina Bergant, Luisa Jordão and Elsa Anes. Cathepsins B and S Content in Mycobacterium Containing Compartments in Human Macrophages and Dendritic cells. Presented at the "Current Opinion in Cellular Host-Pathogen Interactions" 2010 Conference in Amsterdam, The Netherlands. (Poster).

6.   David Pires, Paulo Bettencourt, **Nuno Carmo**, Tina Bergant, Luisa Jordão and Elsa Anes. Interference of *Mycobacterium tuberculosis* with the endocytic pathways on macrophages and dendritic cells from healthy donors: role of Cathepsins. Presented at the 3rd International Symposium "Celular Delivery of Therapeutic Macromolecules 2010" in Cardiff, Wales (UK). (Poster).

7.   David Pires, Paulo Bettencourt, **Nuno Carmo**, Michael Niederweis and Elsa Anes. Role of *Mycobacterium tuberculosis* outer-membrane porins in bacterial survival within macrophages. Presented at the 3rd International Symposium "Celular Delivery of Therapeutic Macromolecules 2010" in Cardiff, Wales (UK). (Poster).

8.   **Nuno Carmo** and Elsa Anes 2009. "Searching for host factors involved in Mycobacterium tuberculosis infection" URIA Workshop Mycobacterium Biology and Pathogenesis Faculdade de Farmácia, April 8.

Acknowledgments

This work was possible due to Professor Elsa, she supervised my project let me work in her laboratory. She believed in me and in my work always with a positive, a mind solving attitude and enless patience for my "problems of expression". Thank you so very much.

To Professor Moniz-Pereira for accepting me in CPM-URIA and for providing all the logistic and equipment required by my project and for letting me work in CPM-URIA.

To Professor Michael Niederweis, from the Department of Microbiology of the University of Alabama (USA), for helping me in the production of fluorescent far red expressing mycobacteria.

To Professor Luís Constantino, for giving me all the compounds I used in this work and his motivating and positive attitude.

To Luís Moita, for supervising me in the beginning of this work and providing the bacterial glycerol stock containing the shRNAs vesicular traffic library.

To Claudio Correia, from the informatics services of the Faculty of Pharmacy of the University of Lisbon (Portugal), for helping me in the implementation a schedule system for reservation of laboratory equipment.

To every lab members who contributed to my formation as a research scientist, as a critical thinker, but above all as a better human being.

David Pires. Thank you very much David for your help in most projects of my PhD! I felt privileged to work with such a brilliant scientist, enthusiastic colleague, and friendly person. Thank you for your inspiring hard-work and intelligent comments!

To Paulo Bettencourt, for the exciting debates and brainstorming we had in our office.

Resumo

A tuberculose (TB) é a manifestação patológica da infecção do *Mycobacterium tuberculosis* no seu hospedeiro: os humanos. Esta doença afecta os humanos há milénios e constitui ainda um problema de saúde pública a nível global. A reemergência da TB após decadas de declínio resulta sobretudo da co-infecção com o vírus da imunodeficiência humana e do aparecimento de estirpes de *M. tuberculosis* resistentes aos antibióticos.

O *M. tuberculosis* é um parasita intracelular facultativo, cujo principal nicho de sobrevivência são os macrófagos: as células do sistema imune cuja função é a destruição dos microrganismos. Após fagocitado pelo macrófago, o *M. tuberculosis* subverte o normal funcionamento do seu hospedeiro. Os fagossomas contendo o bacilo da tuberculose não maturam para fagolisossomas, não fundindo com endossomas tardios ou lisossomas, protegendo o bacilo dos factores microbicidas do macrófago. Apesar de o fagossoma estar bloqueado num estádio precoce da sua maturação este funde com outras vesículas do macrófago hospedeiro, fornecendo à micobactéria recursos para a sobrevivência e replicação.

Em particular, multiplas publicações sugerem que diferentes proteínas do hospedeiro reguladoras do tráfego vesicular ou do citoesqueleto da actina poderão desempenhar um papel relevante na sobrevivência deste patogénio. Contudo, os mecanismos através dos quais é estabelecida esta subversão não são conhecidos.

O desenvolvimento de metodologias de larga escala para triagem no estudo dos factores do hospedeiro envolvidos na infecção de macrófagos, pelo *M. tuberculosis*, têm sido refreados pelas características únicas desta micobactéria. A única metodologia disponível para a quantificação de micobactérias intracelulares é a contagem de unidades formadoras de colónias (UFC), uma técnica laboriosa e dispendiosa. Nesta tese aproveitamos as características das proteínas fluorescentes para desenvolvermos metodologias para a quantificação da internalização e sobrevivência de micobactérias em macrófagos e em culturas líquidas. O desenvolvimento dessas técnicas permitiu:

1) Desenvolver uma metodologia baseada nas propriedades das proteínas fluorescentes para a determinação da sobrevivência de *M. tuberculosis* intracelularmente em macrófagos infectados.

2) Determinar o efeito de cerca de 120 genes humanos do tráfego vesicular na carga do *M. tuberculosis* em macrófagos humanos.

3) Estudar o efeito dos genes validados no ponto 2) e do micro RNA mIR143-3p na internalização do *M. tuberculosis* por macrófagos humanos.

4) Adicionalmente foi estudado o efeito do silenciamento de Rab GTPases na secreção de exosomas.

De forma a desenvolver um método alternativo ao UFC compatível com a possibilidade de rastreamento em larga escala da sobrevivência de micobactérias aproveitamo-nos das características das proteínas fluorescentes com o objectivo de monitorizar a infecção de macrófagos pelo *M.* tuberculosis. Numa primeira fase culturas líquidas de *M. tuberculosis* expressando GFP foram sujeitos à acção microbicida de vários antibióticos e determinadas as suas concentrações mínimas inibitórias por fluorimetria. Posteriormente foram utilizados vários esteres derivados do ácido pirazinóico em *M. tuberculosis* expressando GFP por fluorimetria tendo-se quantificado a sua actividade biológica. Todos os compostos apresentaram uma maior actividade biológica que a pirazinamida ou o ácido pirazinóico. Compostos com maior comprimento da cadeia linear do álcool e maior lipofilia estão positivamente correlacionados com a actividade biológica. Apesar de adequado para a quantificação da inibição de crescimento de *M. tuberculosis* em culturas líquidas, a proteína GFP não se demonstrou propicia para a quantificação de micobactérias intracelulares. A quantificação por fluorimetria de *M. tuberculosis* intracelulares expressando a proteína fluorescente vermelha tdTomato, demonstrou-se uma boa alternativa ao UFC. Adicionalmente, a quantificação da intensidade da fluorescência de macrófagos humanos THP-1 expressando GFP, permitiu quantificar tanto o número como a viabilidade dos macrófagos.

O estabelecimento de uma metodologia de rastreamento em larga escala para a quantificação de *M. tuberculosis* intracelular, permitiu-nos proceder ao silenciamento

sistemático de cerca de 120 genes do tráfego vesicular humano e quantificar o seu efeito na carga de *M. tuberculosis* em macrófagos. Os candidatos obtidos no rastreamento foram posteriormente validados quanto à sua expressão genética. Identificámos 10 genes com efeito na carga intracelular de *M. tuberculosis* em macrófagos, em 2 genes, foi observado um aumento e em 8 genes, uma redução da carga de *M. tuberculosis* em macrófagos humanos. Os candidatos foram maioritariamente proteínas Rab, proteínas reguladoras e efectoras de Rab e proteínas do tráfego vesicular não classificadas.

De forma a quantificar o contributo da internalização nos resultados observados no rastreamento dos 120 genes, desenvolvemos uma metodologia baseada em citometria de fluxo. Determinamos que, para micobactérias virulentas e avirulentas, a grande maioria dos genes testados são, provavelmente, reguladores positivos da internalização. Estas observações justificaram e confirmaram alguns dos resultados obtidos no rastreamento genómico e propõem um papel activo das micobactérias na modulação da sua internalização por macrófagos humanos.

De forma a validar biologicamente alguns dos candidatos, estes foram silenciados novamente e foi quantificada a carga micobacteriana em macrófagos utilizando a metodologia convencional, as unidades formadoras de colónias. Com os resultados observados ficou demonstrado   que a proteína Rab7a induz um aumento da carga macrofágica de *M. tuberculosis*. O silenciamento de Rab34 e Sintaxina 4 induz uma redução da carga de *M. tuberculosis* em macrófagos humanos sendo esta redução, possivelmente devida à redução da internalização nestas células.

Os micro RNAs (miR), recentemente descritos, são uma nova classe de moléculas que controlam eventos pós-transcripcionais durante a expressão genética. Os miR ligam-se a regiões especificas do RNA mensageiro (RNAm) de uma proteína bloqueando a tradução proteica e/ou levando à degradação do RNAm. Os miRs controlam selectivamente a expressão de proteínas de diferentes vias metabólicas das células. Estudos feitos no nosso laboratório demonstraram que o miR-143-3p está sobre-expresso nos estádios iniciais da infecção de *M. tuberculosis* em macrófagos. O miR-143-3p liga-se ao mRNA do gene Wasl controlando a expressão da proteína N-Wasp, um transdutor de receptores membranares e do citoesqueleto

de actina. O silenciamento da N-Wasp reduz a internalização de *M. tuberculosis* pelos macrófagos. Estes resultados demonstram a regulação de N-Wasp pelo *M. tuberculosis* para controlar a sua internalização.

Os exossomas são vesículas com um diâmetro de 30 a 100 nm que são secretadas por diversos tipos de células. Os exossomas desempenham um papel importante na sinalização entre células e em macrófagos têm um papel de apresentação de antigénios. Os exossomas secretados por macrófagos infectados por *M. tuberculosis* são pró-inflamatórios *in vitro e in vivo*. No laboratório do Dr. Amigorena foi desenvolvida uma metodologia para quantificação de exossomas através de pérolas de latex conjugadas dom CD63 e a utilização de citometria de fluxo. Em colaboração com o Dr Ostrwsky, do laboratório do Dr Amigorena, Instituto Curie, Paris, França, efectuei um rastreio de larga escala para determinação dos genes do tráfego intracelular envolvidos na secreção de exossomas em células HeLa B6H4. Nesse estudo a proteína Rab27a e Rab27b foram envolvidas na secreção de exossomas em células humanas. Era nosso objectivo determinar se tal se verificava em macrófagos humanos, no contexto da infecção do *M. tuberculosis*, não foi possível por razões alheias à nossa vontade.

Conjuntamente os dados apresentados nesta tese demonstram o efeito de factores específicos do hospedeiro que influenciam a sobrevivência e/ou internalização do *M. tuberculosis* por macrófagos, alguns deles aparentemente modulados pelo bacilo da tuberculose. Em particular, os dados sugerem que o *M. tuberculosis* desenvolveu um mecanismo específico de invasão dos macrófagos alveolares, provavelmente, para estabelecer o seu nicho replicativo sem activar em demasia o sistema imune do hospedeiro. Estes factores do hospedeiro, e em especial as proteínas que as codificam ou regulam são potenciais alvos para o desenvolvimento de drogas orientadas para a modulação do hospedeiro de forma a inibir ou controlar a infecção por *M. tuberculosis*. O desenvolvimento de novas drogas em formulações que inibam estirpes de *M. tuberculosis* resistentes é outra estratégia de erradicação deste patogénio nos humanos.

Palavras-chave: Macrófago humano, *Mycobacterium tuberculosis*, tráfego vesicular, micro RNAs, exossomas, RNAi.

Abstract

Tuberculosis is a pathological manifestation of the infection by *Mycobacterium tuberculosis* in humans. Facultative intracellular parasites, like *M. tuberculosis*, evolved mechanisms to subvert the proper functioning of their host cells to their benefit.

In this thesis we token advantage of the characteristics of the fluorescent proteins to develop methodologies based on fluorimetry to quantify the macrophage internalization and the number of intracellular mycobacteria. The application of these techniques allowed: 1) to demonstrate that the GFP expressing mycobacteria may be used to test the effects of new drugs namely pyrazinoic acid esters against *M. tuberculosis* growth in liquid cultures. However GFP is not a good fluorophore to quantify intracellular mycobacteria. Instead we found tdTomato the election fluorophore to this purpose 2) To determine the effect of 120 genes in the host vesicular traffic during macrophage infection with *M. tuberculosis*. We identified 10 genes, 8 lead to a reduction and 2 an increase of macrophage *M. tuberculosis* burden. 3) To demonstrate that a reduction in macrophage internalization was the cause for the reduction in intracellular *M. tuberculosis* observed in some of the genes identified in 2) and the modulation of internalization by the microRNA miR-142-3p. Additionally, we studied the effect of Rab GTPases silencing in exosome secretion.

MicroRNAs (miR) are small non-coding RNA molecules that regulate gene expression. Previous studies in our laboratory shown that miR-142-3p was up-regulated during early stages of *M. tuberculosis* macrophage infection. MiR142-3p binds to Wasl gene controlling the expression of N-wasp protein involved in signal transduction of membrane receptors and actin cytoskeleton. N-wasp silencing reduces *M. tuberculosis* internalization by macrophage. These studies demonstrate that *M. tuberculosis* regulates its internalization through N-Wasp.

Taken together our results demonstrate the effect of specific host factors in the survival and/or internalization of *M. tuberculosis* by macrophages. Tuberculosis bacilli apparently modulate some of them. The development of new molecules in

formulations that inhibit resistant *M. tuberculosis* strains is another strategy for the eradication of this pathogen from humans.

List of Abreviations

BCG-Bacillus Calmette-Guérin

CFU-Colony forming Units

CR-Complement Receptor

DMSO- Dimethyl Sulfoxide

DOTS-Directly Observed Treatment and Short-course drug therapy

EEA1-Early Endosome Antigen1

ER-Endoplasmic Reticulum

EM-Electron Microscopy

ESX1-ESAT-6 secretion system

FcγR- Receptors for the constant region of immunoglobulin G

FI-Fluorescent Intensity

FP-Fluorescent Proteins

GAP-GTPase Activating Proteins

GAPDH - Glyceraldehyde-3-Phosphate Dehydrogenase

GDF-GDI Dissociation Factor

GDI-GDP Dissociation Inhibitor

GEF-GDP-GTP Exchange Factor

GFP-Green Fluorescent Protein

HMDM- Human Monocyte-Derived Macrophages

HTS- High-throughput Screening

hU6-U6 promoter

IFNγ-Iterferon gamma

ILVs-Intraluminal Vesicles

LAM-Lipoarabinomannan

LM- Lipomannan

LTB-Latent tuberculosis

ManLam-Mannose-capped LAM

MCP-Mycobacteria Containing Phagosome

MDHM-Monocyte Derived Human Macrophages

MDR-TB-Multidrug Resitant Tuberculosis

MHC-Major Histocompatibility Complex

MIC-Minimum Inhibitory Concentration

miR-Micro RNA

MR-Mannose Receptor

MTC-*Mycobacterium tuberculosis* complex

MVB-Multivesicular Bodies

Ndk-Nucleoside diphosphate kinase

NSF- N-ethylmaleimide-sensitive factor

OD-Optical Density

PAMP-pathogen associated molecular pattern

PGE2-prostaglandin E2

PI-Phosphate Inorganic

PI(3)P-phosphatidylinositol 3-phosphate

PS -phosphatidyl-serine

PIM-phosphatidyl-myo-inositol mannosides

PknG-Protein kinase G

PMA-phorbol 12-myristate 13-acetate

POA-Pyrazinoic Acid

PRR-Pattern Recognition Receptor

PZA-Pyrazinamide

qRT-PCR- quantitative Real Time PCR

Rab -Rat Brain Protein Ras-related

RD1-Region of Difference 1

RFU-Relative Fluorescence Units

RILP-Rab-Interacting Lysosomal Protein

SNAP-NSF Attachment Protein

SNARE -Soluble N-ethylmaleimide-sensitive-factor Attachment Receptor

Stx-Syntaxin

TB-Tuberculosis

TGN-Trans-Golgi Network

TLR-Toll Like Receptor

TNFα-Tumour Necrosis Factor alpha

List of Figures

Chapter 1

Chapter 2

Chapter 3

Chapter 4

Chapter 5

Chapter 6

List of Tables

Chapter 2

Chapter 3

List of Equations

Chapter 3

Table of contents

Chapter 1
General Introduction

General Introduction

Tuberculosis

Tuberculosis (TB) afflicts human kind for millennia. It is thought that TB was originated in Africa and accompanied the "Out-of-Africa" migrations of modern humans approximately 40-70 thousand years ago[1]. Recently, a study from Turkey reported TB like lesions in 500000 years *Homo erectus* making this disease probably even older than modern humans[2,3].

The ancient known mention of TB was brought to us through Assyrian clay tablets from 600 BC[4,5]. During the industrial revolution in Europe the rapid demographic explosion of the urban populations together with poor life conditions were the major reasons for the high mortality due to TB. Significant scientific achievements for the elucidation of the pathogenesis of the disease where possible after the discovery of the etiologic agent in 1882 by Robert [6].

During the second half of the XX century, with improving live conditions, sanitation and housing, diet and education, with the launch of sanatoria (where patients were isolated and exposed to the sun and circulating air) and a healthy diet, deaths from TB drastically decreased. Actually, the decline in TB incidence in Europe occurred even before the discovery of antibiotics, stressing the importance of living conditions and social factors in containing TB, and highlighting some of the difficulties that are still faced in low-income countries today[7].

Albert Calmette and his associate Camille Guérin developed the Bacille Calmette Guérin (BCG) vaccine, a live attenuated variant of *Mycobacterium bovis*, available since the early 1921[8]. In the 1948 UNICEF started a massive BCG vaccination campaign the first disease control program undertaken by an agency of the World Health Organization[9]. Despite this, the single available vaccine for TB prevention

their efficacy was proven to be limited over the years[10]. Although not being fully able to protect against the infection, the sickness in adults upon vaccination has less morbidity and it was demonstrated to be effective in preventing the meningitis forms in infants [11].

The modern era for TB treatment born with the discovery of antituberculous effect of antibiotics, such as streptomycin in 1948 and isoniazid in 1953 [12,13]. TB became a preventable and medically treatable disease and their incidence continued to drop in industrialized countries throughout the XX century[14,15]. This fact, led to TB being neglected by governments and public health agencies until the end of the 20th century[7].

However, the pandemic of AIDS with increased susceptibility to TB of immunodepressed HIV infected individuals, the increasing cases of multi drug resistant strains (MDR-TB) together with a vaccine that has proven unsuccessful, and with the increased mobilization of people due to globalization have put TB back on the agenda during the past twenty years[16,17].

With the dawn of the new millennia the prevalence of tuberculosis has been decreasing since 2005, while the incidence has decreased since 2002 and a reduction in mortality of 45% between 1990 and 2012[18]. Nevertheless, TB still has a huge impact in public health worldwide, due to its high morbidity and mortality. It´s estimated that one third of the human population has been infected with *M. tuberculosis*, with about 5-10% (100-200 million) that will develop the disease. Co-infection with HIV, malnutrition, diabetes or any immunosuppressive condition increases the probability for developing TB. In 2012, an estimated 8.6 million people developed TB and 1.3 million died from the disease (almost 150 people each hour), from which 320 thousand were HIV positive[19].

Public health and financial efforts including improved access to health care, better control of transmission and increased treatment efficacy are urgently needed. Indeed, new scientific knowledge about the basic mechanisms underlying TB and for the elucidation of the host-*M. tuberculosis* interactions, are mandatory in order to find

new targets to develop alternative strategies for improved vaccines or new drugs that tackle the emergence of antibiotic resistance[7,20].

Mycobacterium tuberculosis

TB is caused by bacteria belonging to the *Mycobacterium tuberculosis* species complex: MTC (*M. tuberculosis, Mycobacterium canettii, Mycobacterium africanum, Mycobacterium microti, M. bovis, Mycobacterium caprae* and *Mycobacterium pinnipedii, Mycobacterium mungi, Dassie bacillus and Mycobacterium orygis* [21–23]. Although these species have 99.9% similarity at the nucleotide level and identical 16S rRNA sequences, they differ widely in terms of their host tropisms, phenotypes and pathogenicity [24]. From these species, *M. tuberculosis*, *M. africanum, M. bovis* and *M. canettii* are important human pathogens and *M. microti* has been reported to infect immunocompromised human patients[21].

M. tuberculosis is a rod-shaped, slow-growing and obligate aerobe bacterium, which the only known natural host is the human species[25,26]. This aerobic facultative intracellular pathogen has characteristic features that include its slow growth, the capability to enter and exit into dormancy, and a special metabolism adapted to intracellular survival, together with a robust genetic homogeneity [27]. Another remarkable characteristic of this pathogen is the ability to switch metabolic pathways after detection of specific environment [28]. The tubercle bacilli is fitted out with a protein secretion system that can deliver virulent effectors to host cells [29].

The etiologic agent of human tuberculosis has a cell wall characterized by a very complex thick cell wall (Figure 1.1) that shares characteristics of both gram positive and negative bacteria[30]. Composed partly by mycolic acids, renders this pathogen with intrinsic resistance to some antibiotics being also responsible for the acid-fast staining property used to identify mycobacteria, in Zhiel-Neelsen acid-fast stain [31]. The cell wall long-chain mycolic acids are linked to arabinogalactan, which is attached to the peptidoglycan. In addition, the cell wall contains several lipoglycans

including lipoarabinomannan (LAM), its precursor's lipomannan (LM), and phosphatidyl-*myo*-inositol mannosides (PIM). LAM acts as a virulence effector of *M. tuberculosis*, contributing to the inhibition of macrophage functions important for killing the pathogen by inhibiting phagosomal maturation and interfering with cell signalling and shifting the cytokine response from pro- to anti-inflammatory [32–34]. Virulent, slow-growing mycobacteria like *M. tuberculosis* harbour mannose-capped LAM (ManLAM) in their cell wall the type of capping is important for virulence [34]. The cell wall of virulent mycobacteria also contains a 19-kDa lipoprotein of unknown function which has been implicated in virulence through a role in host cell death and manipulation of bactericidal mechanisms [35].
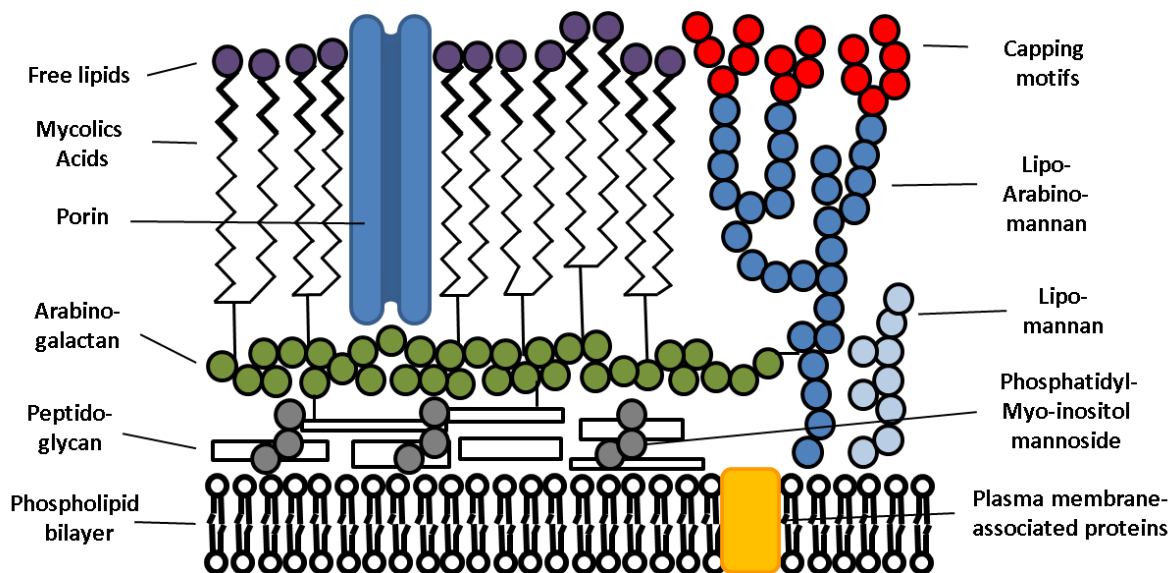
Figure 1.1. Schematic representation of the complex *Mycobacterium tuberculosis* cell wall. Arabinogalactan is attached to the peptidoglycan. Mycolic acids and glycolipids extend through the cell wall[152].

The majority of the species that compose this genus are non-pathogenic environmental bacteria, such as *Mycobacterium smegmatis,* which presents similarities to saprophytic bacteria from the genus *Streptomyces.* The strain H37 is a laboratory variant that was isolated from a 19-year old pulmonary TB patient in 1905, and later dissociated into a virulent strain (H37Rv) and an avirulent strain (H37Ra),

based on virulence in guinea pigs[36]. Although both strains can be cultured in suitable medium in the laboratory, only the H37Rv strain is capable of replication ~~inside~~ within human macrophages[37]. It has recently been described how H37Rv and H37Ra differ genetically and phenotypically, and the major difference lies in a mutation in the *phoP* gene, which is necessary for adaptation to the intracellular environment and PE/PPE/PE-PGRS genes involved in diverse functions such as virulence, fibronectin binding, and cell surface antigenic variations to evade the immune system[38].

From infection to disease

The infection by *M. tuberculosis* follows a sequence of events relatively well known (Figure 1.2). *M. tuberculosis* is transmitted by aerosol route from infected individuals with TB. Once inhaled the bacilli containing aerosols reach the lungs, cross the mucosal barrier and encounters the alveolar macrophages[39]. After macrophage phagocytosis, the infected host cells secrets cytokines that induce a local inflammatory response leading to the recruitment of mononuclear cells from the blood stream[40]. The recruited cells get organized in a structure aiming to contain the infection called granuloma, a defining pathologic feature of *M. tuberculosis* infection[40,41].

The granuloma is a structure composed by a mass of various cell types around the infected alveolar macrophages, consisting of other macrophages, monocytes, neutrophils, giant cells, foamy macrophages, and epithelioid macrophages[40,42,43]. While their function remains not completely understood, it is clear that constrains further propagation of the bacilli to the rest of the lung, arresting viable mycobacteria within this reservoir for a long period of time. This phase of the primo-infection usually is asymptomatic or confused with a simple cold but rarely will develop TB. However, instead of a full clearance of the bacilli most individuals may progress to a latent tuberculosis infection (LTB). It is estimated that only 5-10% of LTB will develop the disease in their lifetime. Factors that may contribute to this re-activation of the dormant bacilli are accompanied by a weakness of the immune system such as

consequence of malnutrition, ageing, immunosuppressant therapy or HIV co-infection. Under this situation, the granuloma centre becomes necrotic, undergoes caseation, resulting in the destruction of the surrounding host tissue. This leads to the rupture of the granuloma and to the release of infectious bacilli into the airways leading to exhalation of infected aerosols and perpetuation if the infection [40,42,43].
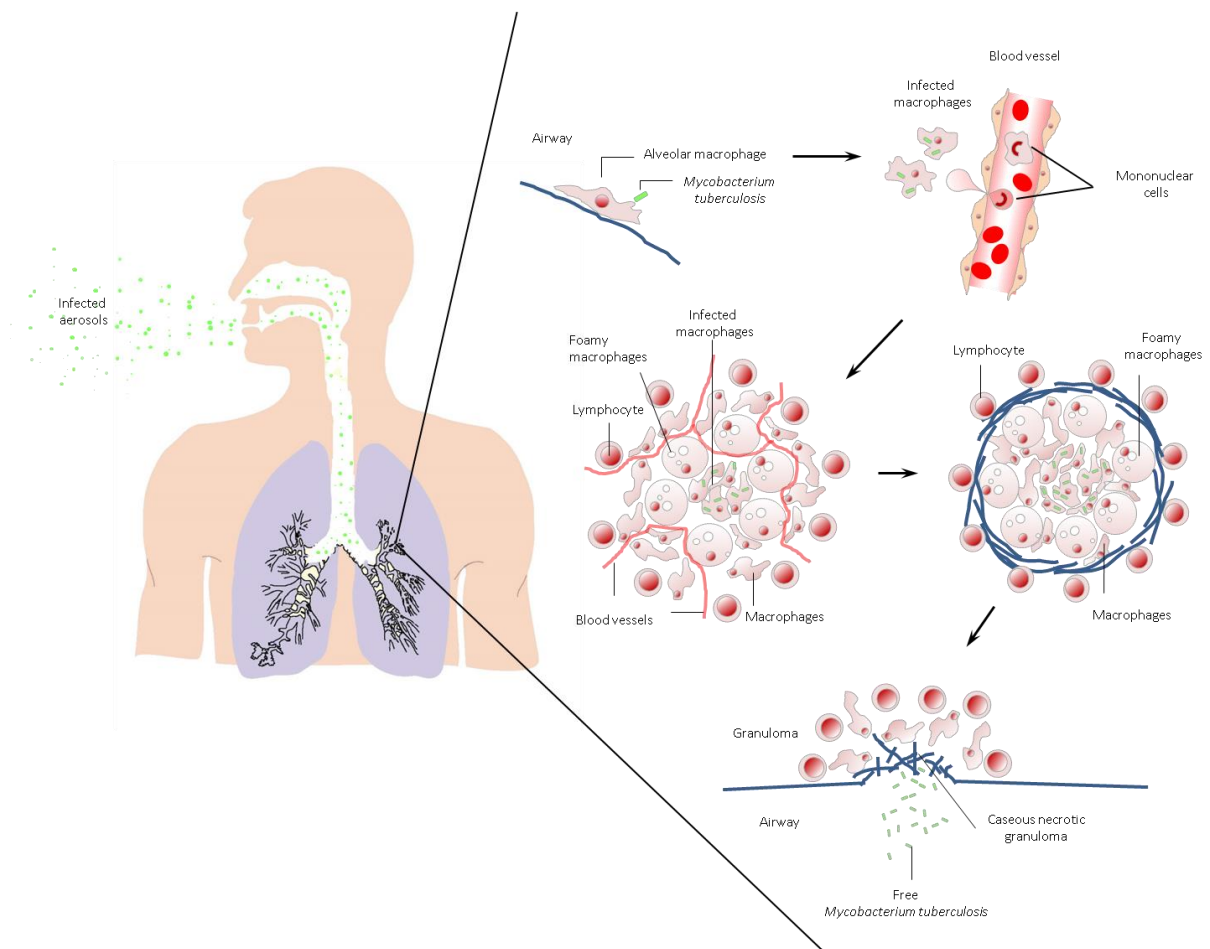
Figure 1.2. *Mycobacterium tuberculosis* **life cycle.** Resident alveolar macrophages phagocytose inhaled bacteria. This leads to a pro-inflammatory response and recruitment of cells of the innate and adaptive immune systems, and the formation of a granuloma. The bacilli can be contained within the structure for long periods of time, but if immune control fails, the bacilli will commence replication, and a necrotic granuloma core develops. The granuloma then ruptures and *M. tuberculosis* is spilled into the airways [40].

TB Chemotherapy and resistance

The current treatment regimen for TB includes a combination of four first line antibiotics, recommended by the WHO, composed of rifampicin, isoniazid, ethambutol and pyrazinamide along 2 months, followed by rifampicin and isoniazid for 4 months[44]. Chemotherapy is administered through directly observed treatment and short-course drug therapy (DOTS) programs, where patients are observed when they take their medication to ensure compliance, as non-compliance is a major contributor to the development of antibiotic resistance[45,46].

In 2012 the WHO estimated the 3,6% of new diagnosed TB cases and 20% of TB previously treated were multi-drug resistant *M. tuberculosis* TB (MDR-TB). Multi-drug-resistant tuberculosis is defined as *M. tuberculosis* that is resistant to at least INH and RMP, the two most powerful first-line treatment anti-TB drugs[47]. In 2012 it was estimated half million people with MDR-TB and 170 thousand resulted deaths. From these 9,6% were extensively drug-resistant TB cases, with bacteria resistance in addition to INH and RMP to quinolones and at least one injectable second line antibiotic (*i.e.* kanamycin, capreomycin, or amikacin) [48].

Resistant TB cases do not respond to conventional short-course antibiotic regimens and the treatment may be extended up to 2 years. The antibiotics used as alternative are less effective, more toxic to the patient and 50 to 100 times more expensive, having also poorer outcomes[48].

Some of the common causes of acquired drug resistance are prescription of inadequate treatment regimen, irregular drug supply, poor drug quality with low bioavailability, and poor compliance[49,50].

Macrophage – *M. tuberculosis* interaction

Macrophages are professional phagocytes relevant for the innate and adaptive immune responses. Resident macrophages are terminally differentiated in the body, *e.g.* alveolar macrophages are stationed in the lungs, Kupffer cells in the liver and microglia in the nervous system. The precursors of macrophages, the monocytes, circulate in the blood stream and are recruited into sites of infection or tissue damage upon cytokine challenge. The adhesion to specific extracellular matrix induces their differentiation to macrophages, cells with increased phagocytic capacity, different morphology and adhesive properties[51].

During infection, macrophages are one of the first line of defence, able to internalize and destroy pathogens, through a mechanism called phagocytosis[52]. Phagocytosis is an innate defence mechanism that removes foreign particles such as infecting bacteria and clear debris and death cells from among others, airways. The process initiates with adhesion to specific surface membrane receptors and engulfment of the bacterium by a plasma membrane-derived intracellular vacuole termed a phagosome. This is followed by a series of membrane fusion and fission events that massively reorganizes both the composition of phagosomal membranes and the phagosomal contents, a process known as phagosome maturation[52]. The pathway ends with the formation of the phagolysosome, a compartment competent to kill intracellular bacterium through their low pH, hydrolytic enzymes and the oxidative burst [53]. Bacterial protein and lipid debris became sources of antigens for antigen-specific T cells presentation, bridging innate to adaptive immune responses[51]. The resulted activated macrophages upon inflammatory or microbial stimulation acquire the antimicrobial properties necessary for elimination of the invader. However pathogens such as *M. tuberculosis*, have evolved means to circumvent most macrophage microbicidal responses [52,54,55].

Detection and internalization of M. tuberculosis by macrophages

M. tuberculosis is recognized by a set of macrophage surface receptors, thereby initiating specific signalling pathways and modulating several immunobiological processes during and after internalization[56,57]. The uptake of *M. tuberculosis* bacilli by macrophages involves the recognition of some bacterial components pathogen associated molecular patterns (PAMPs) through several of macrophage pattern recognition receptors (PRR) toll like receptors (TLR)[58] ,scavenger receptors, lectin receptors and other immune receptors including complement receptors (CR)[59], mannose receptors (MR)[60], receptors for the constant region of immunoglobulin G (FcγR), and, glycoproteins[61]. The type of receptors used for detection and/or internalization of *M. tuberculosis* might affect the fate of the bacteria: for instance internalization via CR or MR reduces pro-inflammation and macrophage activation[57] allowing a silence invasion of host cells. In opposition the engagement of FcγR leads to phagolysosomal maturation of *M. tuberculosis* containing vesicles and therefore may be an advantage for the host[62].

Manipulation of host vesicular traffic pathways

Upon internalization by macrophages, the newly formed phagosome containing *M. tuberculosis* redirects the host vesicular traffic pathways. *M. tuberculosis*´s virulence factors interfere with host phagolysosome biogenesis, by promoting homotypic fusion of early endosomes to provide nutrients to sustain replication[63]. Pioneering studies by Hart and Armstrong showed that phagosomes containing virulent *M. tuberculosis* do not fuse with lysosomes[64,65]. Several other studies shown that virulent mycobacteria containing phagosomes shared characteristics with early phagosomes, with a low acidified lumen (pH≈6) due to absence of V-ATPase[66]. Another important aspect of the mycobacterial phagosome is that the vacuole seems to retain access to markers derived from plasma membrane[67–69], allowing acquisition of nutrients, such as iron[70].

As described for other intracellular pathogens, *M. tuberculosis* secretes virulence factors redirects the host vesicular traffic through selective exclusion or retention of

Rab GTPases and SNARE proteins a major group of proteins responsible for coordination of vesicle traffic and fusion [71–73].

Rabs and SNAREs proteins

Rab proteins are a large family of monomeric GTPases with more than 70 members already identified in the human genome. These proteins help to define the organelle identity consequence of their distinct intracellular localization [74,75]. Nevertheless, different Rabs are able to bond the same membrane organelle forming distinct membrane microdomains bearing different functions [75,76].

Another typical feature of these family of proteins is the molecular switches alternating between two conformational states: the GTP-bound "active" form and the GDP-bound "inactive" form [74,77,78] (Figure 1.3). The spatial and temporal recruitment of GDP-GTP exchange factors (GEFs) and GTPase activating proteins (GAPs) is responsible for the correct transitions between Rabs in organelle membranes. Briefly, the soluble inactive GDP-bound Rab is a substrate for GDP dissociation inhibitor (GDI). At the acceptor membrane, the complex interacts with GDI dissociation factor (GDF), which removes GDI from the complex, allowing the insertion of the Rab in the membrane. At this stage, GEF acts on the membrane-inserted Rab to convert it to a GTP-bound active state, which in turn interacts with specific effectors, such as phosphatidylinositol kinases and phosphatases[75,77,79,80]. Through their effectors, Rabs mediate many key steps of membrane trafficking, including cargo selection, vesicle budding and transport, membrane tethering and fusion (Figure 1.3).

Several components of the fusion machinery participate in this process, including N-ethylmaleimide-sensitive factors (NSFs), NSF attachment proteins (SNAPs) and SNAREs (soluble NSF attachment receptor) [81–83]. The pairing of an organelle target SNARE with the vesicle SNARE originates a four-helix trans-SNARE bundle that pulls membranes together, allowing the fusion of lipid bilayers. Posterior to membrane fusion, the pair of SNAREs bound to the membrane is designated as cis-

SNARE and is separated into t-SNARE and v-SNARE through the recognition of the cis-SNARE complex by α-SNAP and the action of the NSF ATPase that interacts with α-SNAP [81–83]. Since SNAREs have some degree of promiscuity, Rab GTPases and their effectors also regulate docking and fusion specificity[84].

M. tuberculosis manipulation of host vesicular traffic

Phagosomes undergo a series of fusion and fission events along the endocytic pathway termed phagosome maturation[85] that results in the biogenesis of phagolysosomes[85]. After sealing, nascent phagosomes rapidly lose some of the cytosolic membrane components. Rab5 became associated with early phagosomes immediately after their formation. Active Rab5 recruits several effectors such as rabaptin 5 and rabex 5, promoting a loop with early endosome antigen1 (EEA1)[86]. EEA1 effector thereafter binds to Syntaxin (STX) 13 modulating, transiently the association and pore like fusion between phagosomes and vesicles on the same level of maturation: early endosomes[87]. At this stage early phagosomes possess a moderate pH and a poor hydrolytic lumen [52]. It is though that phagosomes maturation requires Rab5 conversion to Rab7 on the membrane organelle[88].

Recruitment of Rab7 to phagosomes is not completely understood. During this phase active Rab5 binds to its effector Vps34, a Phosphoinositide 3 Kinase typeII (PI3K) inducing the production of Phosphoinositide 3-phosphate (PI(3)P) in the phagosomal membrane[89]. Importantly, Rab5 also prompts, indirectly, the recruitment and GTP-loading (activation) of Rab7[90]. The newly acquired Rab7 proceeds to direct the centripetal displacement of phagosomes towards lysosomes through acquisition of RILP (Rab7 interacting lysosomal protein) which binds to dynein and promotes the interaction between phagosomes and lysosomes[91]. The SNARE STX7 is recruited to late endosomes/lysosomes[92] and is associated with phagosomes. This protein is recruited to phagosomes later than STX13 and accumulates throughout maturation probably promoting fusion between late endosomes/lysosomes and the phagosome.
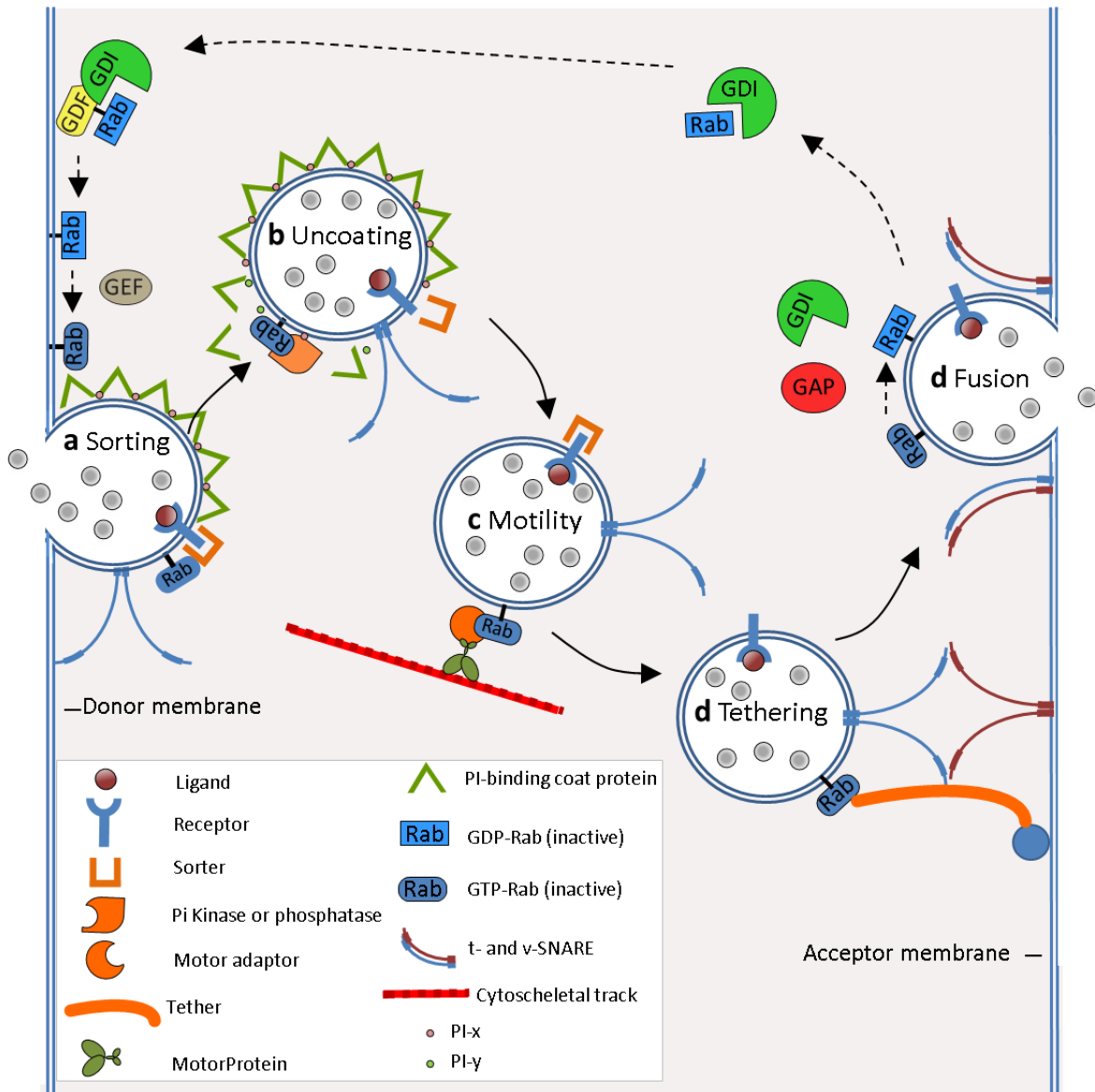
Figure 1.3. Distinct membrane trafficking steps that can be controlled by a Rab GTPase and its effectors (indicated in orange).a | An active GTP-bound Rab can activate a sorting adaptor to sort a receptor into a budding vesicle. b | Through recruitment of phosphoinositide (PI) kinases or phosphatases, the PI composition of a transport vesicle might be altered (the conversion of PI-x into PI-y) and thereby cause uncoating through the dissociation of PI-binding coat proteins. c | Rab GTPases can mediate vesicle transport along actin filaments or microtubules (collectively referred to as cytoskeletal tracts) by recruiting motor adaptors or by binding directly to motors (not shown). d | Rab GTPases can mediate vesicle tethering by recruiting rod-shaped tethering factors that interact with molecules in the acceptor membrane. Such factors might interact with SNAREs and their regulators to activate SNARE complex formation, which results in membrane fusion. e | Following membrane fusion and exocytosis, the Rab GTPase is converted to its inactive GDP-bound form through hydrolysis of GTP, which is stimulated by a GTPase-activating protein (GAP). Targeting of the Rab–GDP dissociation inhibitor (GDI) complex back to the donor membrane is mediated by interaction with a membrane-bound GDI displacement factor (GDF). Conversion of the GDP-bound Rab into the GTP-bound form is catalysed by a guanine nucleotide exchange factor (GEF)[75].

The phagolysosome contains an arsenal of highly hydrolytic enzymes that works in an acidic environment (pH bellow 5,5) designed to effectively eliminate invading microbes. Activated macrophages in addition to M0 ones are reprogrammed to high killing via free radicals and less extend of hydrolysis, fundamental for antigen presentation to the adaptive immune cells[93]. Several other Rabs and SNAREs proteins have been associated with phagosomes[71,85].

M. tuberculosis has the ability to invade macrophages, survive and, even replicate in phagosomes that do not maturate to phagolysosomes[94]. For long has been observed that *M. tuberculosis* block phagosome-lysosome fusion[64]. However, *M. tuberculosis* containing phagosome is a dynamic compartment: rather than static retaining the characteristics of an early phagosome. It has a pH of 6.3, mainly due to reduced recruitment of the V-ATPase and has access to transferrin[95–97] thus indicating that they are competent to fuse with endosomes for nutrient acquisition. It also lacks mature lysosomal hydrolases [98] and, the interactions between the phagosome and the TGN are limited[99]. Increasing body of evidence suggests that *M. tuberculosis* is able to manipulate macrophage vesicular traffic pathways. First, studies on phagosomal blockade by *M. tuberculosis* containing phagosomes indicate that the process is arrested during Rab5-Rab7 conversion[94]. More recent studies shows the presence of Rab7 in mycobacterial phagosomes, indicating that *M. tuberculosis*-containing phagosomes has the machinery for Rab7 and therefore the maturation block could occur subsequently to Rab7 acquisition or were influenced by other components [100]. A more recent study by Seto and colleagues helped to clarify the previous results, by demonstrating that Rab7 is transiently recruited to and subsequently released from mycobacterial phagosomes[101]. This phenomenon contributes to maturation block, by limiting the recruitment of the cathepsin D protease and the Rab-interacting lysosomal protein (RILP), a Rab 7 effector, to phagosomes [101]. Rab14 and Rab22a, were also demonstrated to be involved in the inhibition of *M. tuberculosis* phagosome maturation[102,103]. Recently Seto and colleagues made a comprehensive study on the localization and function of 42 Rab GTPases in both *Staphylococcus aureus* and *M. tuberculosis* during phagosome maturation progress[104]. The authors observed 22 Rab GTPases recruited to *S. aureus* phagosomes, and 17 of these showed different recruitment kinetics relatively to *M. tuberculosis* phagosomes. Similarly to Rab7, Rab34 is a late endosomal Rab

involved in the recruitment of cathepsin D to phagosomes and transiently associated with *M. tuberculosis* phagosomes. The authors suggest that modulation of the recruitment of these proteins to *M. tuberculosis* phagosome is involved in the arrest of phagosome maturation and inhibition of phagolysosome biogenesis.

In addition to Rab GTPases, proteins of the fusion machinery were also suggested to be targets for mycobacterial manipulation. The v-SNARE cellubrevin, also known as VAMP3, is involved in endosomal recycling and endosomal interactions with post-Golgi compartments, and is usually acquired in phagosomes. Fratti et al. appointed cellubrevin as a mycobacterial target due to the observation of a discrete degradation of this SNARE during mycobacterial infection [105]. Other SNARE that appears to be a target of *M. tuberculosis* is Stx4, which is a recycling endosomal and plasma membrane t-SNARE[106]. It was observed that Stx4 is retained in phagosomes containing PIM-coated latex beads, whereas the accumulation of this SNARE is lower in phagosomes containing uncoated beads. Since PIM is a mycobacterial glycolipid that impregnates host cell endomembranes, these findings indicate that PIM contributes to the fusion of *M. tuberculosis*-containing phagosomes with endosomal compartments, by retention of Stx4 in the phagosomal membrane [63].

Despite recent advances little is known about the *M. tuberculosis* mechanisms for retention or exclusion of this proteins or effect in *M. tuberculosis* replication or killing for these proteins.

Mycobacterium tuberculosis virulence effectors modulate host vesicular traffic

To successfully modulate host macrophage vesicular traffic *M. tuberculosis* relies on virulence effectors that specific alter proteins to inhibit phagolysosome biogenesis and direct transport to MCP for obtaining nutrients for replication[73]. LAM and particularly ManLAM was found to be a virulence effector by reducing acquisition of EEA1 and Stx6 to MCP altering calcium signalling and promoting trans-Golgi to phagosome maturation block [107]. Another described virulence factors affecting vesicular traffic is an acid phosphatase termed SapM secreted within the macrophage [33]. SapM hydrolyzes PI(3)p accumulated on phagosomal membranes,

eliminating the docking site of EEA1 involved in phagosome maturation[33]. The use of in vitro organellar preparations lead to the finding that phosphatidylinositol manoside (PIM) specifically promotes early endosomal fusion in a ATP-, cytosol- and NSF-dependent manner with absolute requirement of Rabs[63]. PIM stimulates phagosome-early endosome defining a novel route for MCP acquisition of nutrients. *M. tuberculosis* nucleoside diphosphate kinase (Ndk) exhibits GTPase activating protein (GAP) activity towards Rab5 and Rab7a blocking phagosome maturation through inhibition of recruitment of EEa1 and RILP effectors to Rab5 and Rab7a respectively[108].

Tyrosine phosphatases secreted by *M. tuberculosis* protein kinase G (PknG), is secreted into the cytosol of infected macrophages and prevents the intracellular destruction of mycobacteria by blocking phagosome-lysosome fusion[109]. PtpA is secreted into the macrophage cytosol to inactivate the human VPS33B, a component of the Class C VPS complex that regulates endosomal membrane fusion[109]. VPS33B dephosphorylation by PtpA results in the inhibition of phagosome-lysosome fusion. In addition to its phosphatase activity, PtpA is also capable of binding to subunit H of the macrophage V-ATPase complex, indicating that PtpA can directly disrupt phagosome acidification[109].

For the release of some virulence effector molecules that interfere with host responses, *M. tuberculosis* possesses a specialized protein secretion system, the so-called early secretory antigenic target system 1 (ESX-1). Esx-1, encoded by the RD1 (region of difference 1) genomic region represents a major virulence determinant [110].

M. tuberculosis induction of macrophage exosome secretion

Exosomes are small (50-100 nm) vesicles secreted by a range of cell types including macrophages. Exosomes biogenesis occurs by the inward invagination and budding of the limiting membrane of endosomal compartments forming multivesicular bodies (MVB)[111]. When MVB membranes fuse with the plasma membrane, exosomes are secreted to the extracellular space where they can interact with other cells[112,113]. Exosomes derived from antigen presenting cells are enriched in Major Histocompatibility Complex (MHC) class II, MHC class I and in co-stimulatory molecules, and are capable of efficiently inducing T cell responses both *in vitro* and *in vivo* when injected into mice[114]. Exosomes derived from cancer cells can participate both in the induction of anti-tumour immune responses, and in tumour-induced immunosuppression *in vivo*, depending on the tumour model studied or the physiological state of the patient[115].

In addition, these vesicles have been implicated in the pathogenesis of several infectious diseases as those caused by virus, prion or bacteria infected cells [116,117]. Particularly, recent studies report that exosomes produced by macrophages infected with different intracellular pathogens, are pro-inflammatory, which highlight a new role of these structures in innate immunity[118]. This is truth also for mycobacteria as several recent reports show that exosomes are secreted by macrophages infected with several mycobacteria species. Exosomes secreted by BCG infected macrophages administered intra-nasally into naïve mice they stimulated antigen-specific CD4+ and CD8+ T cells[119]. Identification of exosomes secreted by macrophages infected with *M. tuberculosis* revelled 41 mycobacterial proteins some already described to have antigenic properties[120]. Yet, these exosomes, derived from *M. tuberculosis* H37Rv-infected macrophages, inhibited IFN-γ induced MHC class II and CD63 expression on mice bone marrow derived macrophages, suggesting that exosomes, as carriers of *M. tuberculosis* PAMPs, may provide a mechanism by which *M. tuberculosis* may exert its suppression of a host immune response beyond the infected cell[121].

18

Although exosomes from *M. tuberculosis* infected macrophages have a huge potential in vaccine and diagnosis development for TB, the intracellular membrane traffic mechanisms underlying exosome secretion are still not understood.

Macrophage MicroRNAs as a target for *M. tuberculosis* host subversion

MicroRNAs (miRs) are small non-coding, single-stranded RNA molecules, with approximately 22 nucleotides length. In the cytosol, miRs bind specifically to the 3'-UTR regions of target mRNAs in a sequence-specific manner, causing translational repression or mRNA degradation, promoting a reduction in the protein translation and availability, which leads to the consequent repression of biological functions [122].

miRs are important to control a wide-range of biological processes, including development, cellular differentiation, proliferation, apoptosis, metabolism, immune response and in response to bacterial infections [123–126]. Expression of several miRs were demonstrated to be to be altered during *M. tuberculosis* infection[127]. On both murine and human derived macrophages an altered expression of miR-155, a miR associated with enhanced TNF-α biosynthesis, was observed [128,129]. Curiously, an opposite pattern of expression was shown in in human macrophages *M. tuberculosis* infection relatively to murine macrophages. In the case of *M. smegmatis* infection of human macrophages the gene is up regulated[128,129]. This suggests dependence in the regulation of the miR155 of the host cells and virulence of mycobacteria. To the best of our knowledge these are the only studies that systematically screened the miR expression on macrophage *M. tuberculosis* infection.

M. tuberculosis control of macrophage cell death

Infected cells can undergo a programmed death, dependent of apoptotic caspases, to deprive intracellular pathogens of their survival niche and to expose them to immune cell recruitment[130]. *M. tuberculosis* is able to manipulate the host macrophage cell death response to its own advantage. For a long time, there was a discrepancy in the results obtained concerning host macrophage death upon *M. tuberculosis* infection, as some studies have shown *M. tuberculosis* to be pro-apoptotic [131–134], while others have shown the bacterium to induce an anti-apoptotic effect in macrophages [135,136]. However, it is becoming clear that virulent *M. tuberculosis* is able to inhibit apoptosis initially upon infection, through several strategies, in order to retain its intracellular niche. *M. tuberculosis* protects cells against apoptosis via two key pathways: first, through induction of TLR-2–dependent activation of the nuclear factor kappa-light-chain-enhancer of activated B cells (NF-kB) cell survival pathway and second by enhancing the production of soluble TNF receptor 2 (sTNFR2), which neutralizes the pro-apoptotic activity of tumour necrosis factor alpha (TNF-α) [137–139]. Additionally, *M. tuberculosis* down regulation of host expression of the anti-apoptotic protein BCL-2 is also evident in *M. tuberculosis*-infected macrophages, although the mechanism of this gene repression is not known. This is achieved in part by the product of the gene *nuoG*, as deletion of this gene from mycobacteria results in elevated levels of apoptosis [135,136].

On the other hand, accumulating evidence shows that virulent *M. tuberculosis* induces necrosis of the infected macrophages upon infection. Necrosis particularly pyroptosis is a particular type of cell death which occurs in response to excessive stress, microbial invasion or tissue damage.

Furthermore, recent work shows that *M. tuberculosis* is capable of inhibiting the production of the prostaglandin E2 (PGE2), which plays a role in preventing mitochondrial damage as well as repairing the plasma membrane. This leads to necrosis rather than apoptosis, a situation which favours the bacterium to escape the macrophage and survive [134,140]. Additionally, *M. tuberculosis* H37Rv can prevent

20

completion of the apoptotic envelope by removing a domain from annexin-1, and this is also thought to play a role in inducing necrosis rather than the more hostile apoptotic event, allowing bacterial dissemination in the lung [141]. Thus, induction of necrosis is an important step in the pathogenesis of TB, enabling rupture of the host cell and spread to other cells once the bacterial load is sufficiently high.

M. tuberculosis clearance by autophagy

Autophagy is another form of programmed cell death by a separate pathway in which the cell ingests and degrades its own components, and this mechanism has been implicated in the delivery of cellular material and intracellular bacteria to phagolysosomes[142]. Induction of this mechanism has been shown to play a role in *M. tuberculosis* clearance. *M. tuberculosis* is eliminated from infected macrophages by the induction of autophagy as a consequence of nutrient starvation, drug inducer or IFN γ [143,144]. Autophagy also potentially controls the intracellular burdens of *M. tuberculosis* in macrophages[145]. Autophagy can be seen as an alternative induction of phagolysosome biogenesis and a tool for *M. tuberculosis* clearance.

Development of fluorescent based methods for studying host-mycobacteria interaction

 The "gold" standard for quantification of intracellular mycobacteria, colony forming units (CFU), relies on plating serial dilutions of lysed infected cells in solid media culture plates[146]. This technique is laborious, expensive and time consuming. CFU counting of mycobacterial species with fastidious growth-rates is only possible after several weeks of incubation. This approach is not suitable for high throughput

screens and therefore is essential the development of faster and more suitable methods[147]. The discovery of the green fluorescent protein (GFP) in the 1960's was the basis of a revolution in molecular and cell biology[148], presently researchers have a broad spectrum of colours and applications[149]. Fluorescent proteins allow the motorization of the cellular growth with high spatial and temporal resolution by fluorimetric detection using fluorimeters. Several fluorescent reporters are nontoxic cytoplasmic proteins and are continuously synthesized, which minimizes the effect of fluorescence signal dilution during cell replication [150]. These reporters don't require addition of co-factors or sample lysis and allow multiple labelling of the biological sample[151].

Thesis Goals

The overall objective of this thesis is to dissect the role of human vesicular traffic proteins, specifically Rab GTPases and SNARE proteins, in the survival/persistence of intracellular *M. tuberculosis* in an *in vitro* macrophage infection model. Vesicular traffic proteins, namely Rab GTPases and SNARE, coordinate vesicular traffic and membrane fusion[75,82]. Intracellular *M. tuberculosis* selectively excludes or retains specific vesicular traffic proteins in their phagosomes[73,104]. Our hypothesis was whether or not these vesicular traffic proteins have a role in the survival/persistence of intracellular *M. tuberculosis.* To achieve this goal we designed a high throughput screen based in a dual fluorescence method using two different fluorescent proteins as reporters of *M. tuberculosis* and of human macrophages for quantification intracellular mycobacteria. Additionally, we used RNA interference (RNAi) to knockdown host vesicular traffic genes. The genes whose knockdown reduced or increase the intracellular mycobacteria obtained from the genomic screen were phenotypically validated and gene knockdown confirmed by RT-PCR. In order to define if the different genes obtained from the genomic screen had a role in macrophage internalization of *M. tuberculosis* we optimized an internalization assay based on flow cytometry. We demonstrated that some genes whose knockdown led

to a reduction in intracellular *M. tuberculosis* in the genomic screen showed a reduction in mycobacteria internalization by human macrophages.

Additionally, previous results of our laboratory indicate that miR-142-3p is induced upon macrophage infection by mycobacteria. A gain-of-function experiment by inducing an increase of miR-142-3p led to a reduction in N-Wasp protein and, consequently to a reduced internalization of mycobacteria by murine macrophages. Likewise, virulent *M. tuberculosis* induced miR-142-3p expression and decreased N-Wasp in monocyte derived human primary macrophages (MDHM). In this study we show that miR-142-3p induction and consequent N-Wasp reduction of protein amount in MDHM is specifically induced by virulent *M. tuberculosis* but not by the non-pathogenic species *M. smegmatis* or by latex beads. To address whether or not reduction of N-Wasp by RNAi induced a decrease of *M. tuberculosis* internalization in monocyte derived human macrophages we used the optimized internalization assay. The presented results show a possible mechanism by which *M. tuberculosis* controls the rate of human macrophage internalization.

Finally, in order to dissect the role of Rab GTPases in exosome secretion we carried out a medium throughput genomic screen using a semi quantitative technique for ovalbumin and exosome secretion and systematically silenced 59 Rab GTPases. With this approach we were able to identify four Rabs, including Rab27a and Rab27b, proteins specifically involved in exosome secretion but not in ovalbumin. We also aimed to apply this technology to dissect the vesicular traffic genes involved in exosome secretion in *M. tuberculosis* infected macrophages. However it was not logistically possible to achieve this objective.

References

1. Comas I, Coscolla M, Luo T, et al. Out-of-Africa migration and Neolithic coexpansion of Mycobacterium tuberculosis with modern humans. *Nat Genet*. 2013;45(10):1176–82.

2. Gagneux S. Host-pathogen coevolution in human tuberculosis. *Philos Trans R Soc Lond B Biol Sci*. 2012;367(1590):850–9.

3. Wirth T, Hildebrand F, Allix-Béguec C, et al. Origin, spread and demography of the Mycobacterium tuberculosis complex. *PLoS Pathog*. 2008;4(9):e1000160..

4. Scurlock JA. *Diagnoses in Assyrian and Babylonian Medicine: Ancient Sources, Translations, and Modern Medical Analyses*.; 2005..

5. Smith I. Mycobacterium tuberculosis Pathogenesis and Molecular Determinants of Virulence. 2003;16(3):463–496.

6. Sakula a. Robert koch: centenary of the discovery of the tubercle bacillus, 1882. *Can Vet J*. 1983;24(4):127–31.

7. Snowden FM. Emerging and reemerging diseases: a historical perspective. *Immunol Rev*. 2008;225:9–26..

8. Luca S, Mihaescu T. History of BCG Vaccine. *Mædica*. 2013;8(1):53–8.

9. Daniel TM. The history of tuberculosis. *Respir Med*. 2006;100(11):1862–70.

10. Comstock GW. Simple, practical ways to assess the protective efficacy of a new tuberculosis vaccine. *Clin Infect Dis*. 2000;30 Suppl 3(Supplement_3):S250–3.

11. Trunz BB, Fine P, Dye C. Effect of BCG vaccination on childhood tuberculous meningitis and miliary tuberculosis worldwide: a meta-analysis and assessment of cost-effectiveness. *Lancet*. 2006;367(9517):1173–80.

12. STREPTOMYCIN treatment of pulmonary tuberculosis. *Br Med J*. 1948;2(4582):769–82.

13. ISONIAZID in the treatment of pulmonary tuberculosis; second report to the Medical Research Council by their Tuberculosis Chemotherapy Trials Committee. *Br Med J*. 1953;1(4809):521–36.

14. Smith I. Mycobacterium tuberculosis Pathogenesis and Molecular Determinants of Virulence Mycobacterium tuberculosis Pathogenesis and Molecular Determinants of Virulence. 2003;16(3):463–496.

15. Mitchison D, Davies G. The chemotherapy of tuberculosis: past, present and future. *Int J Tuberc Lung Dis*. 2012;16(6):724–32.

16. Navin TR, McNabb SJN, Crawford JT. The continued threat of tuberculosis. *Emerg Infect Dis*. 2002;8(11):1187.

17. Gandhi NR, Nunn P, Dheda K, et al. Multidrug-resistant and extensively drug-resistant tuberculosis: a threat to global control of tuberculosis. *Lancet*. 2010;375(9728):1830–43.

18.   *Global Tuberculosis Report 2011*. Geneva, Switzerland: World Health Organization; 2011.

19.   WHO. *Global tuberculosis report 2013*. Geneva, Switzerland: World Health Organization; 2013.

20.   Korbel DS, Schneider BE, Schaible UE. Innate immunity in tuberculosis: myths and truth. *Microbes Infect*. 2008;10(9):995–1004.

21.   Forrellad M a, Klepp LI, Gioffré A, et al. Virulence factors of the Mycobacterium tuberculosis complex. *Virulence*. 2013;4(1):3–66.

22.   Alexander K a, Laver PN, Michel AL, et al. Novel Mycobacterium tuberculosis complex pathogen, M. mungi. *Emerg Infect Dis*. 2010;16(8):1296–9.

23.   Characterization of Mycobacterium orygis as M. tuberculosis Complex Subspecies - Volume 18, Number 4—April 2012 - Emerging Infectious Disease journal - CDC.

24.   Brosch R, Gordon S V, Marmiesse M, et al. A new evolutionary scenario for the Mycobacterium tuberculosis complex. *Proc Natl Acad Sci U S A*. 2002;99(6):3684–9.

25.   Cosma CL, Sherman DR, Ramakrishnan L. The secret lives of the pathogenic mycobacteria. *Annu Rev Microbiol*. 2003;57:641–76.

26.   Pieters J. Entry and survival of pathogenic mycobacteria in macrophages. *Microbes Infect*. 2001;3(3):249–55.

27.   Cole ST, Brosch R, Parkhill J, et al. Deciphering the biology of Mycobacterium tuberculosis from the complete genome sequence. *Nature*. 1998;393(6685):537–44.

28.   Boshoff HIM, Barry CE. Tuberculosis - metabolism and respiration in the absence of growth. *Nat Rev Microbiol*. 2005;3(1):70–80.

29.   Champion PAD, Cox JS, DiGiuseppe Champion P a. Protein secretion systems in Mycobacteria. *Cell Microbiol*. 2007;9(6):1376–84.

30.   Fu L., Fu-Liu C. Is Mycobacterium tuberculosis a closer relative to Gram-positive or Gram–negative bacterial pathogens? *Tuberculosis*. 2002;82(2-3):85–90.

31.   Barry CE, Lee RE, Mdluli K, et al. Mycolic acids: structure, biosynthesis and physiological functions. *Prog Lipid Res*. 1998;37(2-3):143–79.

32.   Pathak SK, Basu S, Bhattacharyya A, Pathak S, Kundu M, Basu J. Mycobacterium tuberculosis lipoarabinomannan-mediated IRAK-M induction negatively regulates Toll-like receptor-dependent interleukin-12 p40 production in macrophages. *J Biol Chem*. 2005;280(52):42794–800.

33.   Vergne I, Chua J, Lee H-H, Lucas M, Belisle J, Deretic V. Mechanism of phagolysosome biogenesis block by viable Mycobacterium tuberculosis. *Proc Natl Acad Sci U S A*. 2005;102(11):4033–8.

34.   Dao DN, Kremer L, Guérardel Y, et al. Mycobacterium tuberculosis lipomannan induces apoptosis and interleukin-12 production in macrophages. *Infect Immun*. 2004;72(4):2067–74.

35.   Ciaramella a, Martino a, Cicconi R, Colizzi V, Fraziano M. Mycobacterial 19-kDa lipoprotein mediates Mycobacterium tuberculosis-induced apoptosis in monocytes/macrophages at early stages of infection. *Cell Death Differ*. 2000;7(12):1270–2.

36. Steenken W, Oatway WH, Petroff SA. BIOLOGICAL STUDIES OF THE TUBERCLE BACILLUS : III. DISSOCIATION AND PATHOGENICITY OF THE R AND S VARIANTS OF THE HUMAN TUBERCLE BACILLUS (H(37)). *J Exp Med*. 1934;60(4):515–40.

37. Zhang M, Gong J, Lin Y, Barnes PF. Growth of virulent and avirulent Mycobacterium tuberculosis strains in human macrophages. *Infect Immun*. 1998;66(2):794–9.

38. Zheng H, Lu L, Wang B, et al. Genetic basis of virulence attenuation revealed by comparative genomic analysis of Mycobacterium tuberculosis strain H37Ra versus H37Rv. Davis D, ed. *PLoS One*. 2008;3(6):e2375.

39. Kaufmann SHE, McMichael AJ. Annulling a dangerous liaison: vaccination strategies against AIDS and tuberculosis. *Nat Med*. 2005;11(4 Suppl):S33–44.

40. Russell DG. Who puts the tubercle in tuberculosis? *Nat Rev Microbiol*. 2007;5(1):39–47.

41. Beatty WL, Russell DG. Identification of mycobacterial surface proteins released into subcellular compartments of infected macrophages. *Infect Immun*. 2000;68(12):6997–7002.

42. Russell DG, Cardona P, Kim M, Allain S. NIH Public Access. 2009;10(9):943–948.

43. Russell DG, Barry CE, Flynn JL. Tuberculosis: what we don't know can, and does, hurt us. *Science*. 2010;328(5980):852–6.

44. Caminero JA, Sotgiu G, Zumla A, Migliori GB. Best drug treatment for multidrug-resistant and extensively drug-resistant tuberculosis. *Lancet Infect Dis*. 2010;10(9):621–629.

45. Bishai JD, Bishai WR, Bishai DM. Heightened vulnerability to MDR-TB epidemics after controlling drug-susceptible TB. Hill PC, ed. *PLoS One*. 2010;5(9):e12843.

46. Dye C, Williams BG. The population dynamics and control of tuberculosis. *Science*. 2010;328(5980):856–61.

47. Dalton T, Cegielski P, Akksilp S, et al. Prevalence of and risk factors for resistance to second-line drugs in people with multidrug-resistant tuberculosis in eight countries: a prospective cohort study. *Lancet*. 2012;380(9851):1406–17.

48. WHO. WHO Global Task Force outlines measures to combat XDR-TB worldwide. 2006. Available at: http://www.who.int/mediacentre/news/notes/2006/np29/en/

49. Almeida Da Silva PEA, Palomino JC. Molecular basis and mechanisms of drug resistance in Mycobacterium tuberculosis: classical and new drugs. *J Antimicrob Chemother*. 2011;66(7):1417–30.

50. Nachega JB, Chaisson RE. Tuberculosis drug resistance: a global threat. *Clin Infect Dis*. 2003;36(Suppl 1):S24–30.

51. Janeway C. *Immunobiology*. 5th ed. New York: Garland Science; 2001.

52. Flannagan RS, Jaumouillé V, Grinstein S. The cell biology of phagocytosis. *Annu Rev Pathol*. 2012;7:61–98.

53. Stuart LM, Ezekowitz RAB. Phagocytosis: elegant complexity. *Immunity*. 2005;22(5):539–50.

54. Benoit M, Desnues B, Mege J-L. Macrophage polarization in bacterial infections. *J Immunol*. 2008;181(6):3733–9.

55. Flannagan RS, Cosío G, Grinstein S. Antimicrobial mechanisms of phagocytes and bacterial evasion strategies. *Nat Rev Microbiol*. 2009;7(5):355–66.

56. Kleinnijenhuis J, Oosting M, Joosten L a B, Netea MG, Van Crevel R. Innate immune recognition of Mycobacterium tuberculosis. *Clin Dev Immunol*. 2011;2011:405310.

57. Ernst JD. Macrophage Receptors for Mycobacterium tuberculosis. *Infect Immun*. 1998;66(4):1277–1281.

58. Wang C, Peyron P, Mestre O, et al. Innate immune response to Mycobacterium tuberculosis Beijing and other genotypes. *PLoS One*. 2010;5(10):e13594.

59. Schäfer G, Jacobs M, Wilkinson RJ, Brown GD. Non-opsonic recognition of Mycobacterium tuberculosis by phagocytes. *J Innate Immun*. 2009;1(3):231–43.

60. Kang PB, Azad AK, Torrelles JB, et al. The human macrophage mannose receptor directs Mycobacterium tuberculosis lipoarabinomannan-mediated phagosome biogenesis. *J Exp Med*. 2005;202(7):987–99.

61. Clara Espitia, Eden Rodríguez, Lucero Ramón-Luing, Gabriela Echeverría-Valencia and Antonio J. Vallecillo. Host–Pathogen Interactions in Tuberculosis, Understanding Tuberculosis - Analyzing the Origin of Mycobacterium Tuberculosis Pathogenicity, Dr. Pere-Joan Cardona (Ed.), 2012. ISBN: 978-953-307-942-4, InTech, DOI: 10.5772/30310. Available from: http://www.intechopen.com/books/understanding-tuberculosis-analyzing-the-origin-of-mycobacterium-tuberculosis-pathogenicity/host-pathogen-interactions-in-tuberculosis

62. Hill M, Armstrong JA, Hart PD. Phagosome-lysosome interactions in cultured macrophages infected with virulent tubercle bacilli. Reversal of the usual nonfusion pattern and observations on bacterial survival. *J Exp Med*. 1975;142(1):1–16.

63. Vergne I, Fratti RA, Hill PJ, Chua J, Belisle J, Deretic V. Mycobacterium tuberculosis Phagosome Maturation Arrest : Mycobacterial Phosphatidylinositol Analog Phosphatidylinositol Mannoside Stimulates Early Endosomal Fusion. 2004;15(February):751–760.

64. Armstrong JA, Hart PD. Response of cultured macrophages to Mycobacterium tuberculosis, with observations on fusion of lysosomes with phagosomes. *J Exp Med*. 1971;134(3 Pt 1):713–40..

65. Hart PD, Armstrong J a. Strain virulence and the lysosomal response in macrophages infected with Mycobacterium tuberculosis. *Infect Immun*. 1974;10(4):742–6.

66. Sturgill-Koszycki S, Schlesinger PH, Chakraborty P, et al. Lack of acidification in Mycobacterium phagosomes produced by exclusion of the vesicular proton-ATPase. *Science*. 1994;263(5147):678–81.

67. Clemens DL, Horwitz MA. The Mycobacterium tuberculosis phagosome interacts with early endosomes and is accessible to exogenously administered transferrin. *J Exp Med*. 1996;184(4):1349–55.

68. Russell DG, Dant J, Sturgill-Koszycki S. Mycobacterium avium- and Mycobacterium tuberculosis-containing vacuoles are dynamic, fusion-competent vesicles that are accessible to glycosphingolipids from the host cell plasmalemma. *J Immunol*. 1996;156(12):4764–73.

69. Sturgill-Koszycki S, Schaible UE, Russell DG. Mycobacterium-containing phagosomes are accessible to early endosomes and reflect a transitional state in normal phagosome biogenesis. *EMBO J*. 1996;15(24):6960–8.

70. Schaible UE, Collins HL, Priem F, Kaufmann SHE. Correction of the iron overload defect in beta-2-microglobulin knockout mice by lactoferrin abolishes their increased susceptibility to tuberculosis. *J Exp Med*. 2002;196(11):1507–13.

71. Brumell JH, Scidmore M a. Manipulation of rab GTPase function by intracellular bacterial pathogens. *Microbiol Mol Biol Rev*. 2007;71(4):636–52.

72. Stein M-P, Müller MP, Wandinger-Ness A. Bacterial pathogens commandeer Rab GTPases to establish intracellular niches. *Traffic*. 2012;13(12):1565–88.

73. Vergne I, Chua J, Singh SB, Deretic V. Cell biology of mycobacterium tuberculosis phagosome. *Annu Rev Cell Dev Biol*. 2004;20:367–94.

74. Zerial M, McBride H. Rab proteins as membrane organizers. *Nat Rev Mol Cell Biol*. 2001;2(2):107–17.

75. Stenmark H. Rab GTPases as coordinators of vesicle traffic. *Nat Rev Mol Cell Biol*. 2009;10(8):513–25.

76. Sönnichsen B, De Renzis S, Nielsen E, Rietdorf J, Zerial M. Distinct membrane domains on endosomes in the recycling pathway visualized by multicolor imaging of Rab4, Rab5, and Rab11. *J Cell Biol*. 2000;149(4):901–14.

77. Hutagalung AH, Novick PJ, NOVICK AHH and PJ. Role of Rab GTPases in Membrane Traffic and Cell Physiology. *Physiol Rev*. 2011;91(1):119–149.

78. Mizuno-Yamasaki E, Rivera-Molina F, Novick P. GTPase networks in membrane traffic. *Annu Rev Biochem*. 2012;81:637–59.

79. Somsel Rodman J, Wandinger-Ness a. Rab GTPases coordinate endocytosis. *J Cell Sci*. 2000;113 Pt 2:183–92.

80. Grosshans BL, Ortiz D, Novick P. Rabs and their effectors: achieving specificity in membrane traffic. *Proc Natl Acad Sci U S A*. 2006;103(32):11821–7.

81. Weber T, Zemelman B V, McNew JA, et al. SNAREpins: Minimal Machinery for Membrane Fusion. *Cell*. 1998;92(6):759–772.

82. Jahn R, Scheller RH. SNAREs--engines for membrane fusion. *Nat Rev Mol Cell Biol*. 2006;7(9):631–43.

83. Hong W. SNAREs and traffic. *Biochim Biophys Acta*. 2005;1744(2):120–44.

84. McNew JA. Regulation of SNARE-mediated membrane fusion during exocytosis. *Chem Rev*. 2008;108(5):1669–86. doi:10.1021/cr0782325.

85. Vieira O V, Botelho RJ, Grinstein S. Phagosome maturation: aging gracefully. *Biochem J*. 2002;366(Pt 3):689–704.

86. McBride HM, Rybin V, Murphy C, Giner a, Teasdale R, Zerial M. Oligomeric complexes link Rab5 effectors with NSF and drive membrane fusion via interactions between EEA1 and syntaxin 13. *Cell*. 1999;98(3):377–86.

87. Vieira O V., Bucci C, Harrison RE, et al. Modulation of Rab5 and Rab7 Recruitment to Phagosomes by Phosphatidylinositol 3-Kinase. *Mol Cell Biol*. 2003;23(7):2501–2514.

88. Desjardins M, Huber L a, Parton RG, Griffiths G. Biogenesis of phagolysosomes proceeds through a sequential series of interactions with the endocytic apparatus. *J Cell Biol*. 1994;124(5):677–88.

89. Vieira O V, Botelho RJ, Rameh L, et al. Distinct roles of class I and class III phosphatidylinositol 3-kinases in phagosome formation and maturation. *J Cell Biol*. 2001;155(1):19–25.

90. Vieira O V., Bucci C, Harrison RE, et al. Modulation of Rab5 and Rab7 recruitment to phagosomes by phosphatidylinositol 3-kinase. *Mol Cell Biol*. 2003;23(7):2501–14.

91. Jordens I, Fernandez-Borja M, Marsman M, et al. The Rab7 effector protein RILP controls lysosomal transport by inducing the recruitment of dynein-dynactin motors. *Curr Biol*. 2001;11(21):1680–5.

92. Mullock BM, Smith CW, Ihrke G, et al. Syntaxin 7 is localized to late endosome compartments, associates with Vamp 8, and Is required for late endosome-lysosome fusion. *Mol Biol Cell*. 2000;11(9):3137–53.

93. Stendahl O. *Phagocytosis of Bacteria and Bacterial Pathogenicity*. (Ernst JD, Stendahl O, eds.). Cambridge: Cambridge University Press; 2006.

94. Via LE. Arrest of Mycobacterial Phagosome Maturation Is Caused by a Block in Vesicle Fusion between Stages Controlled by rab5 and rab7. *J Biol Chem*. 1997;272(20):13326–13331.

95. Clemens DL. The Mycobacterium tuberculosis phagosome interacts with early endosomes and is accessible to exogenously administered transferrin. *J Exp Med*. 1996;184(4):1349–1355.

96. Clemens DL, Horwitz MA. Characterization of the Mycobacterium tuberculosis phagosome and evidence that phagosomal maturation is inhibited. *J Exp Med*. 1995;181(1):257–70.

97. Sturgill-koszycki S, Schaible UE, Russell DG. Mycobacterium-containing phagosomes. Science. 1996;15(24):6960–6968.

98. Rohde K, Yates RM, Purdy GE, Russell DG. Mycobacterium tuberculosis and the environment within the phagosome. *Immunol Rev*. 2007;219:37–54.

99. Vergne I, Chua J, Deretic V. Mycobacterium tuberculosis phagosome maturation arrest: selective targeting of PI3P-dependent membrane trafficking. *Traffic*. 2003;4(9):600–6.

100. Clemens DL, Lee B, Horwitz MA. Deviant Expression of Rab5 on Phagosomes Containing the Intracellular Pathogens Mycobacterium tuberculosis and Legionella pneumophila Is Associated with Altered Phagosomal Fate Deviant Expression of Rab5 on Phagosomes Containing the Intracellular Pathogen. Infect Immun. 2000; 68(5):2671-84..

101. Seto S, Matsumoto S, Ohta I, Tsujimura K, Koide Y. Dissection of Rab7 localization on Mycobacterium tuberculosis phagosome. *Biochem Biophys Res Commun*. 2009;387(2):272–7.

102. Kyei GB, Vergne I, Roberts E, et al. Rab14 is critical for maintenance of Mycobacterium tuberculosis phagosome maturation arrest. *EMBO J*. 2006;25(22):5250–5259.

103. Roberts E a, Chua J, Kyei GB, Deretic V. Higher order Rab programming in phagolysosome biogenesis. *J Cell Biol*. 2006;174(7):923–9.

104. Seto S, Tsujimura K, Koide Y. Rab GTPases regulating phagosome maturation are differentially recruited to mycobacterial phagosomes. *Traffic*. 2011;12(4):407–20.

105. Fratti R a, Chua J, Deretic V. Cellubrevin alterations and Mycobacterium tuberculosis phagosome maturation arrest. *J Biol Chem*. 2002;277(19):17320–6.

106. Band AM, Ali H, Vartiainen MK, et al. Endogenous plasma membrane t-SNARE syntaxin 4 is present in rab11 positive endosomal membranes and associates with cortical actin cytoskeleton. *FEBS Lett*. 2002;531(3):513–9.

107. Fratti RA, Backer JM, Gruenberg J, Corvera S, Deretic V. Role of phosphatidylinositol 3-kinase and Rab5 effectors in phagosomal biogenesis and mycobacterial phagosome maturation arrest. J Cell Biol. 1997:631–644.

108. Sun J, Wang X, Lau A, Liao T-YA, Bucci C, Hmama Z. Mycobacterial nucleoside diphosphate kinase blocks phagosome maturation in murine RAW 264.7 macrophages. *PLoS One*. 2010;5(1):e8769.

109. Wong D, Bach H, Sun J, Hmama Z, Av-Gay Y. Mycobacterium tuberculosis protein tyrosine phosphatase (PtpA) excludes host vacuolar-H+-ATPase to inhibit phagosome acidification. *Proc Natl Acad Sci U S A*. 2011;108(48):19371–6.

110. MacGurn J a, Cox JS. A genetic screen for Mycobacterium tuberculosis mutants defective for phagosome maturation arrest identifies components of the ESX-1 secretion system. *Infect Immun*. 2007;75(6):2668–78.

111. Huotari J, Helenius A. Endosome maturation. *EMBO J*. 2011;30(17):3481–500.

112. Stoorvogel W, Kleijmeer MJ, Geuze HJ, Raposo G. The biogenesis and functions of exosomes. *Traffic*. 2002;3(5):321–30.

113. Théry C, Ostrowski M, Segura E. Membrane vesicles as conveyors of immune responses. *Nat Rev Immunol*. 2009;9(8):581–93.

114. Raposo G, Nijman HW, Stoorvogel W, et al. B lymphocytes secrete antigen-presenting vesicles. *J Exp Med*. 1996;183(3):1161–72.

115. Iero M, Valenti R, Huber V, et al. Tumour-released exosomes and their implications in cancer immunity. *Cell Death Differ*. 2008;15(1):80–8.

116. Wiley RD, Gummuluru S. Immature dendritic cell-derived exosomes can mediate HIV-1 trans infection. *Proc Natl Acad Sci U S A*. 2006;103(3):738–43.

117. Fevrier B, Vilette D, Archer F, et al. Cells release prions in association with exosomes. *Proc Natl Acad Sci U S A*. 2004;101(26):9683–8.

118. Bhatnagar S, Shinagawa K, Castellino FJ, Schorey JS. Exosomes released from macrophages infected with intracellular pathogens stimulate a proinflammatory response in vitro and in vivo. *Blood*. 2007;110(9):3234–44.

119. Giri PK, Schorey JS. Exosomes derived from M. Bovis BCG infected macrophages activate antigen-specific CD4+ and CD8+ T cells in vitro and in vivo. Bishai W, ed. *PLoS One*. 2008;3(6):e2461.

120. Giri PK, Kruh NA, Dobos KM, Schorey JS. Proteomic analysis identifies highly antigenic proteins in exosomes from M. tuberculosis-infected and culture filtrate protein-treated macrophages. *Proteomics*. 2010;10(17):3190–202.

121. Singh PP, LeMaire C, Tan JC, Zeng E, Schorey JS. Exosomes released from M. tuberculosis infected cells can suppress IFN-γ mediated activation of naïve macrophages. *PLoS One*. 2011;6(4):e18564.

122. Libri V, Miesen P, van Rij RP, Buck AH. Regulation of microRNA biogenesis and turnover by animals and their viruses. *Cell Mol Life Sci*. 2013;70(19):3525–44.

123. Bueno MJ, Pérez de Castro I, Malumbres M. Control of cell proliferation pathways by microRNAs. *Cell Cycle*. 2008;7(20):3143–8.

124. Kedde M, Agami R. Interplay between microRNAs and RNA-binding proteins determines developmental processes. *Cell Cycle*. 2008;7(7):899–903.

125. O'Connell RM, Rao DS, Chaudhuri AA, Baltimore D. Physiological and pathological roles for microRNAs in the immune system. *Nat Rev Immunol*. 2010;10(2):111–22.

126. Eulalio A, Schulte L, Vogel J. The mammalian microRNA response to bacterial infections. *RNA Biol*. 2012;9(6):742–50.

127. Singh PK, Singh AV, Chauhan DS. Current understanding on micro RNAs and its regulation in response to Mycobacterial infections. *J Biomed Sci*. 2013;20:14.

128. Rajaram MV1, Ni B, Morris JD, Brooks MN, Carlson TK, Bakthavachalu B, Schoenberg DR, Torrelles JB, Schlesinger LS. Mycobacterium tuberculosis lipomannan blocks TNF biosynthesis by regulating macrophage MAPK-activated protein kinase 2 (MK2) and microRNA miR-125b. Proc Natl Acad Sci U S A. 2011 Oct 18;108(42):17408-13..

129. Kumar D, Nath L, Kamal MA, et al. Genome-wide analysis of the host intracellular network that regulates survival of Mycobacterium tuberculosis. *Cell*. 2010;140(5):731–43.

130. Lamkanfi M, Dixit VM. Manipulation of host cell death pathways during microbial infections. *Cell Host Microbe*. 2010;8(1):44–54.

131. Chen M, Gan H, Remold HG. A mechanism of virulence: virulent Mycobacterium tuberculosis strain H37Rv, but not attenuated H37Ra, causes significant mitochondrial inner membrane disruption in macrophages leading to necrosis. *J Immunol*. 2006;176(6):3707–16.

132. Lee J, Remold HG, Ieong MH, Kornfeld H. Macrophage apoptosis in response to high intracellular burden of Mycobacterium tuberculosis is mediated by a novel caspase-independent pathway. *J Immunol*. 2006;176(7):4267–74.

133. O'Sullivan MP, O'Leary S, Kelly DM, Keane J. A caspase-independent pathway mediates macrophage cell death in response to Mycobacterium tuberculosis infection. *Infect Immun*. 2007;75(4):1984–93.

134. Chen M, Divangahi M, Gan H, et al. Lipid mediators in innate immunity against tuberculosis: opposing roles of PGE2 and LXA4 in the induction of macrophage death. *J Exp Med*. 2008;205(12):2791–801.

135. Velmurugan K, Chen B, Miller JL, et al. Mycobacterium tuberculosis nuoG is a virulence gene that inhibits apoptosis of infected host cells. *PLoS Pathog*. 2007;3(7):e110.

136. Briken V, Miller JL. Living on the edge: inhibition of host cell apoptosis by Mycobacterium tuberculosis. *Future Microbiol*. 2008;3(4):415–22.

137. Balcewicz-Sablinska MK, Keane J, Kornfeld H, Remold HG. Pathogenic Mycobacterium tuberculosis evades apoptosis of host macrophages by release of TNF-R2, resulting in inactivation of TNF-alpha. *J Immunol*. 1998;161(5):2636–41.

138. Repasy T, Lee J, Marino S, et al. Intracellular Bacillary Burden Reflects a Burst Size for Mycobacterium tuberculosis In Vivo. *PLoS Pathog*. 2013;9(2):e1003190.

139. Kornfeld H, Mancino G, Colizzi V. The role of macrophage cell death in tuberculosis. *Cell Death Differ*. 1999;6(1):71–8.

140. Divangahi M, Chen M, Gan H, et al. Mycobacterium tuberculosis evades macrophage defenses by inhibiting plasma membrane repair. *Nat Immunol*. 2009;10(8):899–906.

141. Gan H, Lee J, Ren F, Chen M, Kornfeld H, Remold HG. Mycobacterium tuberculosis blocks crosslinking of annexin-1 and apoptotic envelope formation on infected macrophages to maintain virulence. *Nat Immunol*. 2008;9(10):1189–97.

142. Yuk JM, Yoshimori T, Jo EK. Autophagy and bacterial infectious diseases. *Exp Mol Med*. 2012;44(2):99–108.

143. Singh SB, Davis AS, Taylor GA, Deretic V. Human IRGM induces autophagy to eliminate intracellular mycobacteria. *Science*. 2006;313(5792):1438–41.

144. Deretic V, Singh S, Master S, et al. Microreview Mycobacterium tuberculosis inhibition of phagolysosome biogenesis and autophagy as a host defence mechanism. 2006;8(March):719–727.

145. Jayaswal S, Kamal MA, Dua R, et al. Identification of host-dependent survival factors for intracellular Mycobacterium tuberculosis through an siRNA screen. Rubin EJ, ed. *PLoS Pathog*. 2010;6(4):e1000839.

146. P. Bettencourt, D. Pires NC and EA. Application of Confocal Microscopy for Quantification of Intracellular Mycobacteria in Macrophages. In: Díaz M-V and J, ed. *Microscopy: Science, Technology, Applications and Education*. ©FORMATEX.; 2010:614–621.

147. Meyers PR, Bourn WR, Steyn LM, van Helden PD, Beyers AD, Brown GD. Novel method for rapid measurement of growth of mycobacteria in detergent-free media. *J Clin Microbiol*. 1998;36(9):2752–4.

148. Via LE, Dhandayuthapani S, Deretic D, Deretic V. Green fluorescent protein. A tool for gene expression and cell biology in mycobacteria. Methods Mol Biol. 1998;101:245-60.

149. Giepmans BNG, Adams SR, Ellisman MH, Tsien RY. The fluorescent toolbox for assessing protein location and function. *Science*. 2006;312(5771):217–24.

150. Müller-Taubenberger A, Ishikawa-Ankerhold HC. Fluorescent reporters and methods to analyse fluorescent signals. *Methods Mol Biol*. 2013;983:93–112.

151. Shaner NC, Steinbach PA, Tsien RY. A guide to choosing fluorescent proteins. *Nat Methods*. 2005;2(12):905–9.

152. Park SH, Bendelac A. CD1-restricted T-cell responses and microbial infection. Nature. 2000 Aug 17;406(6797):788-92.

Chapter 2

Development of a dual fluorescence method for quantification of intracellular survival of mycobacteria within viable macrophages.

Development of a dual fluorescence method for quantification of intracellular survival of mycobacteria within viable macrophages.

Abstract

Mycobacterium tuberculosis evolved strategies to invade, survive intracellularly and egress human macrophages. Effective and fast methods for evaluation of *M. tuberculosis* intracellular survival are important tools to decipher host factors required for effective bacteria killing and indeed for new antimicrobial drug screenings. Conventional colony forming units counting (CFU) for quantification of *Mycobacterium tuberculosis* internalized by macrophages, is a labour intensive method with long incubation requirements that can take up to several weeks. Alternative fast and save methods, urge to be developed especially to be applied for mycobacteria intracellular survival assessments required in high-throughput screens (HTS). Other methods such as luminescence are not well suited for HTS, using multiple 96 wells plates because they need a disruption of the infected macrophages for release the substrate for the assay. Here we took advantage of fluorescent reporter proteins to accurately evaluate the amounts of mycobacteria that were internalized by macrophages in cell cultures. We developed a dual fluorescent assay, a method based in the use of two different fluorescent proteins as reporters, one for macrophage viability and the other for intracellular survival of *M. tuberculosis*. The method is cost-effective, suitable for HTS and is an alternative to traditional methods for quantification of intracellular mycobacteria. The assessment and quantification of infected host cells may provide additional information on the toxicity effects of new drugs on host viability, and give insights on host factors that impair *M. tuberculosis* survival/persistence.

Introduction

Tuberculosis (TB) is still a major global public health problem. The etiologic agent, *M. tuberculosis*, infects one third of the human population, especially in the poorest countries. The emergence of multi drug resistant strains has been reported all over the world. Additionally, co-infection with HIV represents the major risk factor for development of active TB [1]. All these factors account for the TB global emergence due to the high prevalence of this disease that kills 1,3 million people annually [2].

M. tuberculosis can survive and even grow within macrophages, within phagosomes, a cellular compartment that provides camouflage from the immune system and limits the access and activity of some antibiotics. Actually, for any drug to reach the intracellular compartment containing the bacilli it will be needed their uptake either by membrane translocation or via endocytosis, depending on the physiochemical characteristics of the molecular structure. After reaching the same compartment of the bacteria, the lumen will need to have a proper pH or ionic content for drug activity or for preventing their extrusion through efflux pumps expressed by the host cell and the mycobacteria [3,4]. Additionally, *M. tuberculosis* has been shown to shift their transcriptional gene profile after macrophage uptake which may alter their susceptibility to drugs [5]. Therefore, the identification of new potential anti-tubercular drugs using *in vitro* systems in broth culture screens may prove to be ineffective when *in vitro* assays are performed in infected cell cultures [6]. Furthermore some pathogens such as *M. tuberculosis* or some host proteins when silenced or overexpressed may induce host cell death or toxicity. Therefore novel screening methods for drugs or host factors that may be involved in the killing of mycobacteria should evaluate in parallel the amount of intracellular pathogens and the ratio of the host infected viable cells.

The current CFU method for determination of the number of live intracellular bacteria, involves methodologies such harvesting bacilli and growing them for quantification on solid media and subsequent counting of colonies. The principle drawbacks of such method is that of being labour-intensive and expensive due to the long period of time needed for *M. tuberculosis* grow (generation time of 18 to 24 hours), associated with the possibility of contamination. Furthermore, non-specific binding of *M. tuberculosis* to both plastic ware and macrophage membranes generates an added obstacle. The lack of a fast, sample friendly and reliable alternative technique for intracellular quantification of *M. tuberculosis* has been limitations when HTS are required for assess host factors affecting intracellular pathogen survival/persistence.

The identification of GFP from Aequorea or in other organisms together with the subsequent expansion in the identification of different fluorescent proteins (FP) through GFP mutagenesis led to a "revolution" in cell biology [7]. The ability to monitor in real time, live cellular mechanisms without cell toxicity or the need of adding any cofactor make these proteins perfect reporters of cell and organism viability.

In this study we developed a dual fluorescence assay by making use of the expression of two different fluorescent proteins one addressing mycobacteria and the other human macrophages. The dual fluorescence assay provides us means to quantify intracellular *M. tuberculosis* and, simultaneously, macrophage viability during infection for HTS. During the development of this methodology we tested the biological effect of pyrazinoic acid esters in *M. tuberculosis* broth cultures and identified some pitfalls of this kind of approach. Effective methods for the evaluation of the survival/killing of intracellular pathogens in their intracellular niche will be important for future research of host-pathogen interactions and will enable the identification of both new drugs that can target *M. tuberculosis* or host factors to impair pathogen intracellular survival in a rapid cost-effective way.

Results

M. tuberculosis fluorescent intensity is correlated with the amount of mycobacteria

The measurement of the optical density is commonly used to quantify the number of mycobacteria in a broth culture and is correlated with the number of viable mycobacteria [8]. However this approach can lead to artifacts due to the clumpy nature of these bacteria. In order to develop a fluorescence-based method to effectively test mycobacterial sensitivity to antibiotics we used the *M. tuberculosis* strain H37ra expressing GFP. Mycobacteria were incubated in broth cultures with serial two fold dilutions of three different antibiotics (amikacin, hygromycin B and kanamycin) and were quantified by measuring the fluorescence intensities (FI; excitation: 488nm; emission: 520nm; Gain: 150) in parallel to the optical density at 600 nm (OD_{600}). The samples were recorded during the following 7 days (Figure

2.1). We observed an increase both on fluorescence intensity and on OD_{600} in the control samples. In all the antibiotics samples tested we detected inhibitory concentrations for bacterial growth with exception of hygromycin B. This result was already expected since pMN042, used in this strain for GFP expression, has a hygromycin B resistance gene. The minimum inhibitory concentration (MICs) for *M. tuberculosis* H37Ra GFP was determined considering the highest concentration that led to 90% of inhibition compared with the control both by FI and OD, after 7 days of incubation (Table 2.1). MIC values obtained by OD measurement were higher than those by FI in an order of 2-4 folds. The MIC for the amikacin by FI measurements was similar to those reported in a similar study [9]. Although expression of GFP by mycobacteria, measured by FI, had higher sensitivity for assessment of cell viability in latter time points and OD_{600} was more sensitive in low cell concentrations for readings below 0,1, still the methods present a strong correlation (r^2=0,94, Pearson's correlation; $p<0,05$) (Figure 2.2). These results indicate that, within a specific range, IF is a good alternative method to evaluate *M. tuberculosis* susceptibility to new anti-tubercular drugs.
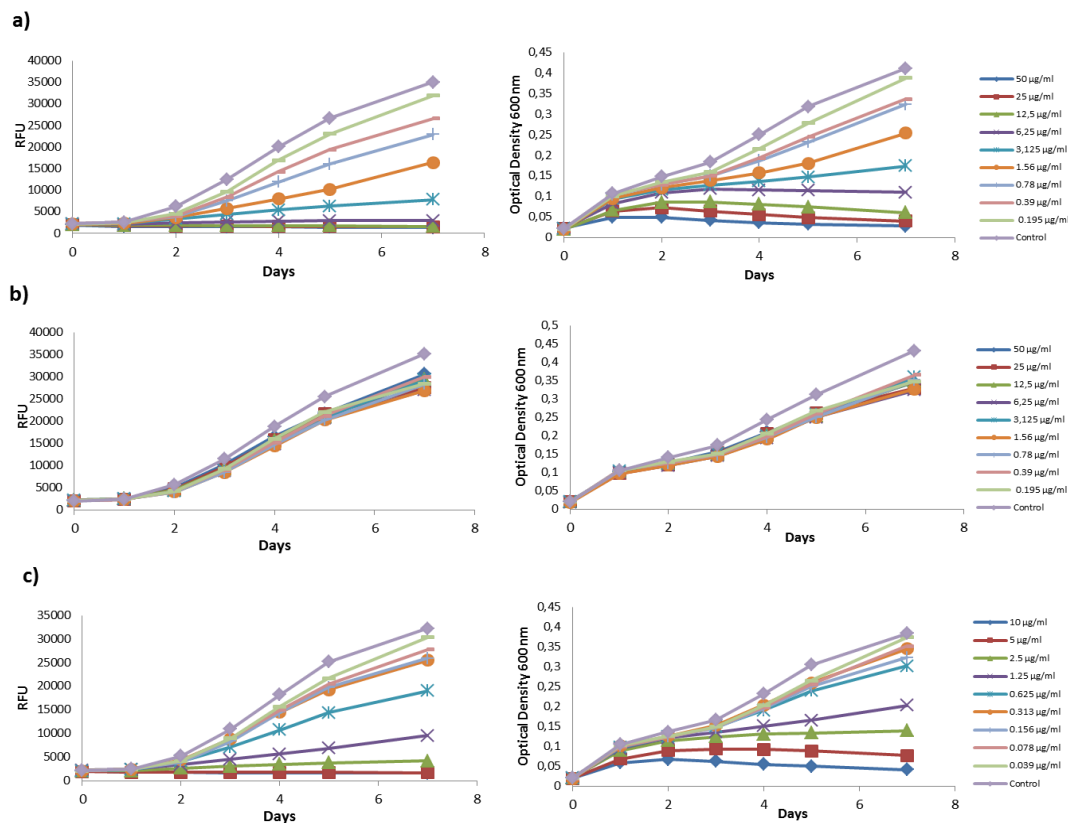
Figure 2.1.Growth kinetics of *M. tuberculosis* expressing GFP to serial two fold dilutions of three antibiotics.Growth kinetic curves were determined by fluorescence intensity (left) and Optical Density at 600nm (right), during 7 days. A) Amikacin B) Hygromycin B and C) Kanamycin. RFU express relative fluorescence units. Blank medium wells were used as a background subtraction for all sample test wells and bacterial control wells.

Table 2.1. Minimum inhibitory concentrations (MIC) of 3 antibiotics against *M. tuberculosis* H37Ra expressing GFP determined by fluorescence intensity (FI) and OD600 after 7 days incubation.

Antibiotic	MIC (µg/ml)	
	RFU	OD_{600}
Amikacin	6,25	25
Hygromycin B	>50	>50
Kanamycin	5	10
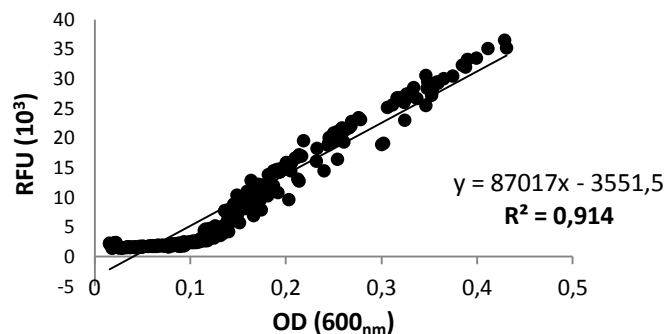
Figure 2.2. Fluorescent Intensity is correlated with OD600 for quantification of *M. tuberculosis* H37Ra expressing GFP. Linear correlation between relative fluorescence unit (RFU) and optical density at 600 nm of *M. tuberculosis* expressing GFP. These two different methods were used to monitor bacterial growth in the presence of antibiotics. Data corresponds to the values obtained with all drugs used in the assay. ($p < 0,05$ by Pearson Product Moment Correlation).

Testing the method for evaluating the anti-mycobacterial activity of new Pyrazinoic acid esters.

To evaluate the relevance of GFP as a reporter for mycobacterial growth we tested the biological activity of new pyrazinoic acid esters in broth cultures. Pyrazinoic acid derivatives, such as esters, may be used to overcome *M. tuberculosis* resistance attributed to *pncA* gene mutations. The pncA gene encodes the pyrazinamidase essential for converting pyrazinamide (PZA) to its active form pyrazinoic acid (POA) [10]. Previous studies showed that long chain esters of POA have adequate plasma and rat liver homogenate stability and can easily be activated by esterases other than pyrazinamidase to liberate POA [11].

In order to test the feasibility of the fluorescence intensity method to determine the antimicrobial effect of new drugs against mycobacteria expressing GFP we determined the MICs of twenty eight pyrazinoic acid ester derivatives (Supplemental information). For this purpose serial two-fold dilutions of each compound was used

with a load of 10^6 mycobacteria per ml and incubated for 5 days. The growth inhibition of each compound was assessed by measuring FI of the GFP emission by mycobacteria. All compounds were screened for growth inhibitory activity against a drug-susceptible strain the avirulent *Mycobacterium tuberculosis* H37Ra (Table 2.2).
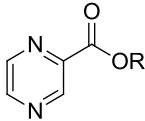
Our results show that all compounds possess higher activity against *M. tuberculosis* H37Ra than PZA or POA in the same experimental conditions. Compounds **3g**, **4h** and **4i** are the most active, with MIC's ranging between 0,085 and 0,095 nM. On the other hand, compounds 5a, 4a, 5d and 5c were the less active with MIC ranging from 1,1 to 1,9 nM.

The Lateral chain length and lipophilicity of pyrazinoic acid derivatives affects their biological activity

Overall, the lateral chain length of pyrazinoic acid derivatives was moderately correlated with the biological activity against *M. tuberculosis* (R^2=0,558; Pearson correlation; p<0,05) (Figure 2.3). However, in the case of pyrazinoic acid derivatives from primary alcohols we observed a strong correlation between the length of the lateral chain with the biological activity (R^2=0,761; Pearson correlation; p<0,05) (Figure 2.4).

We observed the same trend of biological activity in lipophilicity of pyrazinoic acid derivatives tested, with and moderate correlation of all compounds (Figure 2.5; R^2=0,551; Pearson correlation; p<0,05) and a strong correlation of lipophilicity of pyrazinoic acid derivates from primary alcohols and biological activity (Figure 2.6; R^2=0,769; Pearson correlation; p<0,05). Association between lipophilicity and biological activity might be explained by a better diffusion of more lipophilic compounds through the lipidic mycobacterial cell wall barrier [12].

Table 2.2. Minimum Inhibitory Concentration for pyrazinoic acid derivatives against _M. tuberculosis_ H37Ra.

Compound	R	MIC (mM)	pMIC
PZA	$NH_{2(*)}$	3,249	-0,512
POA	H	3,223	-0,508
3a	C_5H_{11}	0,515	0,288
3b	C_6H_{13}	0,96	0,018
3c	C_7H_{15}	0,45	0,347
3d	C_8H_{17}	0,846	0,072
3e	C_9H_{19}	0,2	0,7
3f	$C_{10}H_{21}$	0,378	0,422
3g	$C_{11}H_{23}$	0,09	1,047
4a	$CH(CH_3)_2$	1,204	-0,08
4b	$CH(CH_3)C_2H_5$	0,555	0,256
4c	$CH(CH_3)C_5H_{11}$	0,45	0,347
4d	$CH(CH_3)C_6H_{13}$	0,423	0,373
4e	$CH(CH_3)C_6H_{13}$	0,847	0,072
4f	$CH(CH_3)C_6H_{13}$	0,424	0,373
4g	$CH(CH_3)C_7H_{15}$	0,2	0,7
4h	$CH(CH_3)C_8H_{17}$	0,095	1,024
4i	$CH(CH_3)C_{10}H_{21}$	0,085	1,068
5a	$C(CH_3)_3$	1,11	-0,045
5b	$C(CH_3)_2C_2H_5$	1,03	-0,013
5c	$C(CH_3)_2C_3H_7$	1,921	-0,283
5d	$C(CH_3)_2C_4H_9$	1,8	-0,255
5e	$C(CH_3)_2C_5H_{11}$	0,846	0,072
6a	$CH_2CH(CH_3)_2$	0,555	0,256
6b	$CH_2CH(CH_3)C_2H_5$	1,03	-0,013
6c	$C_2H_4C(CH_3)_2$	0,515	0,288
6d	C_4H_8Cl	0,93	0,031
6e	C_6H_5	0,5	0,301
6f	C_6H_{11}	0,485	0,314
6g	$(CH_3)C_6H_{10}$	0,908	0,041

(*) instead of OR

42
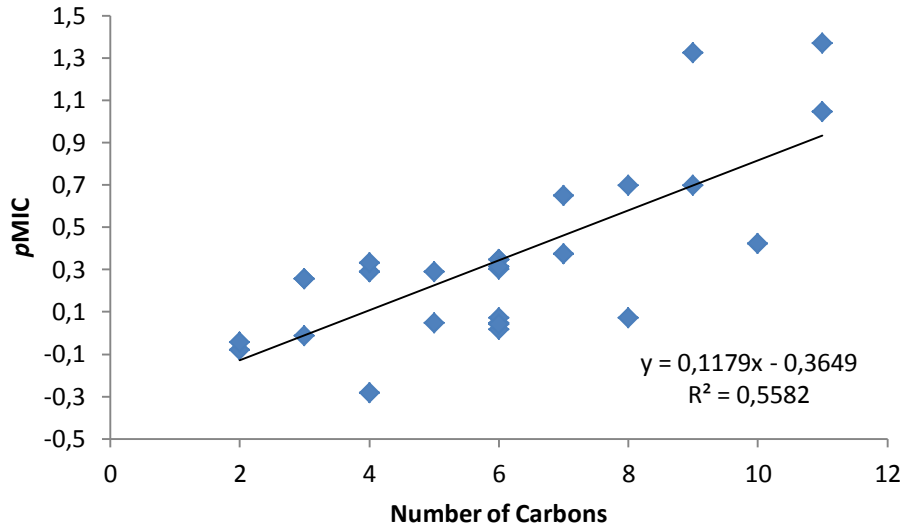
Figure 2.3. Correlation between the number of carbons of the alkyl chain of pyrazinoic acid esters and biological activity in *M. tuberculosis.* (pMIC, biologic activity; R^2=0,558; Pearson correlation; p<0,05).
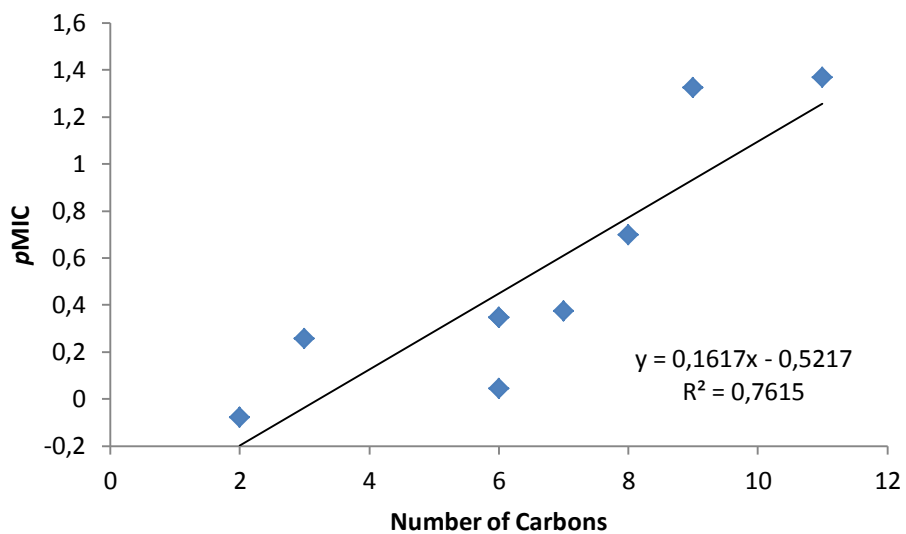
Figure 2.4. Correlation between the number of carbons of the of first order alkyl chain pyrazinoic acid esters and biological activity in *M. tuberculosis.* (pMIC, biological activity; R^2=0,761; Pearson correlation; p<0,05).
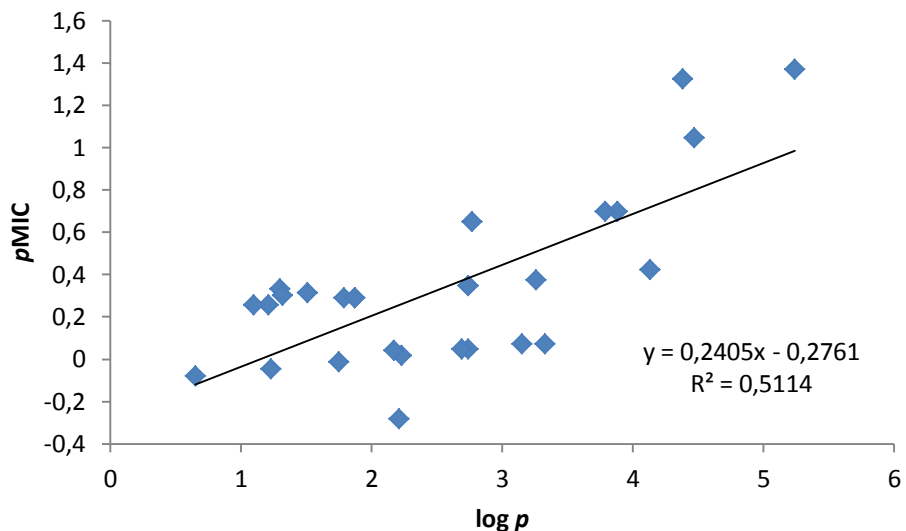
Figure 2.5. Correlation between the lipophilicity of the first order alkyl chain of pyrazinoic acid esters and biological activity in *M. tuberculosis*. (pMIC, biological activity; log *p*, lipophilicity; R^2=0,511; Pearson correlation; p<0,05).
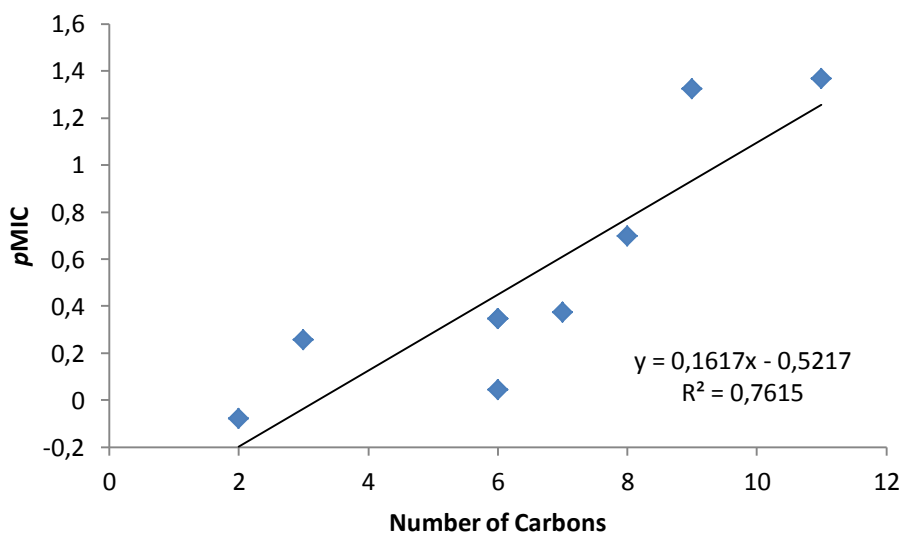
Figure 2.6. Correlation between the lipophilicity of the of pyrazinoic acid esters biological activity in *M. tuberculosis*. (pMIC, biological activity; log *p*, lipophilicity; R^2=0,769; Pearson correlation; p<0,05).

Fluorescence intensity of tdTomato allows *M. tuberculosis* quantification *in vitro*

Although the FI measurement of GFP expressing mycobacteria was useful for quantification of *M. tuberculosis in vitro* we were unable to use this fluorescent protein to quantify intracellular *M. tuberculosis*. This might be due to the interference of autofluorescence from the bacteria sample in the GFP emission channel [13]. To overcome this problem we decided to use a red shifted fluorescent protein: tdTomato one of the brightest red fluorescent proteins available with a bright fluorescence in the red part of the light spectrum [14,15] using *M. tuberculosis* expressing tdTomato, and THP-1 cells expressing eGFP a brighter mutant of GFP [16].

To test if fluorescence intensity of tdTomato could be used to quantify *M. tuberculosis* in our *in vitro* settings, two fold serial dilutions of a mycobacterium inoculum was measured by fluorimetry and the results were compared with the optical density at 600nm (OD_{600}) method commonly used to quantify mycobacteria[8]. The results show a strong statistical correlation (r^2=0,99; p<0,05) between both methods suggesting a positive linear relationship between values in fluorescent intensities and the number of bacilli in the broth culture. This point for a great potential of fluorescent intensity for an accurate quantification of mycobacteria in broth cultures (Figure 2.7). The quantification of *M. tuberculosis* by means of tdTomato fluorescence intensity had already been address by others with similar results [15].

The chart shows a linear regression with the equation:

$$y = 277451x + 351{,}73$$
$$r^2 = 0{,}99$$

X-axis: OD_{600nm} (values 0,00 to 0,12)
Y-axis: RFU ($\times 10^3$) (values 0 to 30)
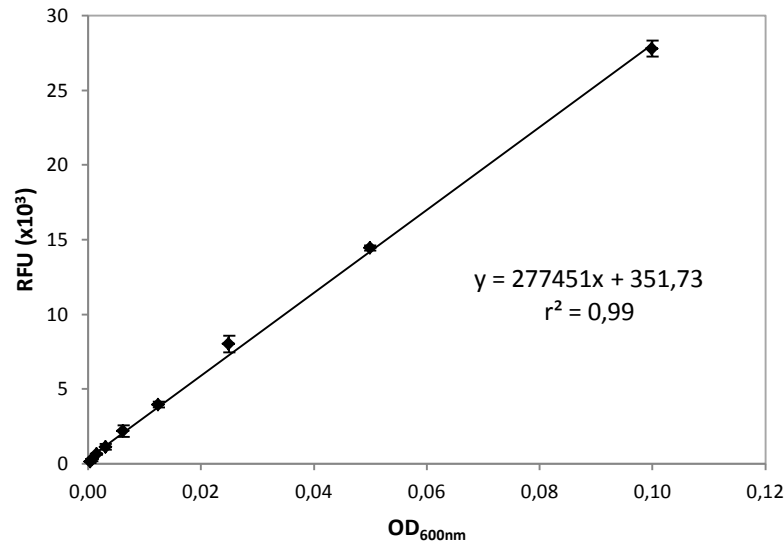
Figure 2.7. Quantification of *M. tuberculosis* H37Ra tdTomato by fluorescence (RFU) and optical density (OD600nm). Data is represented as the mean of RFU (excitation 554, emission 586, gain 200) ± standard deviation of three replicates for each OD600nm value. Wells with tissue culture medium were used as blanks for RFU. The line represents a linear regression between RFU and OD600nm (r2=0.9986; p<0.05 by Pearson Correlation).

Fluorescence intensity of eGFP allows THP-1 quantification *in vitro*

To address if we could quantify the number of THP-1 cells using fluorescent intensity, we transduced THP-1 cells with the plasmid pLEGO-G2 for suitable expression of eGFP. Different numbers of cells were seeded and differentiated into macrophages using black 96 well plates. Following incubation with alamar blue reagent (resazurin), resazurin is commonly used to quantify viable cells, the results were compared with eGFP fluorescent intensities.

As shown in the Figure 2.8, the eGFP intensity was strongly correlated with the THP-1 cell number (r^2=0,98; p<0,05). Nevertheless, there was a reduced sensitivity, compared with alamar blue (r^2=0,98; p<0,05), to a total amount of cells below 12×10^3 in 96 well plates.
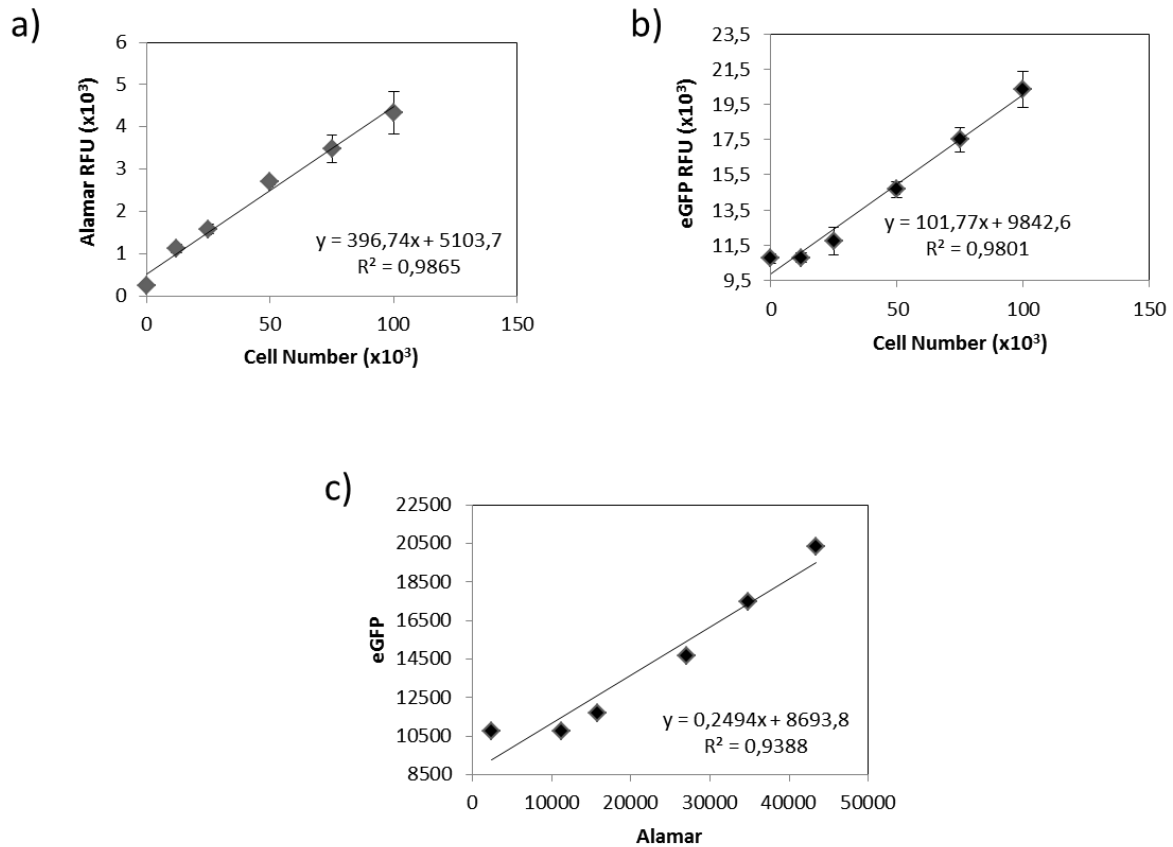
Figure 2.8. The eGFP intensity is a good reporter of THP-1 viability. Different known number of eGFP expressing THP-1 cells were plated and differentiated with PMA in 96 well plate and quantified by a) alamar blue or b) eGFP fluorescence. Both variables were correlated c) (R^2=93,8; Pearson correlation; p<0,05;n=3).

Although less sensitive for very low cell numbers (12×10^3 cells) eGFP fluorescent intensities were strongly correlated to the alamar blue labelled ones (r^2=0,93; p<0,05). The data on eGFP fluorescent intensity shows that this fluorescent reporter can be used to quantify THP-1 cell numbers above 12×10^3. A relation between GFP intensity and cell number has been already described in chinese hamster ovary (CHO) cells [17].

Intracellular *M. tuberculosis* and macrophage viability can be assessed by fluorescence intensity

To address if the above results had any significance in the context of *M. tuberculosis* macrophage infection, we combined the eGFP expressing THP-1 cells with tdTomato expressing mycobacteria in our infection model. After 3 hour pulse, at define time-points after infection, both host cells and mycobacteria fluorescent intensities were recorded and cells were lysed and plated to quantify mycobacteria by CFU. The data presented in the Figure 2.9 shows the results from such experiments.
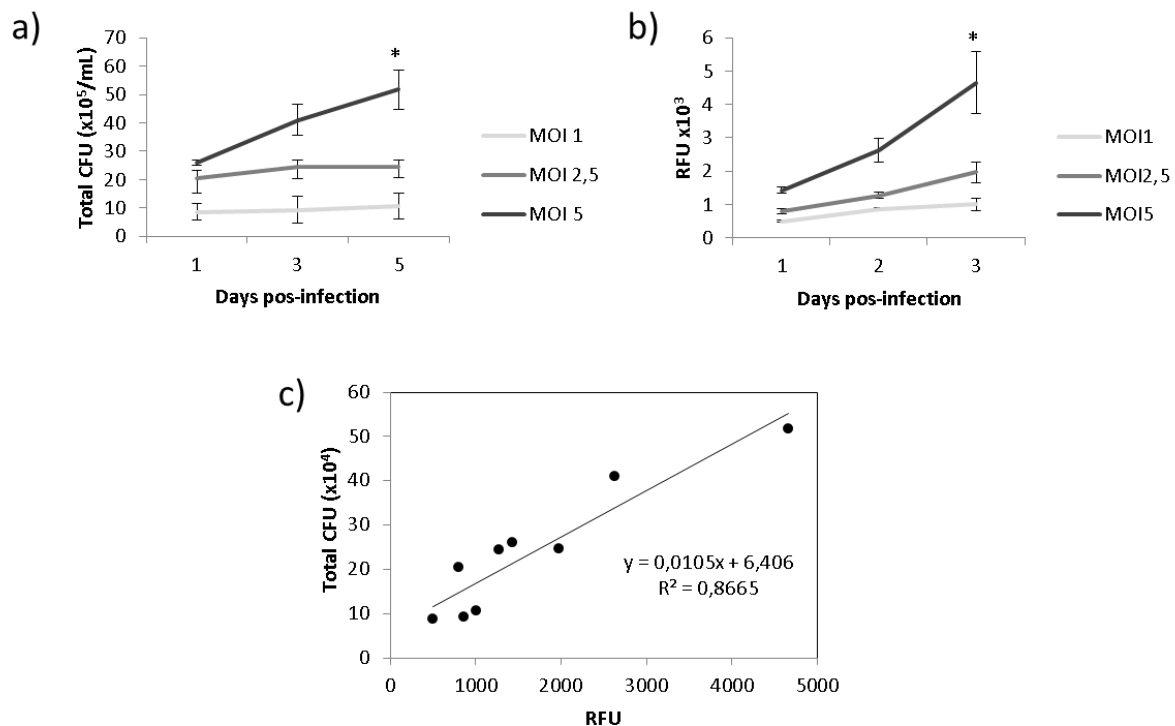
Figure 2.9. Quantification of intracellular *M. tuberculosis* by colony forming units and Fluorescent intensity in THP-1 cells. a) Effect of different MOI in the kinetics of intracellular survival of *M. tuberculosis* by CFU and RFU. At a MOI 5 the *M. tuberculosis* burden significantly increased between day 1 and 5 post-infection C) Correlation between the average values of CFU and RFU for the different time-points post-infection. Values are in mean±SD (*p<0,05; t-test; n=3) MOI, multiplicity of infection.

The survival kinetics of the mycobacteria determined either by fluorescence intensities or CFU shows that the numbers of intracellular *M. tuberculosis* H37Rv are dependent of the initial MOI (Figure 2.9. a and b). In the condition of THP-1 infection with a MOI 5, an increase of fluorescent intensity and CFU over the 5 days of infection was observed, with significant differences between the day 1 and day 5 (t-test: p<0,05). For a MOI 1 or 2,5 the intracellular *M. tuberculosis* load is maintained over the 5 days of infection. At lowest MOIs, THP-1 cells can restrict *M. tuberculosis* growth, with a concomitant rate of replication. The variability in fluorescence intensity of *M. tuberculosis* bacilli is greatly explained by the CFU (Figure 2.9 c) with a strong correlation between the two methodologies (r^2=0,86; p<0,05).This positive linear relationship suggests that fluorescence intensity is dependent of intracellular *M. tuberculosis* expression of tdTomato is a phenotype of the number of viable bacilli within macrophages.

Comparing the results obtained from FI and CFU on day 5 post-infection (Figure 2.10) the FI of tdTomato (Figure 2.10 a) shows enough sensitivity to detect differences between the different MOIs used and the non-infected samples (NI) similar to those obtained by CFU.
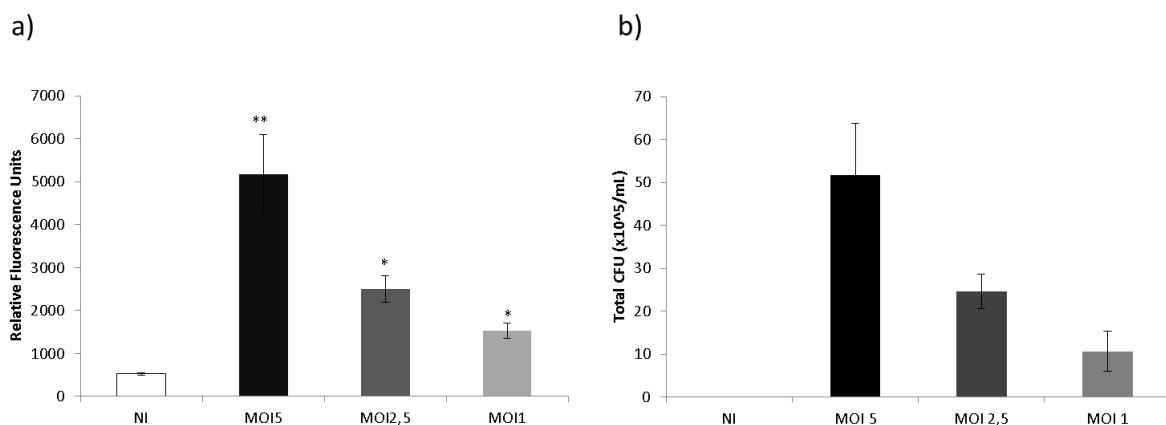
Figure 2.10. Comparison between fluorimetry and CFU counting to quantify *M. tuberculosis* H37Rv in THP-1 cells.THP-1 macrophages were infected with *M. tuberculosis* H37Rv (tdTomato) at MOI 1, 2.5 and 5. a) RFU (excitation 554, emission 586, gain 200) at day 5 post-infection. b) CFU at day 5 post-infection. Data are represented as the mean ± standard deviation of three replicates (ANOVA; Holm-Sidak; p<0.05; n=3). *p<0.05 and ** p<0.001 comparatively to NI (non-infected cells).

The cell viability of the infected cells varies throughout infection and is dependent on the MOI used (Figure 2.11). Nevertheless, there is an increase in fluorescent intensity throughout the experiment time (Figure 2.11a). This may be attributed to artefacts that results from the accumulation of eGFP proteins in the cells or in opposition may reflect proliferation of THP-1 cells after phorbol esters (PMA) withdraw, this reagent was used for macrophage differentiation. THP-1 cell viability at a MOI 1 remained similar to those in the uninfected cells. However, this viability, decreased at higher MOIs, being around one third lower at MOI 5 when compared to of uninfected cells (Figure 2.11b).
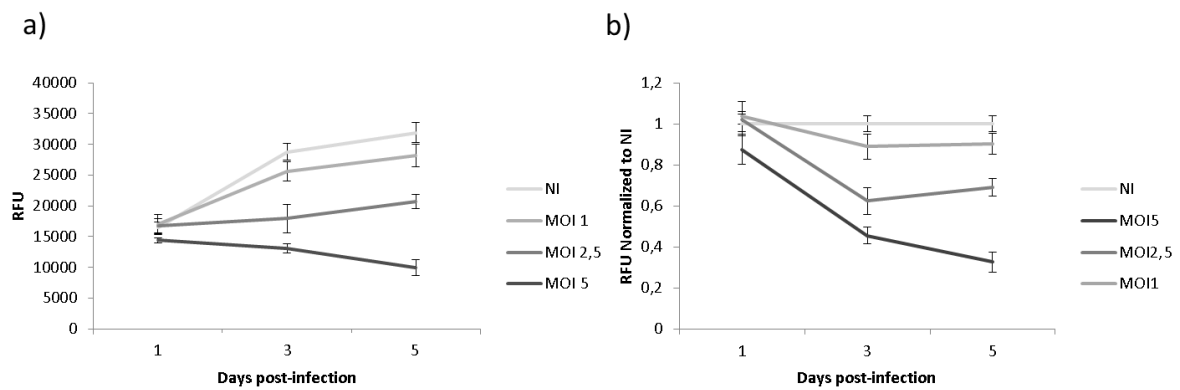
Figure 2.11. Macrophage viability of *M. tuberculosis* infected THP-1 cells by fluorescent intensity. Cells were infected at different multiplicities of infection (MOI) with *M. tuberculosis* and were monitored throughout the following five days post-infection. a) Raw RFU; b) Data normalized to non-infected samples (NI); data Values are in mean±SD; n=3.

Discussion

Broth cultures of *M. tuberculosis* are commonly used for anti-tubercular drug screening. In this work we showed that fluorescence intensity of both GFP and tdTomato can be an alternative method to OD for quantification of mycobacterial growth inhibition (Figure 2.1 and Figure 2.7). In order to confirm this we tested the biological activity of 3 conventional antibiotics and new PZA derivatives, twenty eight pyrazinoic acid esters, as alternative anti-tubercular drugs. All pyrazinoic acid esters tested in this study were demonstrated to be more active against *M. tuberculosis* H37Ra than PZA or POA (Table 2.2). All together our results indicates that the *in vitro* system for quantifying fluorescent mycobacteria has good correlation with the conventional methods such the OD_{600} and the CFU and was demonstrated to be accurate for evaluation of the antimicrobial effect of new drugs.

A major drawback observed during development of the fluorimetric methodology was the impossibility to quantify the effect of pyrazinoic acid esters in intracellular *M. tuberculosis* using our human macrophage model. This may be due to the use of DMSO and/or to the characteristics of the compounds. Nevertheless, this methodology might be useful to identify host factors involved in *M. tuberculosis* macrophage intracellular survival.

In this work we applied fluorescence based methodologies for quantification of intracellular *M. tuberculosis* that can be used as an alternative to traditional CFU. Fluorescence based methods for cell quantification and viability do not requires co-factors as for luciferase assays, or dyes such as resazurin. Furthermore these methods implicate macrophage disruption for substrate quantification or as in the case of CFU, for intracellular bacteria release for plating in culture petri dishes.

Moreover, most fluorescent proteins are small, and have low cell toxicity and are continuously synthesized, which minimizes the effect of fluorescence signal dilution during cell replication [18]. A broad range of fluorescent proteins variants that span

nearly the entire visible spectrum, permits multi-reporter fluorescence [19]. Additionally, this method can be applied for other intracellular pathogens and their host cells.

Replication of *M. tuberculosis* within human macrophages ultimately causes cell death [20]. We observed an increased macrophage cell death with an increase on the MOI used. Similar results on the effect of the initial inoculum in the infection kinetics and cell viability have been published in primary monocyte-derived human macrophages (MDHM) [20]. Welin and co-workers reported that the replication restriction in low inoculation experiments did not led to acquisition of CD63, a maker for fusion of phagosomes with late endosomes and lysosomes but led to acidification and cathepsin D recruitment. In the same report the authors show that increasing *M. tuberculosis* load led to decreasing HMDM viability.

Recently an HTS based microscopic phenotypic assay based on fluorescently labelled *M. tuberculosis* within fluorescently labelled macrophages has been published for drug and genomic screening [21]. Our method outstands on the cost-effectiveness of the detector instrument and using GFP expressing THP-1 cells, does not need time point labelling of cells. Effective methods for the evaluation of intracellular pathogens in their physiological survival niches are important for future research on host-pathogen interactions and will enable screening of compounds, pathogen and host factors that may impair intracellular growth of pathogens in a cost-effective manner.

Material and Methods

Pyrazinoic acid esters

Compounds

The pyrazinoic acid esters used in this study are listed in supplementary information (Table S2.1) and were synthetized in the Professor Luís Constantino's laboratory, Faculty of Pharmacy, University of Lisbon, Portugal.

Determination of compound lipophilicity

Compound lipophilicity (log P) was determined by the logarithm of the partition coefficient, the ratio of concentrations of un-ionized compound in the two phases of water and octanol at equilibrium[22].

Determination of minimum inhibitory concentrations (MIC)

Minimum inhibitory concentrations for the compounds tested were performed by using the broth micro- dilution method [23]. Solutions of each compound were prepared by first dissolving in dimethyl sulfoxide (DMSO; Sigma-Aldrich) to a concentration of 400 µg /ml and then further diluting in the respective culture media. Serial two-fold dilutions were made in 96-well microplates with concentrations ranging from 400 µg/ml to 12,5 µg/ml for each compound. Each well was inoculated with bacterial suspension at a concentration of 10^6 CFU/ml. No inhibitory effects were observed in the presence of DMSO at the concentrations used (1.25%). Isoniazid (Sigma-Aldrich) was used as a reference drug. *Mycobacterium tuberculosis* H37Ra ATCC 25177 harbouring the pMN042 plasmid was incubated in microplates

in appropriate broth medium for 5 days. Following this period they were observed under a light microscope to determine the lowest concentration with no visible mycobacterial growth. The results were confirmed by measuring the optical density at 600 nm and fluorescence intensity (488nm excitation; 520nm emission; gain 200) in a Infinite M200 plate spectrophotometer (Tecan). Due to the inference in compound molecular weight values the MIC concentrations were determined by conversion to molarity.

Bacteria strains maintenance

The avirulent *M. tuberculosis* strain H37Ra (25177™, ATCC) and H37Ra harboring pMN437 plasmid for expression of eGFP2+ [24], was a kind gift of Dr Michael Niederweis of the Microbiology Department of the Alabama University, USA and the virulent *M. tuberculosis* strain H37Rv (25618™, ATCC) were maintained in Middlebrook's 7H9 broth medium (Becton, Dickinson and Company) supplemented with 10% (v/v) OADC (Becton, Dickinson and Company), 0.5% (v/v) glycerol (Sigma-Aldrich) and 0.05% (v/v) Tyloxapol (Sigma-Aldrich) at 37°C with stirring (mycobacterial medium). *M. tuberculosis* H37Ra and H37Rv strains harboring pAsta3 plasmid (Add gene ID: 24657) [15], for expression of codon optimized for expression of mycobacteria gene for tdTomato fluorescent protein under the control of the Psmyc promoter and hygromycin B resistance selector gene were cultured in the same medium supplemented with 50 µg/ml hygromycin B (Sigma-Aldrich) for selection. All manipulations of *M. tuberculosis* were performed in a Biosafety Level 3 environment.

Cell lines

THP-1 cells (ATCC TIB-202)[25] were grown in RPMI media 1640 (GIBCO) supplemented with 10% (v/v) Fetal Bovine Serum (GIBCO), 1% (v/v) Penicillin-Streptomycin (GIBCO), 1% (v/v) Pyruvate (GIBCO), 1% (v/v) L-Glutamine (GIBCO), 1% (v/v) Non-essential aminoacids (GIBCO), 1% (v/v) Hepes buffer (GIBCO). Human Embryonic Kidney 293T (HEK 293T) cells (ATCC CRL-11268) [26] were grown in Dulbecco's modified Eagle's medium (DMEM, GIBCO) supplemented with 10% (v/v) Fetal Bovine Serum (GIBCO), 1% (v/v) Penicillin-Streptomycin (GIBCO). Cells were kept at 37ºC under a 5% carbon dioxide (CO^2) atmosphere.

Mycobacterial electroporation and Generation of a tdTomato expressing H37Rv and H37Ra

M. tuberculosis H37Ra and H37Rv electroporation was made using a method developed elsewhere [27]. Briefly, mycobacteria were grown in mycobacterial medium at 37°C with stirring until $0,5 \leq OD_{600nm} \geq 1$. In order to obtain electrocompetent cells, bacterial suspension was incubated on ice for 90 minutes to improve the transformation efficiency and centrifuged at 3000xg for 10 minutes. The pellet was washed 3 times in ice-cold 10% glycerol, reducing to half of the washing volume each time. After these treatment electrocompetent mycobacteria was stored at -80°C in 20% glycerol until further use.

A mixture containing electrocompetent mycobacteria and 1µg pAsta3 (Figure 2.12) plasmid DNA was left on ice for 10 minutes and transferred to a 0.2 cm electrode-gap electroporation cuvette. The cuvette was placed subjected to one single pulse of 1.8 kV, 25 µF, 200 Ω and then placed on ice for 10 minutes. The transformants were inoculated into mycobacterial medium and incubated at 37°C for 36 h. Mycobacterial

cells were harvested by centrifugation at 3000x*g* for 10 minutes and plated out suitable dilutions on mycobacterial solid medium containing Middlebrook's 7H10 agar (Becton, Dickinson and Company), 0,5% (v/v) glycerol and 10% (v/v) OADC. Mycobacterial red fluorescence was confirmed by fluorescence microscopy after 2 to 3 weeks of incubation at 37°C. Red fluorescent positive colonies were inoculated in mycobacterial broth medium with 50 µg/ml hygromycin B and incubated with stirring at 37°C. The transformants were frozen in 20% glycerol at -80°C [15].
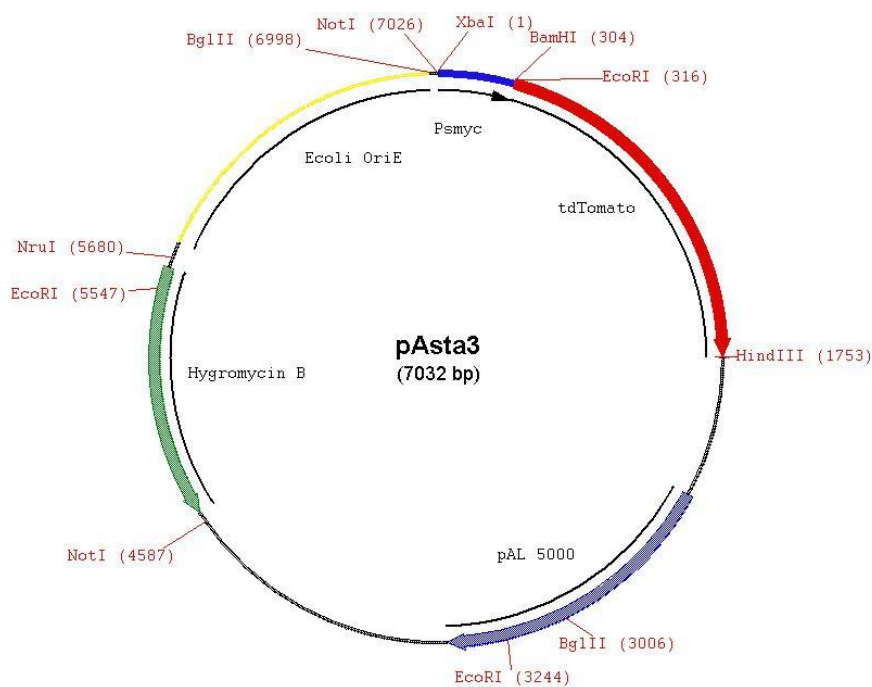
Figure 2.12. pASTA3 plasmid map. pASTA3 plasmid is a vector suitable for mycobacterial expression of a mycobacterial codon-optimised tdTomato fluorescent protein in pSMT3-S. Psmyc, strong mycobacterial promoter; tdTomato, inserted gene that codifies tandem dimmer tomato, a red fluorescent protein; pAL5000, mycobacterial replicon; Hygromycin B, hygromycin B resistance gene for bacterial selection; Ecoli OriE: *E. coli* origin of replication.[15]

Generation and quantification of eGFP expressing THP-1

Lentivirus Production

For generation of a THP-1 expressing enhanced Green Fluorescent Protein (eGFP) we used the lentiviral plasmid the LEGO-vector LeGO-G2, derived from pLentiLox3.7 developed at the MIT HIV-1, a kind gift from Dr. Kristoffer Riecken from the University of Hamburg, School of Medicine and University Hospital of Hamburg-Eppendorf, Germany. This is a fourth generation lentiviral vector for suitable cell marking, with a blasticidin selection cassette. The eGFP transcription is regulated by SFFV promoter (Figure 2.13).
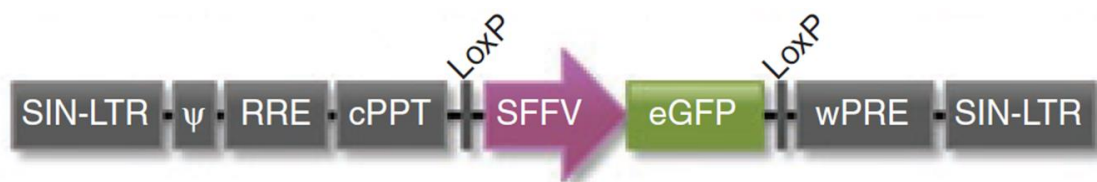
Figure 2.13. Lentivirus Vector Gene Ontology LeGo-G2 detail. LeGo-G2 is a lentiviral vector expressing enhanced green fluorescent protein (eGFP) as a single removable marker gene (using Loxp/Cre system) and a SFFV promoter to ensure sufficient detection. The plamid carries a Blasticidin selection gene. SIN-LTR, self-inactivating-long-terminal-repeat; RRE, rev-responsive element; cPPT, central polypurine tract; SFFV, promoter of spleen focus-forming virus; wPRE, Woodchuck hepatitis virus post-transcriptional regulatory element.[28]

Lentivirus were produced according Moura-Alves *et al* [29,30]. Briefly, HEK 293T cells were seeded at a density of 2.2×10^5 cells/ml (100 μl per well in 96 well plates) in DMEM media without Penicillin-Streptomycin. After 24 hours incubation at cell culture normal conditions, cells were transfected with a mixture of the 3 plasmids, the packaging plasmid (100 ng of pCMV-dR8.91), the envelope plasmid (10 ng of VSV-G/pMD2.G) and 100 ng of the pLeGo-G2 vector, using Fugene HD transfection reagent (Promega) in Optimem medium (GIBCO). After 18 hours of incubation, media was replaced with 170 μl of high serum growth media (30% FBS (v/v) DMEM). Twenty-four hours after media replacement, viruses were harvested (150 μl) and fresh media (150 μl) was added to the cells. The second viral collection was

performed 24 hours later and harvested viruses were pooled with the previous day collection and stored at -80ºC.

Lentiviral transduction of THP-1 cells

Lentiviral transduction was performed according what is described by Pedro Moura-Alves *et al.* [29] Briefly, 10 µl of lentivirus were plated per well in a round bottom 96 well plate. THP-1 cells were resuspended in RPMI medium containing 8 ug/ml of Polybrene (Sigma-Aldrich) at a density of 1.25×10^6 cells/ml, and 40 µl were added on top of the virus containing wells. Plates were spun for 90 minutes at 900xg at 37ºC. After spinoculation, media was removed and replaced with 200 µl of fresh RPMI, and cells incubated at 37ºC under normal cell culture conditions. After 2 days, transduced cell selection was performed by replenish 200 µl of RPMI media containing Blasticidin (Sigma-Aldrich) to a final concentration of 25 ug/ml and selection pressure was maintained for 2 weeks.

Infection procedures

Mycobacterial preparation

Prior to any experiment, infection or broth cultures, mycobacterial cultures at mid log grow phase were centrifuged at 3000xg, 37°C for 10 minutes, washed in Phosphate buffer saline (PBS) pH 7.4 (Gibco) and, in the case of infection experiments, resuspended in in RPMI media 1640 (Gibco) supplemented with 10% (v/v) Fetal Bovine Serum (Gibco), 1% (v/v) Pyruvate (Gibco), 1% (v/v) L-Glutamine (Gibco), 1% (v/v) Non-essential aminoacids (Gibco), 1% (v/v) Hepes buffer (Gibco). To obtain a single-bacillus suspension the medium with the bacilli was passed 20 times through a sterile syringe equipped with a 21 gauge needle, followed by 15 minutes of ultrasonic. The remaining bacterial clumps were eliminated by centrifugation at 350xg for 1 minute and single-cell suspension was verified by light microscopy.

Mycobacterial infection of THP-1 macrophages

All infection experiments were made with RPMI media without phenol or antibiotics. THP-1 cell densities were quantified using a Neubawer chamber. For infection experiments we added $7,5x10^4$ THP-1 cells/well in a black polystyrene 96 wells plate (Corning) and incubated them with 20 nM of phorbol 12-myristate 13-acetate (PMA) (Sigma-Aldrich) RPMI media without phenol for 24 hours for differentiation into macrophages. After this period, cells were allowed to rest in PMA free media for another 24 hours.

In the day of infection, the macrophage media was discarded and was added 100 µl of single bacilli suspensions. The macrophages were infected with H37Rv in at different multiplicities of infection (MOI), proportion of mycobacteria/macrophage. After a specific pulse period, the macrophages were washed with warm media. After washing, 200 µl/well of media containing 10 µg/ml of gentamicin was added, to kill extracellular bacteria. Cells we incubated for 24 hours and replenish with 200 µl/well of media containing no antibiotics. It have been reported that at this range of concentration gentamicin does not accumulate in THP-1 cells and any intracellular gentamicin is also rapidly inactivated [34,35].

Data acquisition and analysis

Quantification of intracellular *M. tuberculosis* by colony forming units

After defined time points post-infection, infected macrophages were washed with PBS and incubated with 0,05% (v/v) solution of IGEPAL at normal cell incubation conditions, for 10 minutes. Serial 10 fold dilutions were made with sterile distilled water, and plated Middlebrook's 7H10 solid medium (Becton, Dickinson and Company) supplemented with 10% (v/v) OADC (Becton, Dickinson and Company),

0.5% (v/v) glycerol (Sigma-Aldrich). Plates were incubated at 37°C for 3 weeks. Microcolonies were count with the help of an optical microscope.

Quantification of eGFP expressing THP-1

Quantification of eGFP expressing THP-1 cells was made using an Infinite M200 spectrophotometer (Tecan). Different number of THP-1 cells were plated in a black polystyrene 96 wells plate and incubated with 20nM of phorbol 12-myristate 13-acetate (Sigma-Aldrich) in RPMI media for 24 hours for differentiation into macrophages. After this period of differentiation, cells were allowed to rest in PMA free media for another 24 hours. After the resting period, cells fluorescence was measured at 488nm excitation and 520nm emission and a gain of 175. Cell media formulation is descried in cell lines maintenance; however we used phenol free and no antibiotics RPMI (Gibco). These settings were also use in the quantification of mycobacterium infected cells. Alternatively, after differentiation THP-1 cells number was also assessed by resazurin fluorescence intensity using alamarBlue (Molecular Probes) following the manufacturer's instructions. Briefly, 10% (v/v) of alamarBlue reagent was added to each well and incubated for 4 h at normal cell conditions. Fluorescence was measure at and excitation of 570nm and emission of 595nm, and a gain of 100.

Quantification of mycobacteria by fluorimetry

Quantification of *M. tuberculosis* H37Ra and H37Rv, harbouring pASTA3 or pMN042, in broth cultures was made by spectrophotometry of absorption and fluorescence in an Infinite M200 spectrophotometer (Tecan). Optical density at 600nm (OD_{600nm}) was measured to determine mycobacterial concentration ($OD600nm=0.1$ is equivalent to $1x10^7$ bacteria/ml) [33]. For Minimum Inhibitory Concentration determination (MIC) experiments, 200µl of 0,01 OD_{600} of *M. tuberculosis* H37Ra or H37Rv bearing the pASTA3 plasmid in different compound concentration. Pyrazinoic acid esters were a kind gift of Professor Luis Constantino,

60

Faculty of Pharmacy, University of Lisbon, Lisbon, Portugal. Hygromycin B (Gibco), Amykacin and Kanamycin (Sigma-Aldrich) were used has controls. After several days of incubation at 37°C fluorescent quantification of mycobacteria was made using spectrophotometer Infinite M200 (Tecan). Fluorescence was measured at an excitation of 554 nm, an emission of 586 nm and a gain of 150 for broth cultures. These settings were also used to quantify intracellular *M. tuberculosis*.

Statistical treatment

The software SigmaPlot 12.0 (*Systat Software Inc.*) was used for statistical analysis. *Student's t-test* was used for comparing two means multiple means comparison was made using one-way ANOVA. To make multiple comparisons versus control group was used the Holm-Sidak method. The differences were considered statistically significant when $p < 0.05$. To determine the correlation between two variables a linear regression was used as well as a Pearson Product Moment Correlation.

References

1. Pawlowski A, Jansson M, Sköld M, Rottenberg ME, Källenius G. Tuberculosis and HIV co-infection. Hobman TC, ed. *PLoS Pathog*. 2012;8(2):e1002464. 4.

2. WHO. *Global tuberculosis report 2013*. Geneva, Switzerland: World Health Organization; 2013.

3. Hartkoorn RC, Chandler B, Owen A, et al. Differential drug susceptibility of intracellular and extracellular tuberculosis, and the impact of P-glycoprotein. *Tuberculosis (Edinb)*. 2007;87(3):248–55.

4. Chanwong S, Maneekarn N, Makonkawkeyoon L, Makonkawkeyoon S. Intracellular growth and drug susceptibility of Mycobacterium tuberculosis in macrophages. *Tuberculosis (Edinb)*. 2007;87(2):130–3.

5. Chatterjee A, Saranath D, Bhatter P, Mistry N. Global transcriptional profiling of longitudinal clinical isolates of Mycobacterium tuberculosis exhibiting rapid accumulation of drug resistance. Dheda K, ed. *PLoS One*. 2013;8(1):e54717.

6. Pethe K, Sequeira PC, Agarwalla S, et al. A chemical genetic screen in Mycobacterium tuberculosis identifies carbon-source-dependent growth inhibitors devoid of in vivo efficacy. *Nat Commun*. 2010;1:57.

7. Day RN, Davidson MW. The fluorescent protein palette: tools for cellular imaging. *Chem Soc Rev*. 2009;38(10):2887–921.

8. Peñuelas-Urquides K, Villarreal-Treviño L, Silva-Ramírez B, Rivadeneyra-Espinoza L, Said-Fernández S, de León MB. Measuring of Mycobacterium tuberculosis growth. A correlation of the optical measurements with colony forming units. *Braz J Microbiol*. 2013;44(1):287–9.

9. Srivastava R, Deb DK, Srivastava KK, Locht C, Srivastava BS. Green fluorescent protein as a reporter in rapid screening of antituberculosis compounds in vitro and in macrophages. *Biochem Biophys Res Commun*. 1998;253(2):431–6.

10. Marttila HJ, Marjamäki M, Vyshnevskaya E, et al. pncA mutations in pyrazinamide-resistant Mycobacterium tuberculosis isolates from northwestern Russia. *Antimicrob Agents Chemother*. 1999;43(7):1764–6.

11. Simões MF, Valente E, Gómez MJR, Anes E, Constantino L. Lipophilic pyrazinoic acid amide and ester prodrugs. *Eur J Pharm Sci*. 2009;37(3):257–263.

12. Lambert P a. Cellular impermeability and uptake of biocides and antibiotics in gram-positive bacteria and mycobacteria. *Symp Ser Soc Appl Microbiol*. 2002;(31):46S–54S.

13. Billinton N, Knight AW. Seeing the wood through the trees: a review of techniques for distinguishing green fluorescent protein from endogenous autofluorescence. *Anal Biochem*. 2001;291(2):175–97.

14. Deliolanis NC, Kasmieh R, Wurdinger T, Tannous B a, Shah K, Ntziachristos V. Performance of the red-shifted fluorescent proteins in deep-tissue molecular imaging applications. *J Biomed Opt*. 2008;13(4):044008.
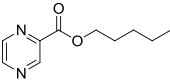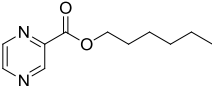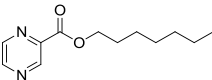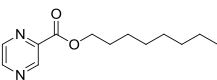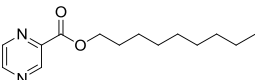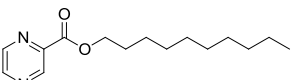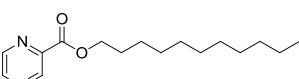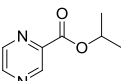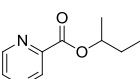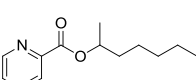
15. Carroll P, Schreuder LJ, Muwanguzi-Karugaba J, et al. Sensitive detection of gene expression in mycobacteria under replicating and non-replicating conditions using optimized far-red reporters. *PLoS One*. 2010;5(3):e9823.

16. Zhang G, Gurtu V, Kain SR. An enhanced green fluorescent protein allows sensitive detection of gene transfer in mammalian cells. *Biochem Biophys Res Commun*. 1996;227(3):707–11.

17. Hunt L, Jordan M, De Jesus M, Wurm FM. GFP-expressing mammalian cells for fast, sensitive, noninvasive cell growth assessment in a kinetic mode. *Biotechnol Bioeng*. 1999;65(2):201–5.

18. Müller-Taubenberger A, Anderson KI. Recent advances using green and red fluorescent protein variants. *Appl Microbiol Biotechnol*. 2007;77(1):1–12.

19. Kremers G-J, Gilbert SG, Cranfill PJ, Davidson MW, Piston DW. Fluorescent proteins at a glance. *J Cell Sci*. 2011;124(Pt 2):157–60.

20. Welin A, Raffetseder J, Eklund D, Stendahl O, Lerm M. Importance of phagosomal functionality for growth restriction of Mycobacterium tuberculosis in primary human macrophages. *J Innate Immun*. 2011;3(5):508–18.

21. Queval CJ, Song O-R, Delorme V, et al. A microscopic phenotypic assay for the quantification of intracellular mycobacteria adapted for high-throughput/high-content screening. *J Vis Exp*. 2014;(83):e51114.

22. Smith DA, Allerton C, Kalgutkar AS, Waterbeemd H, Walker DK. *Pharmacokinetics and Metabolism in Drug Design (Methods and Principles in Medicinal Chemistry)*. Wiley-VCH; 2012:268.

23. Sethi S, Mandal J, Kumar P, et al. Susceptibility testing of Mycobacterium tuberculosis by broth microdilution method: a rapid alternative method. *Diagn Microbiol Infect Dis*. 2007;57(4):447–9.

24. Steinhauer K, Eschenbacher I, Radischat N, Detsch C, Niederweis M, Goroncy-Bermes P. Rapid evaluation of the mycobactericidal efficacy of disinfectants in the quantitative carrier test EN 14563 by using fluorescent Mycobacterium terrae. *Appl Environ Microbiol*. 2010;76(2):546–54.

25. Tsuchiya S, Yamabe M, Yamaguchi Y, Kobayashi Y, Konno T, Tada K. Establishment and characterization of a human acute monocytic leukemia cell line (THP-1). *Int J Cancer*. 1980;26(2):171–176.

26. Pear WS, Nolan GP, Scott ML, Baltimore D. Production of high-titer helper-free retroviruses by transient transfection. *Proc Natl Acad Sci U S A*. 1993;90(18):8392–6.

27. Goude R, Parish T. Electroporation of mycobacteria. *Methods Mol Biol*. 2009;465:203–15.

28. Weber K, Bartsch U, Stocking C, Fehse B. A multicolor panel of novel lentiviral "gene ontology" (LeGO) vectors for functional gene analysis. *Mol Ther*. 2008;16(4):698–706.

29. Moura-Alves P, Neves-Costa A, Raquel H, et al. An shRNA-based screen of splicing regulators identifies SFRS3 as a negative regulator of IL-1β secretion. *PLoS One*. 2011;6(5):e19829.

30. Moffat J, Grueneberg DA, Yang X, et al. A lentiviral RNAi library for human and mouse genes applied to an arrayed viral high-content screen. *Cell*. 2006;124(6):1283–98.

31. Carryn S, Van Bambeke F, Mingeot-Leclercq M-P, Tulkens PM. Comparative intracellular (THP-1 macrophage) and extracellular activities of beta-lactams, azithromycin, gentamicin, and fluoroquinolones against Listeria monocytogenes at clinically relevant concentrations. *Antimicrob Agents Chemother*. 2002;46:2095–2103.

32. Carryn S, Van Bambeke F, Mingeot-Leclercq M-P, Tulkens PM. Activity of beta-lactams (ampicillin, meropenem), gentamicin, azithromycin and moxifloxacin against intracellular Listeria monocytogenes in a 24 h THP-1 human macrophage model. *J Antimicrob Chemother*. 2003;51(4):1051–2.

33. P. Bettencourt, D. Pires NC and EA. Application of Confocal Microscopy for Quantification of Intracellular Mycobacteria in Macrophages. In: Díaz M-V and J, ed. *Microscopy: Science, Technology, Applications and Education*. ©FORMATEX.; 2010:614–621.

34. Carryn S, Van Bambeke F, Mingeot-Leclercq MP, Tulkens PM. Comparative intracellular (THP-1 macrophage) and extracellular activities of beta-lactams, azithromycin, gentamicin, and fluoroquinolones against Listeria monocytogenes at clinically relevant concentrations. Antimicrob Agents Chemother. 2002 Jul;46(7):2095-103.

35. Carryn S, Van Bambeke F, Mingeot-Leclercq MP, Tulkens PM. Activity of beta-lactams (ampicillin, meropenem), gentamicin, azithromycin and moxifloxacin against intracellular Listeria monocytogenes in a 24 h THP-1 human macrophage model. J Antimicrob Chemother. 2003 Apr;51(4):1051-2.
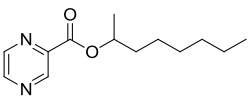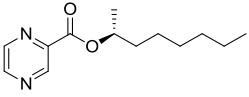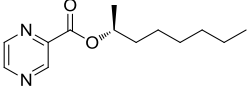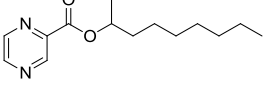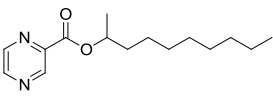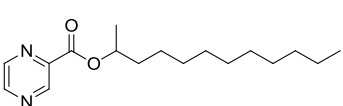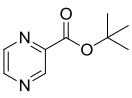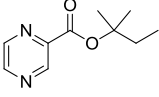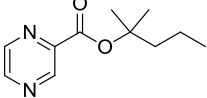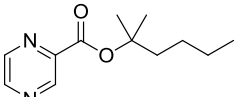
Supplementary information

Table S 2.1. Name, structure and code of the pyrazinoic acid esters used in this study.

Compound	Structure	Code
pentyl pyrazinoate		3a
hexyl pyrazinoate		3b
heptyl pyrazinoate		3c
octyl pyrazinoate		3d
nonyl pyrazinoate		3e
decyl pyrazinoate		3f
undecyl pyrazinoate		3g
isopropyl pyrazinoate		4a
sec-butyl pyrazinoate		4b
1-methyl hexyl pyrazinoate		4c
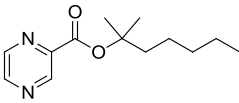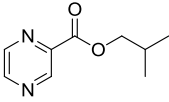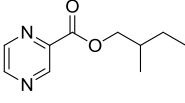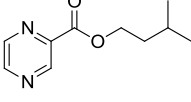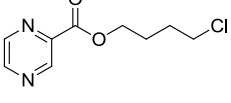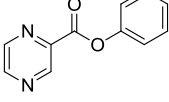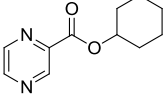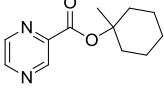
1-methyl heptyl pyrazinoate		4d
R-(-)-1-methyl heptyl pyrazinoate		4e
S-(+)-1-methyl heptyl pyrazinoate		4f
1-methyl octyl pyrazinoate		4g
1-methyl nonyl pyrazinoate		4h
1-methyl undecyl pyrazinoate		4i
tert-butyl pyrazinoate		5a
1,1-dimethylpropyl pyrazinoate		5b
1,1-dimethylbutyl pyrazinoate		5c
1,1-dimethylpentyl pyrazinoate		5d

1,1-dimethylhexyl pyrazinoate		5e
iso-butyl pyrazinoate		6a
2-methylbutyl pyrazinoate		6b
isopentyl pyrazinoate		6c
4-chlorobutyl pyrazinoate		6d
phenyl pyrazinoate		6e
cyclohexyl pyrazinoate		6f
methylcyclohexyl pyrazinoate		6g

Chapter 3

Vesicular traffic genes involved in *Mycobacterium tuberculosis* macrophage infection

Vesicular traffic genes involved in *Mycobacterium tuberculosis* macrophage infection.

Abstract

Mycobacterium tuberculosis is a facultative intracellular pathogen that is able to survive within phagosomes, endosomal vesicles of human phagocytes such as macrophages. The success of *M. tuberculosis* relies on the subversion of the host vesicular traffic events in order to provide the access to nutrients and, in parallel to inhibit the delivery of microbicidal factors to the bacterial containing phagosome. Rab GTPases and SNAREs are proteins that coordinate the trafficking and fusion of cellular vesicles and these are potential targets to be manipulated by *M. tuberculosis* virulence factors. To decipher the role of individual Rabs and SNARES on the intracellular survival of *M. tuberculosis* we developed a high trough put assay based on a dual fluorescent reporter assay that enables the quantification of intracellular mycobacteria and the viability of the infected macrophages along the time.

Using this approach we identified a total of 10 host genes that interfered with intracellular *M. tuberculosis* survival including seven Rab GTPases, two SNAREs and one Rab effector. The silencing of Rab7 and Rab43 led to an increase in *M. tuberculosis* survival within macrophages while the knockdown of two SNAREs, MSD032 and Stx4, five Rabs (Rab27a, Rab31, Rab34, Rab39B and Rab8) and the Rab effector RABEP1 a resulted in a reduction of mycobacteria cellular burden. Our study highlights the potential impact host vesicular traffic in the survival/persistence of intracellular *M. tuberculosis*.

Introduction

Phagocytosis is an evolutionary conserved mechanism that evolved from a nutritional function in primitive unicellular organisms. In higher organisms it occurs mainly in specialized cells, *i.e.* phagocytes and lies at the center of the immune response, providing an innate route for destruction of pathogens, antigen presentation and inflammation [1–3]. Phagocytosis is a highly regulated and complex cellular mechanism in which pathogen detection triggers their internalization in a membrane bound vesicle: the phagosome. Newly formed phagosomes undergoes a maturation process leading to modification in membrane and lumen that lead to the formation of a highly microbicidal organelle: the phagolysosome [4]. During this highly dynamic and complex process the phagosome interacts by a series of fission and fusion events with several organelles [5–7]. At the end of this trafficking pathway phagosomes become competent to fuse with late endosomes and lysosomes, acquiring proteolytic and antimicrobial properties, a mechanism called phagolysosome biogenesis.

Rab GTPases and SNARES are major players directing vesicle traffic and fusion, that regulate phagosome formation, maturation and phagolysosome biogenesis [5]. Upon microorganism attachment to macrophage membrane receptors, a cup formation is provided allowing the sealing, of the nascent phagosome that will consequently fuse with early endosomes [8] by a process modulated by Rab5 [9]. The Rab5 effector, early endosome antigen 1 (EEA1) binds to Stx13 providing a bridge to early endosome fusion [10,11]. Phagosomal bound Rab5 rapidly decreases with the concomitant enrichment of EEA1 allowing Rab7 to reach the maturating phagosome, a phenomena named phagosomal Rab conversion [12]. Consequently Rab7 bound phagosomes associates with Stx7 promoting fusion with late endosomes and lysosomes [11]. After acquisition of Rab7 the phagolysosome biogenesis is accelerated by recruitment of Rab interacting lysosomal protein (RILP) to the phagosome [13].

Mycobacterium tuberculosis is the causative agent of tuberculosis and its success relies, on its ability to avoid destruction by the immune system, surviving and

replicating mostly inside immune cells that are designed to destroy invading microorganisms: macrophages [14]. Presently is though that virulent mycobacteria are able to modulate their internalization and arrest phagosome maturation, avoiding delivery of microbicidal effectors and therefore sustaining intracellular persistence and replication [15]. Several Rab GTPases and SNAREs have been shown to be differentially recruited to *M. tuberculosis* containing phagosomes when compared to avirulent bacteria or latex beads-containing phagosomes [16,17]. It was previously though that *M. tuberculosis* phagosome was blocked on the Rab5-Rab7 stage of phagosome maturation [18]. However, recently it has been shown that Rab7 is initially associated with the *M. tuberculosis* phagosome but is subsequently released, limiting the recruitment of cathepsin D and RILP [19]. Several other Rab GTPases namely Rab14 and Rab22a were also demonstrated to associate with *M. tuberculosis* containing phagosomes preventing phagosomal maturation [20,21]. Recently, Setto *et al.* compared the recruitment of Rab GTPases to phagosomes containing mycobacteria to those containing *Staphylococcus aureus* [16] and observed that Rab proteins associated with *M. tuberculosis* and *S. aureus* were similar. However, with the exception of Rab22b and Rab43, those responsible for cathepsin D recruitment and phagosomal acidification were progressively excluded from *M. tuberculosis* phagosomes. The authors propose a model in which Rab GTPases regulates phagosome maturation and the recruitment of those proteins is modulated by *M. tuberculosis* during inhibition of phagolysosome biogenesis.

Another work by Fratti *et al.* showed that BGC containing phagosomes retain Stx13 and degrades VAMP3 during mycobacterial infection [17]. In neutrophils Stx4 has been described to be retained together with Rab5 in *M. tuberculosis* phagosomes in order to maintain the maturation block [22]. Indeed, in macrophages Stx4 is retained in phagosomes containing phosphatidylinositol mannoside (PIM)-coated latex beads, whereas a decreased accumulation of this SNARE is observed in phagosomes containing just uncoated inert beads. Since PIM is a mycobacterial glycolipid that diffuses and incorporates into host cell endomembranes, these findings indicate that PIM contributes to the fusion of *M. tuberculosis*-containing phagosomes with endosomal compartments, by retention of Stx4 in the phagosomal membrane [23]. Although, several Rab GTPases and SNAREs have been associated differentially to the *M. tuberculosis* containing phagosomes their role on the pathogen survival has

not been yet demonstrated. Certainly for Rab22a, while a RNAi knockdown enhance maturation of *M. tuberculosis* containing phagosome through increase acquisition of Rab7, no significant effect on intracellular *M. tuberculosis* survival was observed [20].

The standard method for quantification of intracellular *M. tuberculosis* involves laborious, time consuming and expensive quantification of colony forming units (CFU) and implicates de destruction of the sample (the infected host cells, in a tissue culture well plate) at a defined time point. The factors affecting accuracy of this method have been identified for more than one century [24]. Specifically, CFU quantification of slow growing mycobacteria provides the additional challenge of an incubation of several weeks. The lack of a fast, sample friendly and reliable alternative technique for intracellular quantification of *M* tuberculosis halted higher throughput studies on factors affecting intracellular *M. tuberculosis* survival/persistence.

The identification of GFP from Aequorea and the subsequent expansion in the identification of different fluorescent proteins (FP) through GFP mutagenesis or in other organisms led to a "revolution" in cell biology [25]. The ability to monitor live cellular mechanisms without cell toxicity or the need of adding any cofactor make these proteins perfect reporters of cell and organism viability.

In this work we proposed to dissect the role of macrophages vesicular traffic proteins in *M. tuberculosis* infection. In order to achieve this we developed a dual fluorescent assay profiting from mycobacteria and human macrophages expressing two different fluorescent proteins (tdTomato and eGFP respectively). Likewise, the dual fluorescence assay provided means to quantify intracellular *M. tuberculosis* and, simultaneously, macrophage viability during infection along time and using the same sample.

In order to identify macrophage vesicular traffic genes with a role in *M. tuberculosis* infection we performed a RNAi based screen. A lentiviral library shRNAs enriched in shRNAs targeting vesicular traffic genes were used to generate loss-of-function phenotypes for those genes. We silenced the expression of around 120

vesicular traffic genes and quantified tdTomato and eGFP fluorescence after 5 days post infection.

Our results show that vesicular traffic genes modulation affects *M. tuberculosis* survival/persistence and affects differently virulent and avirulent mycobacteria strains.

Results

Vesicular traffic genes affect intracellular *M. tuberculosis* macrophage load

In an attempt to identify the vesicular traffic genes involved in *M. tuberculosis* macrophage infection, we have performed RNAi-based screen to systematically silence around 120 genes (listed at Table S3.1 on Supplementary Information) that have already been reported to be involved in intracellular vesicular traffic. This collection of genes was mainly constituted by Rab GTPases and SNAREs but included also some Rab effectors and other vesicular traffic genes. The screening outline is presented on Figure 3.1.

THP1 human monocytic cells stably expressing eGFP were transduced with lentiviral vectors for expression of shRNA targeting a specific gene by RNAi and the positive clones were selected with puromycin. Next, we differentiated the transduced THP-1 cells to macrophages using phorbol 12-myristate 13-acetate (PMA). For infection of transduced macrophages a multiplicity of infection (MOI) of 1 was used (meaning 1 bacillus to 1 cell). Five days post-infection, the fluorescence intensities of both tdTomato, the intracellular M. tuberculosis reporter and, the eGFP, the macrophage viability reporter were recorded for each tested silenced gene of the THP-1 clone library. Samples with an eGFP fluorescent lower than half of the control samples were discarded from the analysis. In order to present the data of all screen, Z-scores calculation were made using the Equation 3.1.

$$Zscore = \frac{AVG(RFU_{shRNA}) - AVG(RFU_{SCR})}{SDV_{SCR}}$$

Equation 3.1. Z-score calculation. Z-score was calculated by the difference of the mean of each shRNA targeting a genes ($AVG(RFU_{shRNA})$) and the mean of the control samples ($AVG(RFU_{SCR})$) divided by the standard deviation of the control samples (SDV_{SCR}).

The results of the screening are shown in Figure 3.2. Genes were considered candidates as having an effect on intracellular *M. tuberculosis* if at least two shRNAs possessed a tdTomato fluorescence increase or decrease that was 2,5 standard deviations from the average of the control (scramble: SCR, a shRNA construct that does not targets any protein mRNA). After several rounds of validation we identified a total of 21 candidate genes with a reduction of the fluorescence observed for 18 genes while an increase was detected in 3 (Table 3.1).
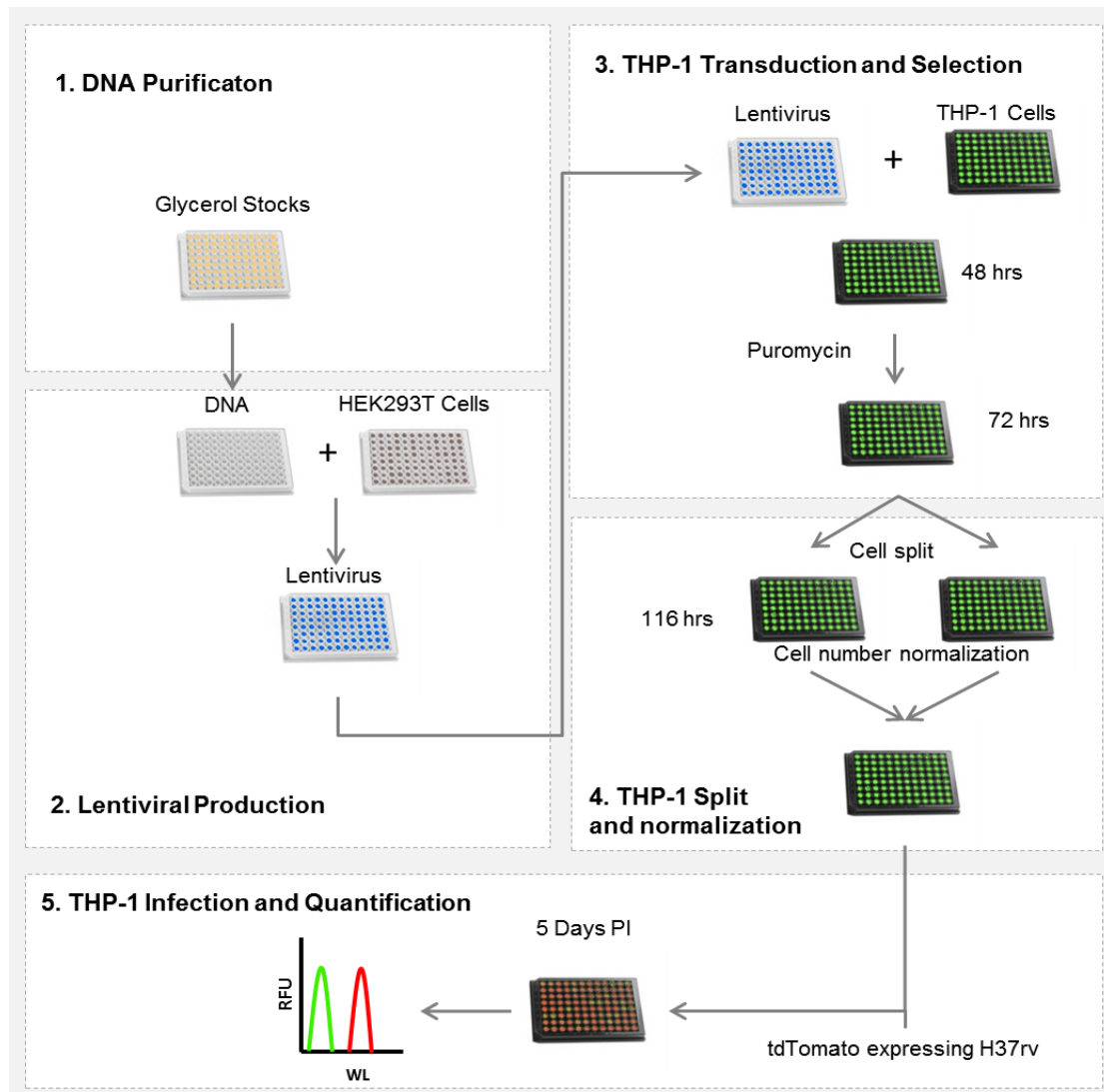
Figure 3.1. Lentiviral production and RNAi based screening outline. Lentiviral library was kept in glycerol stocks at -80°C. **1.** Bacterial stocks transformed with the pLKO.1 plasmids encoding the gene interference hairpins were incubated at 37°C and plasmid DNA was purified by a high through put plasmid purification protocol. **2.** The 293t cells were transfected with a library generated of pLKO.1 and the packaging plasmids, pCMV-dR8.91 (Delta 8.9) plasmid encoding gag, pol and rev genes and pCMV-VSV-G plasmid encoding envelope, to produce the lentiviral vectors. **3.** Lentiviruses were used to transduce THP-1 cells as describe in methods. **4.** After puromycin selection of the transduced cells, each 96 well plate was split and further incubated for 116 hrs. THP-1 cells were count by cytometry and $75x10^3$ per well were seeded in black 96 well plates. **5.** Cells were differentiated with PMA and infected with tdTomato expressing H37Rv at a MOI of 1. Five days post-infection fluorescence intensities of either the cells (eGFP) or the mycobacteria (tdTomato) were recorded.
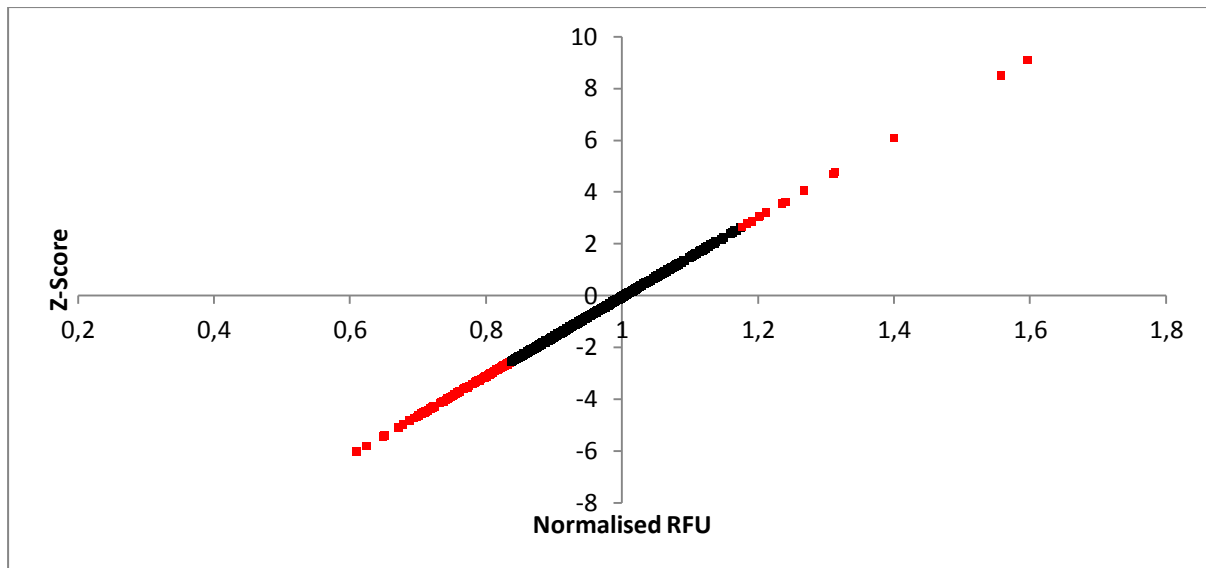
Figure 3.2. Identification of vesicular traffic genes with an effect on intracellular *M. tuberculosis* by RNAi screen. Around 120 vesicular traffic genes were targeted in THP-1 cells by lentiviral shRNA delivery. Five days post-infection intracellular *M. tuberculosis* expressing tdTomato fluorescence was measured (excitation: 554nm; emission: 586; gain: 200). In the y-axis the average fluorescence intensities of each shRNA sample were subtracted by the average of scramble control and divided by the standard deviation of the scramble. In the x-axis the control normalised fluorescence intensities of each shRNA. Highlighted in red the shRNAs with more than 2,5 standard deviations of the control.

Validation of candidate genes obtained in the RNAi screen

Following the RNAi-based screen, and in order to validate if the results observed were due to effective knockdown of a certain gene, the respective mRNA was quantified by qRT-PCR. The knock down efficiency was calculated comparing the expression level of a shRNA from a gene of interest with the level of expression of that gene in control cells. A candidate gene was considered validated if the average level of knock down was higher than 35%. In Figure 3.3 are represented the different values for tdTomato RFU and respective knockdown for the shRNAs validated by qRT-PCR. Table 3.2 summarizes the list of the validated candidates, their classification and function.

Table 3.1. List of candidate genes with potential effect on *M. tuberculosis* intracellular burden.
Resistance genes are those whose silencing leads to an increase of fluorescence and therefore to bacilli survival, while the susceptibility genes have the opposite effect with an effect on bacilli killing.

Susceptibility Genes	Resistance Genes
MDS032	RAB7A
RAB3A	RAB42
RABGAP1	RAB43
RAB7B	
RAB7L1	
RAB8A	
RAB11FIP3	
RAB24	
RAB27A	
RAB31	
RAB33A	
RAB34	
RAB39B	
RABEP1	
RABGGTA	
SNAP23	
STX4	
VAMP2	
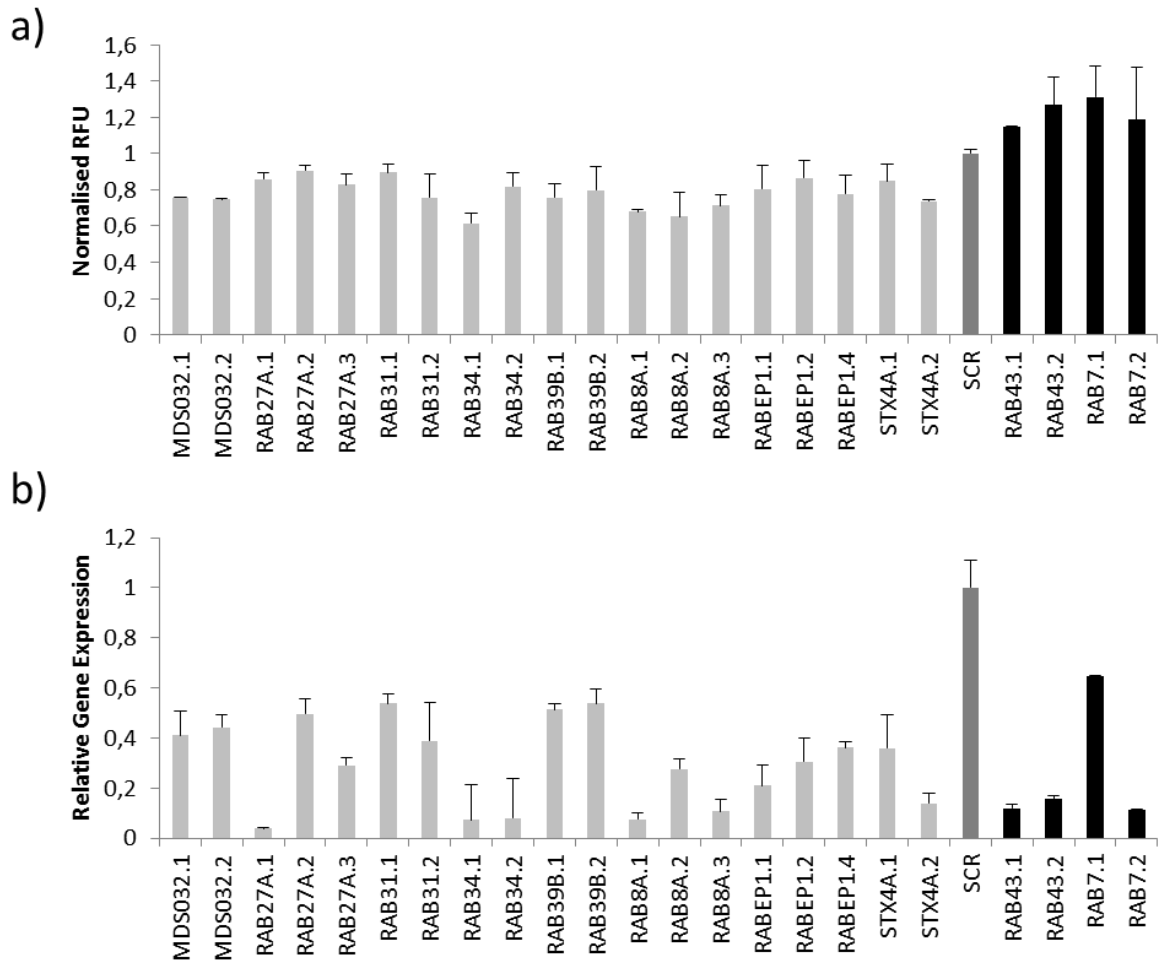
Figure 3.3. Knock down validation of vesicular traffic genes obtained from the shRNA screen.
a) Relative fluorescence intensity determined on tdTomato infected and silenced THP1 cells, for the validated candidates. b) Relative gene expression of the knockdown efficiency for the candidate vesicular traffic genes determined by qRT-PCR. The gene expression relative levels for each candidate gene was normalised relatively to control cells.

Table 3.2. List of validated susceptibility and resistance genes that affect the intracellular *M. tuberculosis* burden and predicted cellular function.

Susceptibility genes	Classification – Function/Subcellular localization
MDS032	SNARE - Golgi-ER transport [26]
RAB27A	Rab GTPase – Lysosomes, Melanosome transport [27]
RAB31	Rab GTPase – early endosomes, Cathepsin D recruitment to phagosomes [16]
RAB34	Rab GTPase – Golgi, Cathepsin D recruitment to phagosomes [16]
RAB39B	Rab GTPase – Golgi, unknown[28].
RAB8A	Rab GTPase – Golgi, Phagosome, unknown function [16]
RABEP1	Rab effector - Homotypic endosome fusion and trafficking of recycling endosomes[29]
STX4	SNARE - Plasma membrane, t-SNARE that mediates docking of transport vesicles[30]

Resistance Genes	
RAB7	Rab GTPase – late endosomes/lysosomes, Phagosome recruitment of cathapsin D and phagosomal acidification. [16]
RAB43	Rab GTPase – ER-Golgi Transport , Phagosome recruitment of cathepsin D.[16]

Biological characterization of vesicular traffic genes involved in *M. tuberculosis* infection

To further biologically validate the susceptibility or resistance genes obtained from Table 3.2 with the effectiveness of gene silencing we did a comparison on the quantification of intracellular *M. tuberculosis* survival obtained by RFU with the results of the gene expression. In addition to validate the RFU results we performed in parallel the quantification of intracellular mycobacteria by CFU. Figure 3.4 summarizes the results obtained from RFU and CFU quantification after infection of THP-1 cells that were knocked down for Rab7, Rab34, Stx4 and Rab14. The results indicate a similar trend between the RFU and the CFU and are supported by the mRNA expression of the selected genes. Also, the figure 3.4 shows the main phenotypes observed. For instance, Rab7 knockdown led to an increase in both tdTomato RFU and CFU as expected while in the case of Rab34 and Stx4 the RNA silencing led to a decrease in intracellular mycobacteria. Surprisingly the Rab14 knockdown had no effect on the amount of intracellular *M. tuberculosis.*

Since avirulent species and strains of *M. tuberculosis* complex are usually used in host-pathogen interactions studies, all over the world, we asked whether the knockdown of the validated genes (Figure 3.4) had similar effect on the strain *M. tuberculosis* H37Ra. The results of macrophage knockdown and posterior infection with *M. tuberculosis* H37Ra are summarized in figure 3.5. For both strains Rab7 knockdown induced an increased survival a indicating a clear role in *M. tuberculosis* intracellular clearance. However for all remaining tested genes contradictory phenotypes were observed. This is the case of Rab34 knockdown were an increased survival of the avirulent strain is detected, in opposition to what is observed for *M. tuberculosis* H37Rv. The knockdown of Rab14 induces a reduction on the amounts of avirulent mycobacteria while no effect was found for virulent *M. tuberculosis.* Similarly, Stx4 knockdown reduced the survival of virulent mycobacteria while with the avirulent *M. tuberculosis* no differences to the control samples were shown.

82
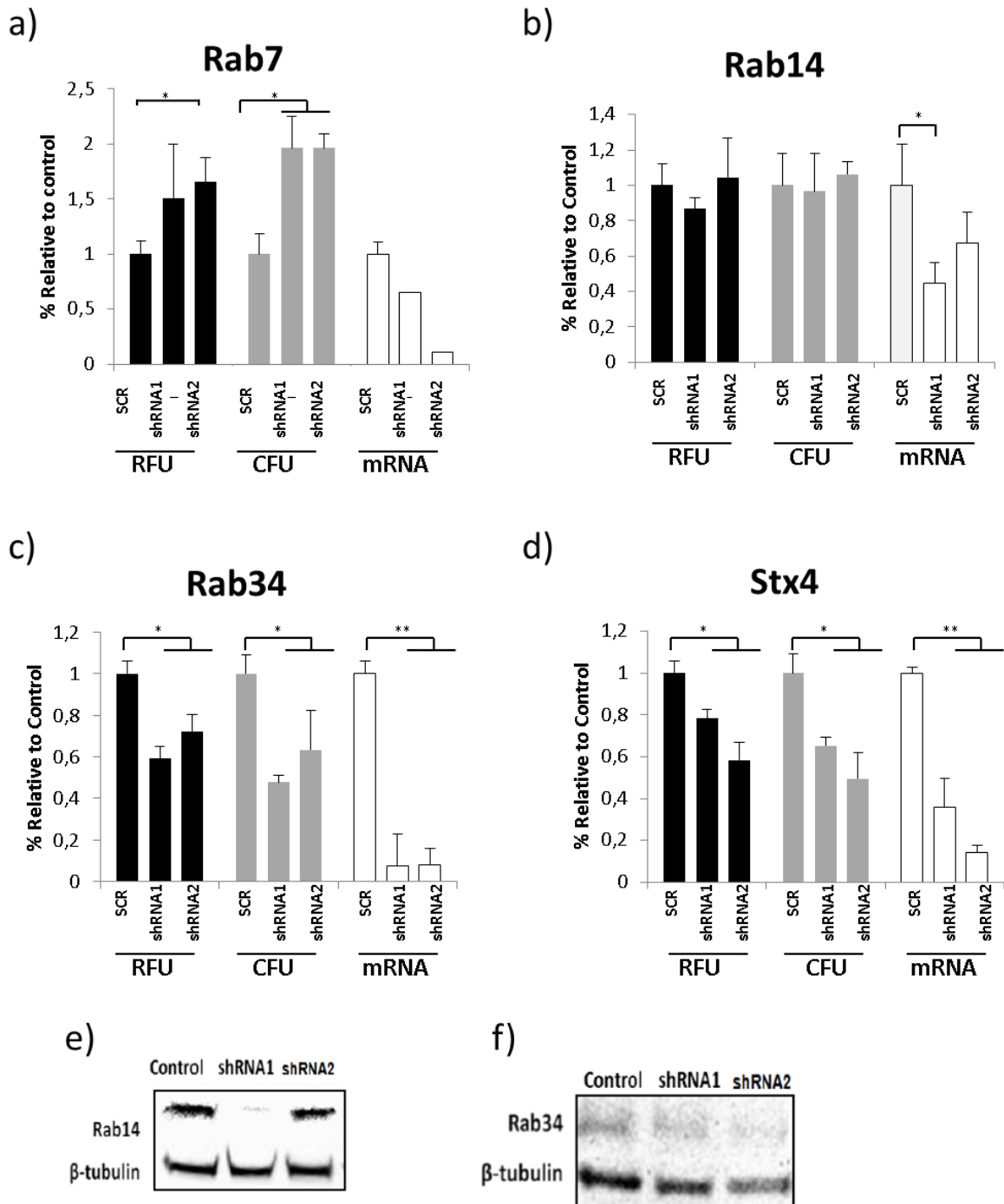
Figure 3.4. Effect of vesicular traffic genes knockdown on intracellular *M. tuberculosis* H37Rv survival. *M. tuberculosis* macrophage burden was measure both by fluorescent intensity of *M. tuberculosis* reporter (tdTomato; black bars) and by CFU (grey bars). White bars represent the relative level of mRNA of the selected gene to the expression of those genes in control samples determined by qt-RT-PCR. a) Rab7; b) Rab34; c) Syntaxin4 and d) Rab14. Data is presented as the average+SD (n=4 for RFU and CFU; n=2 for mRNA; t-test; *p<0.05;**p≤0,01). e) and f) confirmation of protein knockdown for Rab14 and Rab34 by western blot.
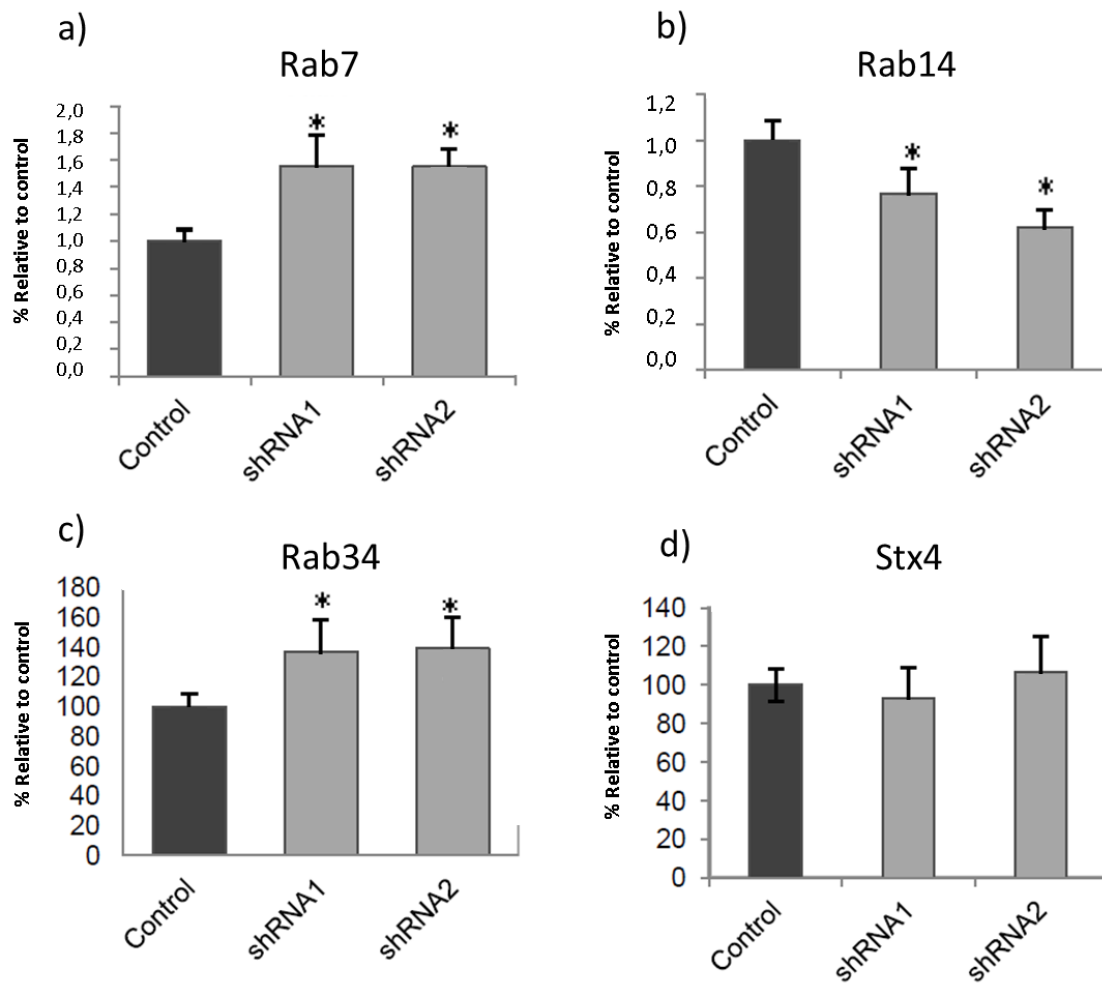
Figure 3.5. Effect of vesicular traffic genes knockdown on intracellular avirulent *M. tuberculosis* H37Ra survival. Black bars represent the CFU normalized to 100% on control samples and grey bars represents the percentage of CFU relatively to control on infected macrophages silenced with two distinct hairpins shRNAs of the same gene, for respectively. a) Rab7;b) Rab34; c) Syntaxin4 and d) Rab14.Data is presented as the average+SD (n=4 for RFU and CFU; n=2 for mRNA; t-test; *p<0.05;**p≤0,01).

Discussion

By RNA silencing of approximately around 120 macrophage genes related with vesicular traffic and membrane fusion and using a dual fluorescent assay set up in our laboratory on *M. tuberculosis* infected host cells we were able to identify a total of 10 genes that affected *M. tuberculosis* macrophage infection. Of all 8 candidate genes led to reduction (susceptible genes) and 2 candidate genes lead to an increase (resistance genes) in *M. tuberculosis* burden within human macrophages.

Among the susceptible genes found was Rab8a meaning that the silencing of this GTPase increase mycobacteria killing within macrophages. Rab8a has been found to be associated to phagosomes in proteomic studies [31–33]. Indeed, in a previous study by Seto and colleagues, Rab8 was demonstrated to be transiently associated with mycobacteria containing phagosomes (MCP) as well in *S. aureus* containing phagosomes during the first hour of [16]. Furthermore these authors showed that the expression of dominant negative proteins had no effect in both latex bead phagosomes (LBP) acidification or on cathepsin D recruitment. These results are in accordance with ours pointing for an effect on phagosome maturation and therefore bacteria intracellular killing drive by Rab8a.

Stx4 another identified susceptible gene target was described in literature as being involved in glucose-activated exocytosis of insulin, by interaction with actin in pancreatic beta cell line MIN6 [34].

Fratti and co-workers showed that MCP retains Stx4 and that Phosphatidylinositol Mannoside (PIM) from *M. tuberculosis* coated latex beads induce Stx4 accumulation in latex bead phagosomes [22,35] suggesting a role in phagolysosome blockade. However since in most studies they usually uses BCG or H37Ra instead of the virulent *M. tuberculosis* H37Rv, it is not surprisingly that they results show the same tendency than ours using H37Ra but not the H37Rv strain.

Rab27a has been found associated with MCP at later stages of infection [16]. Nevertheless, this protein has been reported to negatively modulate complement

receptor mediated phagocytosis of c3bi-zymosam particles in human macrophages [36] suggesting a role in the phase of bacteria internalization within macrophages. Rab27a knockdown induced a shorter coronin1A association to phagosomes and an increase in phagocytic uptake of zymosam particles. The authors describe for the first time that coronin1A is an effector of Rab27a. An association between CoroninA1 and MCP maturation block has been recently described [37]. Coronin1A knockdown results in activation of the p38 MAPK pathway, autophagosome formation around MCP and lead to reduce *M. tuberculosis* survival. We hypothesise that in Rab27a knockdown may be reducing coronin1A association to MCP.

Rab34 was described has being transcriptionally dependent of the transcription factor NF-κB during lysosomal mediated killing of avirulent mycobacteria by macrophages, predicting a role of this Rab GTPase in phagosomal maturation [38]. Moreover, Rab34 has shown to have a role in cathepsin D recruitment to phagosomes [16]. Recently, this Rab GTPase has been reported to mediate phagolysosome fusion by a cargo size dependent mechanism independent of Rab7 [39]. Overexpression of Rab34 led to a decrease in BCG survival concomitantly RNAi interference led to increased survival [39]. However, our results show consistently that Rab34 silencing decreased macrophage intracellular *M. tuberculosis* burden (Figure 3.4). Still, we did observe, an increase in intracellular survival in H37Ra avirulent mycobacteria in Rab34 silenced THP-1 cells (Figure 3.5). We conclude that Rab34 mediated killing of mycobacteria might be specific for avirulent mycobacteria and that virulent *M. tuberculosis* is able to block that mechanism.

Rab31 also known as Rab22b has been firstly describe to had a role in trans-Golgi network (TGN) [40]. Recently, Rab31 was observed in *M. tuberculosis* containing phagosomes early in macrophage infection and is excluded after 60 minutes [16]. On the other hand, this GTPase was implicated in phagosome maturation by recruitment of cathepsin D to latex bead phagosomes [16]. Our results indicate that that Rab31 knockdown reduces the numbers of intracellular *M. tuberculosis*. We speculate that the reduction in cathepsin D recruitment and therefore the vesicle traffic from trans Golgi to late endosomes is not enough to sustain significant replication in our persistence macrophage infection model.

D12, the mouse homolog of MDS032, is a SNARE from the endoplasmic reticulum (ER) [26]. D12 formed a tight complex with stx18) as well as Sec22b and bound to SNAPα, indicating that D12 is a SNARE protein [41]. This complex has been associated with ER membrane involvement of phagocytosis [26]. Analyses of deletion mutants using the opsonized zymosan assay and immunoprecipitation showed that this inhibition is mediated by the interaction with stx18 and/or D12 [26]. We do not know if this has a parallel to human macrophages. Although we observe that MDS032 knockdown intracellular *M. tuberculosis* it would be very interesting to determine if this gene is involved in macrophage internalization of this pathogen. The involvement of ER in *M. tuberculosis* infection could give the pathogen means to control antigen presentation.

Rab39B has 74% similarity to Rab39A and has been isolated in human foetal brain [42]. Mutations of this gene are associated with mental retardation associated with autism, epilepsy, and macrocephaly [28]. This protein has been localized in the TGN and associated with vesicles from the recycling pathway in mouse hippocampal neurons [28]. The silencing of this protein led to a reduction in *M. tuberculosis* burden within macrophages and this may be due to internalization defects related to recruiting recycling endosomes. Our results with Rab39B are the first to identify and associate such effects as susceptible gene target during *M. tuberculosis* infection.

Definitely, knockdown of Rab7 was sufficient to increase intracellular *M. tuberculosis* and thus this protein can be classified has a resistance gene responsible for clearance of this pathogenic bacteria. Rab7 is a key regulatory protein for proper aggregation and fusion of late endocytic structures in the perinuclear region and consequently for the biogenesis and maintenance of the lysosomal compartment [43]. In phagosomes of mammalian cells the recruitment and activation of Rab7 alone is insufficient to induce fusion of phagosomes with late endosomes and lysosomes [44]. Active Rab7 recruits its effector protein RILP (Rab-interacting lysosomal protein) that binds to dynein-dynactin motors and promotes the interaction of Rab7 bearing phagosomes to lysosomes [45]. Curiously, Rab7 is recruited to MCP without RILP association and released afterwards. The same is truth for autophagossomes, Rab7 is also involved in autophagosome maturation and content destruction. *M. tuberculosis* is eliminated from infected macrophages by the induction of autophagy

as a consequence of nutrient starvation, drug inducer or interferon gamma (IFN-γ) [46]. Autophagy potentially controls the intracellular burdens of *M. tuberculosis* in macrophages [47]. All together these and ours results indicate a crucial role of Rab7 for mycobacteria killing. Likewise the control of this GTPase may provide a therapeutic target for *M. tuberculosis* clearance by macrophages.

Rab43 was shown in our results to be another resistance gene target as their silencing induced an increase in intracellular *M. tuberculosis*. Previous studies associate Rab 43 with the ER and the Golgi [48]. This protein was indeed found to be associated with latex beads phagosomes upon macrophage activation by IFN-γ [33]. During infection Rab43 is present in *M. tuberculosis* phagosomes and retained throughout infection, this GTPase is involved in cathepsin D recruitment to latex bead phagosomes this protein [16]. The results suggest that while this protein is associated with recruitment of material associated with phagosome maturation, is not excluded from the *M. tuberculosis* phagosome and its knockdown is associated with a reduction in intracellular pathogen survival/persistence.

Finally, Rab5 was previously described to be retained in *M. tuberculosis* containing phagosomes [22,49–51]. Recently Seto *et al.* observed that this protein exists in 80% of *M. tuberculosis* containing phagosomes [16]. Curiously, Rab5a was found to be the only isoform transcriptionally up-regulated in response to treatment with cytokines such as interleukin-4 or IFN-γ in macrophages [52]. Another up-regulated isoform of Rab5, the Rab5b was identified during Raw264.7 macrophages infection with virulent *M. tuberculosis* [53]. Rab5c was found to co localize with mycobacterial phagosomes in HeLa cells. We speculate that Rab5 isoforms may cooperate in their functions on the endocytic pathway and that the knockdown of one isoform may be complemented by the other. Nevertheless, RABEP1 encodes the protein Rabaptin-5 a Rab5 effector involved in endocytic membrane fusion and homotypic endosome fusion [54,55]. One peculiar characteristic of Rabaptin-5 is to be an effector of both Rab5 and Rab4, linking endosome fusion and recycling [29]. Rabaptin-5 silencing by RNAi caused enlarged endosomes and delayed recycling of transferrin in knockdown HeLa cells [56]. However we don't know if there is a similar mechanism in phagosomes from professional phagocytes. Both latex beads and phagosomes containing BCG do not seems to possess a detectable Rabaptin-5 [57]. Our results

show that RABEP1 is a susceptible gene target which silencing leads to a decrease on mycobacteria burden. The mechanism remains however to decipher.

Seto *et al.* observed that some Rab GTPases that were not recruited to phagosomes containing a virulent *M. tuberculosis* strain were actively associated with phagosomes containing the avirulent *M. tuberculosis* strain H37Ra or *M. bovis* BCG. In parallel these authors show that the recruitment of Rab GTPases implicated in the regulation of phagosome maturation is modulated in a virulence dependent manner. In this work we have found differences in the effect of the knockdown of selected vesicular traffic genes in avirulent and virulent *M. tuberculosis.* The use of clinical strains like CDC 1551 a recent clinical isolate [58] might help to determine the clinical relevance of the genes identified here. Most studies on vesicular traffic genes were made in avirulent mycobacteria and consequently the results obtained don´t have always significance in the virulent *M. tuberculosis* context. Nevertheless, these studies help us to identify the relevance of vesicular traffic genes in macrophage phagocytosis and to highlight the possible vesicular traffic factors exploited by *M. tuberculosis* and intracellular pathogens in general during infection.

The maintenance of *M. tuberculosis´* replication niche within macrophages is highly complex and dynamic. In order to undoubtedly identify the host factors involved in *M. tuberculosis* infection is important to use methods capable of intracellular pathogen quantification. In this work we show that our dual fluorescent reporter assay could be used to perform a high content screen and process hundreds of samples per experiment. This technique can be applied to other mutant *M.* tuberculosis and other intracellular pathogens, using other groups of host targets, or virtually to test the effect of drugs.

Although, several vesicular traffic genes have been found to be differentially recruited/excluded from the *M. tuberculosis* containing phagosomes [16,18] the impact of those genes in the survival or persistence have not been elucidated. Here we showed that a group of vesicular traffic genes have an effect on the survival of intracellular mycobacteria. Nevertheless, the mechanisms associated with some of those phenotypes are still to be elucidated.

Material and Methods

Mycobacteria cultures

Mycobacterium tuberculosis strains H37Rv and H37Ra were cultured in 7H9 medium supplemented with 10% oleic acid albumin dextrose catalase and 0.05% tyloxapol. All manipulations of *M. tuberculosis* were performed in a Biosafety Level 3 environment.

Each of these species of mycobacteria harbours a plasmid constitutively expressing Green Fluorescent Protein (GFP) and a hygromycin resistance as a selection marker. The culture medium contained 50 μg/ml hygromycin B (Sigma-Aldrich) in order to maintain selective pressure on the plasmid carriers.

All cultures were kept at 37°C and were subcultured until achieving exponential phase before being used on experiments: 7-10 days beforehand for *M. tuberculosis.*

Cell lines

The human monocyte cell line THP-1 (ATCC TIB-202) was cultured in RPMI 1640 medium supplemented with 10% (v/v) FBS, 1% (v/v) glutamine, 1% (v/v) penicillin-streptomycin, 1% (v/v) HEPES buffer, 1% (v/v) sodium pyruvate and 1% (v/v) non-essential amino acids.

The HEK 293T cell line (ATCC CRL-11268) was used to amplify the viral constructs of the lentiviral knockdown libraries. They were maintained in DMEM supplemented with 10% (v/v) foetal bovine serum and 1% (v/v) antibiotic – penicillin-streptomycin. Cell lines were maintain at 37°C in an atmosphere containing 5% carbon dioxide.

hairpin-pLKO.1 Plasmid preparation

Plasmids were prepared according to TRC proceedings listed at (https://www.broadinstitute.org/genome_bio/trc/publicProtocols.html). 96 deep well sterile growth plates (Corning) were pre-filled with 1.2 ml of Terrific Broth (TB, Invitrogen) media containing 100 μg/ml carbenicillin (Sigma-Aldrich). The hairpin-pLKO.1 containing bacterial glycerol stocks were inoculated on the TB pre-filled 96 deep well plates and grown for at least 16 hours at 37^oC under agitation, 300 rpm. After incubation, plates were centrifuged for at 1500xg for 8 minutes at 4^oC, and supernatants discarded. Bacterial cell pellets were ressuspended in 200 μl of RNase A containing Ressuspension Buffer (50 mM Tris-HCl, 10 mM EDTA pH 8.0 and 0.1 mg/ml RNase A) and further lysed in 210 μl fresh Alkaline Protease containing lysis buffer (200 mM NaOH, 1% (w/v) SDS and 25 units/ml of Alkaline Protease) for 4 minutes at room temperature. Bacterial cell lysates were neutralized by adding 300 μl Neutralization buffer (3.75 M Guanidinium Hydrochloride, 0.9 M KOAc and 1.4 M HOAc, pH4.35). After 30 minutes at 4^oC, centrifugation at 3000xg, lysates were transferred to a clarification filter plate (Whatman) and centrifuged at 3000xg for additional 5 minutes at 4^oC. Clarified lysates were then incubated at 70^oC for 30 minutes. After incubation, lysates were transferred to a pDNA binding plate (Whatman), centrifuged at 1800xg for 2 minutes at 4^oC and supernatants were discarded. Two washes were performed by centrifuging the pDNA binding plates at 1800xg for 2 minutes at 4^oC in the presence of 600 μl of Wash buffer (480 ml of 100% ethanol added to a 120 ml of a solution containing 15 mM NaCl, 40 mM Tris-HCl and 25 mM Tris, pH 6.65). Plasmid DNA was eluted from the pDNA binding plates by centrifuging at 1800xg for 5 minutes at 4^oC after an incubation of 10 minutes with 140 μl of Elution buffer (10 mM Tris-HCl, pH 8.0). Plasmid DNA concentration was assayed by spectrophotometry in a Tecan Infinite 200 equipment using Quant-iT PicoGreen dsDNA reagent (Invitrogen) following manufacturer's protocol, and further stored at -80^oC.

Lentivirus production

Lentiviruses were produced according to TRC lentiviral proceedings present at the RNAi Consortium website (https://www.broadinstitute.org/genome_bio/trc/publicProtocols.html). Briefly, HEK 293T cells were seeded at a density of $2.2x10^5$ cells/ml (100 µl per well in 96 well plates) in DMEM media without Penicillin-Streptomycin. After 24 hours incubation at cell culture normal conditions, cells were transfected with a mixture of the 3 plasmids, the packaging plasmid (100 ng of pCMV-dR8.91), the envelope plasmid (10 ng of VSV-G/pMD2.G) and 100 ng of the shRNA containing pLKO.1-puro vector (Figure 3.6), using Fugene HD transfection reagent (Promega) in Optimem medium (GIBCO), following TRC transfection proceedings. After 18 hours of incubation, media was replaced with 170 µl of high serum growth media (30% FBS (v/v) DMEM). Twenty-four hours after media replacement, viruses were harvested (150 µl) and fresh media (150 µl) was added to the cells. The second viral collection was performed 24 hours later and harvested viruses were pooled with the previous day collection and stored at -80ºC.

Lentiviral transduction

Lentiviral transduction was performed according what is described at the RNAi Consortium website

(https://www.broadinstitute.org/genome_bio/trc/publicProtocols.html). Briefly, 10 µl of viruses were plated per well in a 96 well plate. THP-1 cells were ressuspended in RPMI medium containing 8 µg/ml of Polybrene (Sigma-Aldrich) at a density of $1.25x10^6$ cells/ml, and 40 ul were added on top of the virus containing wells. Plates were spun for 90 minutes at 900xg at 37ºC. After spinoculation, media was removed

and replaced with 200 µl of fresh THP-1 media, and cells incubated at 37ºC under normal cell culture conditions. After 2 days, transduced cell selection was performed by adding 50 µl of THP-1 media containing puromycin (Calbiochem) to a final concentration of 5 ug/ml. Cells were kept under puromycin selection for 3 days and then were ready to be used in further assays.

Infection procedures

Mycobacterial preparation

Prior to any experiment, infection or broth cultures, mycobacterial cultures at mid log grow phase were centrifuged at 3000xg, 37°C for 10 minutes, washed in Phosphate buffer saline (PBS) pH 7.4 (Gibco) and, in the case of infection experiments, resuspended in in RPMI media 1640 (Gibco) supplemented with 10% (v/v) Foetal Bovine Serum (Gibco), 1% (v/v) Pyruvate (Gibco), 1% (v/v) L-Glutamine (Gibco), 1% (v/v) Non-essential aminoacids (Gibco), 1% (v/v) Hepes buffer (Gibco). To obtain a single-bacillus suspension the medium with the bacilli was passed 20 times through a sterile syringe equipped with a 21 gauge needle, followed by 15 minutes of ultrasonic. The remaining bacterial clumps were eliminated by centrifugation at 350xg for 1 minute and single-cell suspension was verified by light microscopy.

Figure 3.6. Vector map for the pLKO.1 lentiviral vector. The self-inactivating lentiviral vector backbone contains elements for efficient viral packaging and shRNA expression. These include Ψ, the lentiviral packaging site; RRE, the Rev-responsive element; cPPT, central polypurine tract. RSV 5′ LTR is a hybrid of the Rous Sarcoma virus promoter and the HIV 5′ LTR. SIN 3′ LTR is the HIV 3′ LTR with a self-inactivating U3 deletion. Expression of the shRNA is driven by the human U6 promoter (hU6). The lentiviral vector also contains the mammalian selection marker puromycin resistance gene (PAC) under the control of the PGK promoter as a mammalian selection marker. pUCori is the bacterial origin of replication of the plasmid, F1 ori is the single-stranded phage F1 origin of replication, and AmpR is the ampicillin resistance gene.

Mycobacterial infection of THP-1 macrophages

All infection experiments were made with RPMI media without phenol or antibiotics. THP-1 cell densities were quantified using Milipore EasyCyte H6 Guava flow cytometer, using its proprietary InCyte software. $7,5x10^4$ THP-1 cells/well seeded in a black polystyrene 96 well plates (Corning) and incubated with 20 nM of phorbol 12-myristate 13-acetate (PMA) (Sigma-Aldrich) RPMI media without phenol for 24 hours

94

for differentiation into macrophages. After this period, cells were allowed to rest in PMA free media for another 24 hours.

In the day of infection, the cell media was discarded and was added 100 µl of single bacilli suspensions. The macrophages were infected with H37Rv in at a multiplicity of infection (MOI) of 1, proportion of mycobacteria/macrophage. After a specific pulse period, macrophages were washed with warm media. After washing, 200 µl/well of media containing 10 µg/ml of gentamycin was added, to kill extracellular bacteria. Cells were incubated for 24 hours and replenish with 200 ml/well of media containing no antibiotics. It have been reported that at this range of concentration gentamycin does not accumulate in THP-1 cells and any intracellular gentamicin is also rapidly inactivated [59,60]. Cell media was replaced every 48 hours.

Data acquisition and analysis

Quantification of mycobacteria expressing tdTomato and THP-1 expressing eGFP

Quantification of intracellular H37Rv, expressing tdTomato and THP-1 expressing eGFP was made by spectrophotometry of fluorescence in Tecan's M200 spectrophotometer. THP-1 macrophages fluorescence was measured at 488nm excitation and 520nm emission and a gain of 175, and intracellular H37Rv at an excitation of 554nm, an emission of 586nm and a gain of 200.

Quantification of intracellular *M. tuberculosis* by colony forming units

Five days post-infection, infected macrophages were washed with PBS and incubated with 0,05% (v/v) solution of IGEPAL (Sigma-Aldrich) at normal cell incubation conditions, for 10 minutes. Serial 10 fold dilutions were made with sterile distilled water, and plated Middlebrook's 7H10 solid medium (Becton, Dickinson and Company) supplemented with 10% (v/v) OADC (Becton, Dickinson and Company), 0.5% (v/v) glycerol (Sigma-Aldrich). Plates were incubated at 37°C for 3 weeks. Micro colonies were count with the help of an optical microscope.

Quantitative RT-PCR

Total RNA was extracted using TRIzol reagent (Invitrogen) and final RNA quality and concentration determined by spectrophotometry using Nanodrop 2000c equipment (Thermo Scientific). Complementary DNA (cDNA) synthesis was carried out using 1ug of total RNA and Superscript II Reverse Transcriptase (Invitrogen) according to manufacturer's directions. Quantitative RT-PCR (qRT-PCR) was performed in the presence of Power SYBR green PCR Master Mix (Applied Biosystems) and the amplification protocol was performed on a *7300 Real-Time PCR System* (Applied Biosystems). All samples were normalized against the expression of the housekeeping gene glyceraldehyde-3-phosphate dehydrogenase (GAPDH) and the relative expression of each gene was calculated using Pfaffl's method [61]. Primers are listed in supplementary information section (Table S3.2).

Western-blot

Transduced cells were denatured at 95°C for 5 minutes in the presence of Laemmli buffer (BioRad), before loaded 20 µl on 12% Sodium Dodecyl Sulphate polyacrilamide gels. Electrophoresis was performed at 200 V for 1 hour. Proteins were transferred onto nitrocellulose membranes with an electrical intensity of 30 V overnight in a cold room. At the following day, membranes were blocked for 1 hour at room temperature. The blocking buffer contains Tris-buffered saline plus 0.05% (v/v) Tween 20 (TBS-T) and 5% (w/v) Bovine Serum Albumin (BSA) in order to avoid unspecific binding of the detection antibody. Following that, membranes were incubated with primary antibodies (Table 3.3) diluted in TBS-T plus 1% (w/v) BSA for 2 hours at room temperature. After 3 washes in TBS-T, membranes were probed with horseradish peroxidase (HRP)-conjugated secondary antibodies (Table 3.3) for 1 hour at room temperature. After 3 washes in TBS-T, membranes were stained for 5 minutes with the chemiluminescent reagent, Luminata Crescendo Western HRP

Substrate (Millipore). Chemiluminescence was detected and captured with ChemiDoc XRS+ system (Bio-Rad).

Table 3.3. List of Antibodies used to perform WB, dilutions and incubation times.

Antibodies	Reference	Company	Dilution	Incubation	
				Time	Temperature
Rab14	sc-271401	Santa Cruz Biotecnology	1:300	2 hours	RT
Rab 34	ab73383	Abcam	1:1000	2 hours	RT
Beta-tubulin	ab20775	Abcam	1:4000	2 hours	RT
anti-mouse	172-1011	Bio-Rad	1:4000	1 hour	RT
anti-rabbit	170-6515	Bio-Rad	1:4000	1 hour	RT

Statistical treatment

The software SigmaPlot 12.0 (*Systat Software Inc.*) was used for statistical analysis. One tail Student's t-test was used for comparing two means and ANOVA more than two means. Statistical significance was assumed when $P < 0.05$ or $P<0,01$.

References

1. Aderem a, Underhill DM. Mechanisms of phagocytosis in macrophages. *Annu Rev Immunol*. 1999;17:593–623. doi:10.1146/annurev.immunol.17.1.593.

2. Greenberg S, Grinstein S. Phagocytosis and innate immunity. *Curr Opin Immunol*. 2002;14(1):136–45.

3. Jutras I, Desjardins M. Phagocytosis: at the crossroads of innate and adaptive immunity. *Annu Rev Cell Dev Biol*. 2005;21:511–27.

4. Fairn GD, Grinstein S. How nascent phagosomes mature to become phagolysosomes. *Trends Immunol*. 2012;33(8):397–405.

5. Vieira O V, Botelho RJ, Grinstein S. Phagosome maturation: aging gracefully. *Biochem J*. 2002;366(Pt 3):689–704.

6. Desjardins M, Nzala NN, Corsini R, Rondeau C. Maturation of phagosomes is accompanied by changes in their fusion properties and size-selective acquisition of solute materials from endosomes. *J Cell Sci*. 1997;110 (Pt 18):2303–14.

7. Gutierrez MG. Functional role(s) of phagosomal Rab GTPases. *Small GTPases*. 2013;4(3):1–11.

8. Mayorgasq LS, Bertinis F, Stahlqll PD. Fusion of Newly Formed Phagosomes with Endosomes in Intact Cells and in a Cell-free System. J Biol Chem. 1991;266(10):6511-7.

9. Duclos S, Diez R, Garin J, et al. Rab5 regulates the kiss and run fusion between phagosomes and endosomes and the acquisition of phagosome leishmanicidal properties in RAW 264.7 macrophages. *J Cell Sci*. 2000;113 Pt 19:3531–41.

10. McBride HM, Rybin V, Murphy C, Giner a, Teasdale R, Zerial M. Oligomeric complexes link Rab5 effectors with NSF and drive membrane fusion via interactions between EEA1 and syntaxin 13. *Cell*. 1999;98(3):377–86.

11. Collins RF, Schreiber AD, Grinstein S, Trimble WS. Syntaxins 13 and 7 function at distinct steps during phagocytosis. *J Immunol*. 2002;169(6):3250–6.

12. Rink J, Ghigo E, Kalaidzidis Y, Zerial M. Rab conversion as a mechanism of progression from early to late endosomes. *Cell*. 2005;122(5):735–49.

13. Cantalupo G, Alifano P, Roberti V, Bruni CB, Bucci C. Rab-interacting lysosomal protein (RILP): the Rab7 effector required for transport to lysosomes. *EMBO J*. 2001;20(4):683–93.

14. Behar SM, Divangahi M, Remold HG. Evasion of innate immunity by Mycobacterium tuberculosis: is death an exit strategy? *Nat Rev Microbiol*. 2010;8(9):668–74.

15. Vergne I, Chua J, Deretic V. Mycobacterium tuberculosis phagosome maturation arrest: selective targeting of PI3P-dependent membrane trafficking. *Traffic*. 2003;4(9):600–6.

16. Seto S, Tsujimura K, Koide Y. Rab GTPases regulating phagosome maturation are differentially recruited to mycobacterial phagosomes. *Traffic*. 2011;12(4):407–20.

17.   Fratti R a, Chua J, Deretic V. Cellubrevin alterations and Mycobacterium tuberculosis phagosome maturation arrest. *J Biol Chem*. 2002;277(19):17320–6.

18.   Vergne I, Chua J, Singh SB, Deretic V. Cell biology of mycobacterium tuberculosis phagosome. *Annu Rev Cell Dev Biol*. 2004;20:367–94.

19.   Seto S, Matsumoto S, Tsujimura K, Koide Y. Differential recruitment of CD63 and Rab7-interacting-lysosomal-protein to phagosomes containing Mycobacterium tuberculosis in macrophages. *Microbiol Immunol*. 2009;54(3):170–174.

20.   Roberts E a, Chua J, Kyei GB, Deretic V. Higher order Rab programming in phagolysosome biogenesis. *J Cell Biol*. 2006;174(7):923–9.

21.   Kyei GB, Vergne I, Roberts E, et al. Rab14 is critical for maintenance of Mycobacterium tuberculosis phagosome maturation arrest. *EMBO J*. 2006;25(22):5250–5259.

22.   Perskvist N, Roberg K, Kulyté A, Stendahl O. Rab5a GTPase regulates fusion between pathogen-containing phagosomes and cytoplasmic organelles in human neutrophils. *J Cell Sci*. 2002;115(Pt 6):1321–30.

23.   Vergne I, Fratti RA, Hill PJ, Chua J, Belisle J, Deretic V. Mycobacterium tuberculosis Phagosome Maturation Arrest : Mycobacterial Phosphatidylinositol Analog Phosphatidylinositol Mannoside Stimulates Early Endosomal Fusion. 2004;15(February):751–760.

24.   Breed RS, Dotterrer WD. The Number of Colonies Allowable on Satisfactory Agar Plates. *J Bacteriol*. 1916;1(3):321–31.

25.   Day RN, Davidson MW. The fluorescent protein palette: tools for cellular imaging. *Chem Soc Rev*. 2009;38(10):2887–921.

26.   Hatsuzawa K, Hashimoto HH, Arai S, Tamura T, Higa-Nishiyama A, Wada I. Sec22b is a negative regulator of phagocytosis in macrophages. *Mol Biol Cell*. 2009;20(20):4435–43.

27.   Strom M, Hume AN, Tarafder AK, Barkagianni E, Seabra MC. A family of Rab27-binding proteins. Melanophilin links Rab27a and myosin Va function in melanosome transport. *J Biol Chem*. 2002;277(28):25423–30.

28.   Giannandrea M, Bianchi V, Mignogna ML, et al. Mutations in the small GTPase gene RAB39B are responsible for X-linked mental retardation associated with autism, epilepsy, and macrocephaly. *Am J Hum Genet*. 2010;86(2):185–95.

29.   Vitale G, Rybin V, Christoforidis S, et al. Distinct Rab-binding domains mediate the interaction of Rabaptin-5 with GTP-bound Rab4 and Rab5. *EMBO J*. 1998;17(7):1941–51.

30.   Band AM, Ali H, Vartiainen MK, et al. Endogenous plasma membrane t-SNARE syntaxin 4 is present in rab11 positive endosomal membranes and associates with cortical actin cytoskeleton. *FEBS Lett*. 2002;531(3):513–9.

31.   Stuart LM, Boulais J, Charriere GM, et al. A systems biology analysis of the Drosophila phagosome. *Nature*. 2007;445(7123):95–101.

32.   Rogers LD, Foster LJ. The dynamic phagosomal proteome and the contribution of the endoplasmic reticulum. *Proc Natl Acad Sci U S A*. 2007;104(47):18520–5.

33.   Trost M, English L, Lemieux S, Courcelles M, Desjardins M, Thibault P. The phagosomal proteome in interferon-gamma-activated macrophages. *Immunity*. 2009;30(1):143–54.

34.   Jewell JL, Luo W, Oh E, Wang Z, Thurmond DC. Filamentous actin regulates insulin exocytosis through direct interaction with Syntaxin 4. *J Biol Chem*. 2008;283(16):10716–26.

35.   Fratti R a, Chua J, Vergne I, Deretic V. Mycobacterium tuberculosis glycosylated phosphatidylinositol causes phagosome maturation arrest. *Proc Natl Acad Sci U S A*. 2003;100(9):5437–42.

36.   Yokoyama K, Kaji H, He J, et al. Rab27a negatively regulates phagocytosis by prolongation of the actin-coating stage around phagosomes. *J Biol Chem*. 2011;286(7):5375–82.

37.   Seto S, Tsujimura K, Koide Y. Coronin-1a inhibits autophagosome formation around Mycobacterium tuberculosis-containing phagosomes and assists mycobacterial survival in macrophages. *Cell Microbiol*. 2012;14(5):710–27.

38.   Gutierrez MG, Mishra BB, Jordao L, Elliott E, Anes E, Griffiths G. NF-kappa B activation controls phagolysosome fusion-mediated killing of mycobacteria by macrophages. *J Immunol*. 2008;181(4):2651–63.

39.   Kasmapour B, Gronow A, Bleck CKE, Hong W, Gutierrez MG. Size-dependent mechanism of cargo sorting during lysosome-phagosome fusion is controlled by Rab34. *Proc Natl Acad Sci U S A*. 2012;109(50):20485–90.

40.   Ng EL, Wang Y, Tang BL. Rab22B's role in trans-Golgi network membrane dynamics. *Biochem Biophys Res Commun*. 2007;361(3):751–757.

41.   Okumura AJ, Hatsuzawa K, Tamura T, et al. Involvement of a novel Q-SNARE, D12, in quality control of the endomembrane system. *J Biol Chem*. 2006;281(7):4495–506.

42.   Cheng H, Ma Y, Ni X, et al. Isolation and characterization of a human novel RAB (RAB39B) gene. *Cytogenet Genome Res*. 2002;97(1-2):72–5.

43.   Bucci C, Thomsen P, Nicoziani P, McCarthy J, van Deurs B. Rab7: a key to lysosome biogenesis. *Mol Biol Cell*. 2000;11(2):467–80.

44.   Vieira O V., Bucci C, Harrison RE, et al. Modulation of Rab5 and Rab7 Recruitment to Phagosomes by Phosphatidylinositol 3-Kinase. *Mol Cell Biol*. 2003;23(7):2501–2514.

45.   Jordens I, Fernandez-Borja M, Marsman M, et al. The Rab7 effector protein RILP controls lysosomal transport by inducing the recruitment of dynein-dynactin motors. *Curr Biol*. 2001;11(21):1680–5.

46.   Singh SB, Davis AS, Taylor GA, Deretic V. Human IRGM induces autophagy to eliminate intracellular mycobacteria. *Science*. 2006;313(5792):1438–41.

47.   Kumar D, Nath L, Kamal MA, et al. Genome-wide analysis of the host intracellular network that regulates survival of Mycobacterium tuberculosis. *Cell*. 2010;140(5):731–43.

48.   Hutagalung AH, Novick PJ, NOVICK AHH and PJ. Role of Rab GTPases in Membrane Traffic and Cell Physiology. *Physiol Rev*. 2011;91(1):119–149.

49.   Clemens DL, Lee BY, Horwitz M a. Deviant expression of Rab5 on phagosomes containing the intracellular pathogens Mycobacterium tuberculosis and Legionella pneumophila is associated with altered phagosomal fate. *Infect Immun*. 2000;68(5):2671–84.

50.   Via LE, Deretic D, Ulmer RJ, Hibler NS, Huber LA, Deretic V. Arrest of Mycobacterial Phagosome Maturation Is Caused by a Block in Vesicle Fusion between Stages Controlled by rab5 and rab7. *J Biol Chem*. 1997;272(20):13326–13331.

51. Kelley VA, Schorey JS, Dame N. Mycobacterium ' s Arrest of Phagosome Maturation in Macrophages Requires Rab5 Activity and Accessibility to Iron. 2003;14(August):3366–3377.

52. Wainszelbaum MJ, Proctor BM, Pontow SE, Stahl PD, Barbieri MA. IL4/PGE2 induction of an enlarged early endosomal compartment in mouse macrophages is Rab5-dependent. *Exp Cell Res.* 2006;312(12):2238–51.

53. Pan F, Zhao Y, Zhu S, et al. Different transcriptional profiles of RAW264.7 infected with Mycobacterium tuberculosis H37Rv and BCG identified via deep sequencing. *PLoS One.* 2012;7(12):e51988.

54. Gournier H, Stenmark H, Rybin V, Lippé R, Zerial M. Two distinct effectors of the small GTPase Rab5 cooperate in endocytic membrane fusion. *EMBO J.* 1998;17(7):1930–40.

55. Lippé R, Miaczynska M, Rybin V, Runge A, Zerial M. Functional synergy between Rab5 effector Rabaptin-5 and exchange factor Rabex-5 when physically associated in a complex. *Mol Biol Cell.* 2001;12(7):2219–28.

56. Deneka M, Neeft M, Popa I, et al. Rabaptin-5alpha/rabaptin-4 serves as a linker between rab4 and gamma(1)-adaptin in membrane recycling from endosomes. *EMBO J.* 2003;22(11):2645–57.

57. Fratti RA. Role of phosphatidylinositol 3-kinase and Rab5 effectors in phagosomal biogenesis and mycobacterial phagosome maturation arrest. *J Cell Biol.* 2001;154(3):631–644.

58. Valway SE, Sanchez MP, Shinnick TF, et al. An outbreak involving extensive transmission of a virulent strain of Mycobacterium tuberculosis. *N Engl J Med.* 1998;338(10):633–9.

59. Carryn S, Van Bambeke F, Mingeot-Leclercq M-P, Tulkens PM. Comparative intracellular (THP-1 macrophage) and extracellular activities of beta-lactams, azithromycin, gentamicin, and fluoroquinolones against Listeria monocytogenes at clinically relevant concentrations. *Antimicrob Agents Chemother.* 2002;46:2095–2103.

60. Carryn S, Van Bambeke F, Mingeot-Leclercq M-P, Tulkens PM. Activity of beta-lactams (ampicillin, meropenem), gentamicin, azithromycin and moxifloxacin against intracellular Listeria monocytogenes in a 24 h THP-1 human macrophage model. *J Antimicrob Chemother.* 2003;51(4):1051–2.

61. Pfaffl MW. A new mathematical model for relative quantification in real-time RT-PCR. *Nucleic Acids Res.* 2001;29(9):e45.

Supplementary Information

Table S3.1. List of vesicular traffic genes targeted to knockdown by shRNA.

Gene Name	NM_ID	Gene Name	NM_ID
BET1	NM_005868	RAB33B	NM_031296
BET1L	NM_016526	RAB34	NM_031934
BNIP1	NM_001205	RAB35	NM_006861
EPIM	NM_001980	RAB36	NM_004914
GOSR1	NM_004871	RAB36	NM_004914
GOSR2	NM_004287	RAB37	NM_175738
MDS032	NM_018467	RAB37	NM_175738
RAB10	NM_016131	RAB38	NM_022337
RAB11A	NM_004663	RAB39	NM_017516
RAB11B	NM_004218	RAB39B	NM_171998
RAB11FIP1	NM_025151	RAB3A	NM_002866
RAB11FIP2	NM_014904	RAB3A	NM_002866
RAB11FIP3	NM_014700	RAB3B	NM_002867
RAB11FIP4	NM_032932	RAB3C	NM_138453
RAB11FIP5	NM_015470	RAB3C	NM_138453
RAB13	NM_002870	RAB3GAP2	NM_012414
RAB14	NM_016322	RAB3IL1	NM_013401
RAB15	NM_198686	RAB3IP	NM_022456
RAB17	NM_022449	RAB40B	NM_006822
RAB18	NM_021252	RAB40B	NM_006822
RAB19B	XM_376681	RAB40C	NM_021168
RAB1A	NM_004161	RAB41	NM_001032726
RAB1B	NM_030981	RAB42	NM_152304
RAB2	NM_002865	RAB43	NM_198490
RAB20	NM_017817	RAB4B	NM_016154
RAB21	NM_014999	RAB5A	NM_004162

Gene Name	NM_ID	Gene Name	NM_ID
RAB22A	NM_020673	RAB5A	NM_004162
RAB23	NM_016277	RAB5B	NM_002868
RAB24	NM_130781	RAB5B	NM_002868
RAB25	NM_020387	RAB5C	NM_004583
RAB26	NM_014353	RAB6A	NM_002869
RAB27A	NM_004580	RAB6B	NM_016577
RAB27B	NM_004163	RAB6C	NM_032144
RAB28	NM_004249	RAB7	NM_004637
RAB2B	NM_032846	RAB7B	NM_177403
RAB30	NM_014488	RAB7B	NM_177403
RAB31	NM_006868	RAB7L1	NM_003929
RAB32	NM_006834	RAB8A	NM_005370
RAB33A	NM_004794	RAB9A	NM_004251
RAB9B	NM_016370	SNAP29	NM_004782
RABEP1	NM_004703	STX11	NM_003764
RABEP2	NM_024816	STX12	NM_177424
RABEPK	NM_005833	STX17	NM_017919
RABGAP1	NM_012197	STX18	NM_016930
RABGAP1L	NM_014857	STX1A	NM_004603
RABGEF1	NM_014504	STX3A	NM_004177
RABGGTA	NM_004581	STX4A	NM_004604
RABGGTB	NM_004582	STX5A	NM_003164
RABIF	NM_002871	STX6	NM_005819
RABL2A	NM_007082	STX7	NM_003569
RABL2B	NM_001003789	STX8	NM_004853
RABL3	NM_173825	SYBL1	NM_005638
RABL4	NM_006860	VAMP2	NM_014232
RABL5	NM_022777	VAMP3	NM_004781
SEC22B	NM_004892	VAMP4	NM_003762
SEC22L2	NM_012430	VAMP5	NM_006634

Table S3.1. (Continued)

Gene Name	NM_ID	Gene Name	NM_ID
SEC22L3	NM_004206	VTI1A	NM_145206
SNAP23	NM_003825	VTI1B	NM_006370
SNAP25	NM_003081	YKT6	NM_006555

Table S 3.2. List of primers used in qRT-PCR.

Gene Name	Primer	Sequence
GAPDH	HGAPDH-L	AAGGTGAAGGTCGGAGTCAA
	HGAPDH-R	AATGAAGGGGTCATTGATGG
MDS032	MDS032-L	CCACAAAGACGGTGCATCT
	MDS032-R	TCCTTACGTCCATCTCAGGC
RAB11FIP3	RAB11FIP3-L	GTTTGCTACGGTCTACGGGG
	RAB11FIP3-R	GGCTGTGATCCCTTGGTAGA
RAB27A	RAB27A-L	ACAAGCGGTTCTCTACCCTG
	RAB27A-R	CCCTACACCAGAGTCTCCCA
RAB31	RAB31-L	AGGATGCTGCTGAGCCC
	RAB31-R	ACGATGCTTGATTTCCCAAC
RAB33A	RAB33A-L	AGGGAGAAGACCGTGGAAAT
	RAB33A-R	TTGCGGTAGTAATGCTCGAC
RAB34	RAB34-L	GCACAAAGACTTCCACCCC
	RAB34-R	CCCACCACAATGATCTTGGA
RAB3A	RAB3A-L	GACCATCTATCGCAACGACA
	RAB37-R	CATAGCGCCCCGGTAGTAT
RAB39B	RAB39B-L	GGAGATCGAGCCAGGAAAAC
	RAB39B-R	AGTTCCTGTAGTAGGCGCGA
RAB42	RAB42-L	CGTGGAGACCTCGGTTAAAA
	RAB42-R	TCTAGCTTGATGTCCCCCTG
RAB43	RAB43-L	ACCATGAAGACGCTGGAGAT
	RAB43-R	CTGCGGTAGTAGCTCTGGGT
RAB7B	RAB7B-L	GATGCAGCCATCGGAGCCCTTGT
	RAB7B-R	GGCCAGCATCCTCTCCAAGATTATC
RAB7A	RAB7A-L	CCGTTTAGTCTCCTCCTCGG
	RAB7A-R	CCTTCAGCAACACTTTCTTCCT
RAB8A	RAB8A-L	GACGCCTTCAACTCCACTTT
	RAB8A-R	ACCGGCTGTGTCCCATATCT
RABEP1	RABEP1-L	GGCTTCCCAGCCTGACG
	RABEP1-R	TGTTCAAGCTGCTGTTGTGC
RABGGTA	RABGGTA-L	AGATGGAGTATGCCGAGGTG
	RABGGTA-R	CAAGTCAAGATGGGTGACCA
SNAP23	SNAP23-L	GTTGGGGTGTCCGAGTTG
	SNAP23-R	TCTGGTGAGCTCTCTGTTGAA

Table S 3.2. (Continued)

Gene Name	Primer	Sequence
STX4	STX4-L	ATAGAGCCCCAGAAGGAGGA
	STX4-R	TTGATGAGCTCCACGAATTG
VAMP2	VAMP2-L	GCGCAAATACTGGTGGAAAA
	VAMP2-R	CTCCTCGGGGATTTAAGAGC
RABGAP1	RABGAP1-L	GCGCAAATACTGGTGGAAAA
	RABGAP1-R	TCTTCGAGGAGAAGTCTGGC
RAB24	RAB24-L	AAGGTGATGTCGGTCGGA
	RAB24-R	CTTGGCACCCCGATAGTAGA
RAB7L1	RAB42-L	CAGGACAGCTTCAGCAAACA
	RAB42-R	TGAAGCCGCACTATCTCGTA

Chapter 4

Host factors involved in *Mycobacterium tuberculosis* internalization within macrophages

Host factors involved in *Mycobacterium tuberculosis* internalization within macrophages

Abstract

An assay based on flow cytometry was developed to assess and quantify mycobacteria macrophage phagocytosis *in vitro*. Different origin species of macrophage cell cultures were used and infected with several GFP expressing strains and species of virulent and avirulent mycobacteria. Additionally, we knockdown distinct vesicular traffic genes selected from a genomic screen as potential candidates with a role in *M. tuberculosis* macrophage infection. Our results indicate that the rate of internalization is dependent on the species/strain doubling time and on the virulence, being the virulent *M. tuberculosis* H37Rv the strain with the lowest internalization rate of all tested. Additionally, we show that mycobacteria uptake occurs very fast within the first half hour of infection. Furthermore here we demonstrate that the method is feasible as allowed to identify several vesicular traffic genes demonstrated previously with a role in *M. tuberculosis* macrophage infection as positive regulators of mycobacteria internalization by host cells.

Introduction

Phagocytosis of invading microorganisms by macrophages is a multi-step process that involves detection, uptake, destruction and presentation of antigens to adaptive immune system[1]. Macrophage entry is the first critical step in *M. tuberculosis* infection. The process involves the interaction between pathogens´

ligands and macrophage surface receptors. To survive inside macrophages the bacilli evolved strategies for engaging specific receptors to gain entrance without triggering immune activation and degradation inside the macrophage [2]. *M. tuberculosis* is able to engage several macrophage receptors probably due to the complex structure of its cell wall [3]. Although, various macrophage receptors already described, such as complement receptors, mannose receptor, lung surfactant protein receptors, CD14, scavenger receptors, Toll like receptors and Fc receptors, their contribution in the intracellular fate and survival of M. tuberculosis is still far from being understood [4,5]. However, virulent *M. tuberculosis* macrophage uptake through Fcγ receptor-mediated phagocytosis leads to fusion of mycobacteria containing phagosomes with lysosomes [4].

After pathogen detection, internalization and phagosome biogenesis induces an increase of macrophage membrane area to compensate the gradual apposition of plasma membrane onto invading microorganisms [6]. Rather than originating only from plasma membrane, the excess of membrane for phagosome biogenesis is obtained from different macrophage organelles by a process called focal exocytosis [7]. Rab GTPases and SNARE proteins have been implicated with the recruiting of membrane to the nascent phagosome [8]. Indeed, it was shown that the SNARE Vamp3 and Rab11 were involved in early and recycling endosomes and Vamp7 in late endosome recruitment to the phagocytic cup [7,9]. In addition to organelles related to the endosome/lysosome pathway, the endoplasmic reticulum (ER) has also been implicated in phagosome formation. ER-derived membrane has been observed in the bottom of forming phagosomes, and some ER-resident SNAREs were detected in a proteomics analysis of isolated phagosomes (Gagnon et al., 2002; Desjardins, 2003). Recently, a proteomic study by Campbell-Valois identified the plasma membrane, endosomes/lysosomes, Golgi, ER and mitochondria as contributors to the phagosome membrane and also identified several Rab GTPases and SNARE proteins from those organelles associated with nascent phagosomes [10]. Most data on membrane recruitment during phagocytic uptake comes from Fcγ receptor-mediated phagocytosis studies [11]. However it is expected that different phagocytic receptors and other factors may influence the machinery engaged for engulfment [11].

The vesicular traffic proteins involved in the uptake of *M. tuberculosis* are still to be deciphered. Here we took advantage of the powerful potential of fluorescence-activated cell sorting (FACS) flow cytometry to develop and optimize a macrophage internalization assay for mycobacteria. This approach provided us tools for further biologically characterise the role of several vesicular traffic gene, after siRNA knockdown of macrophages, in mycobacteria internalization. Our data shows that mycobacteria/macrophage internalization rates are dependent on ~~of~~ the cell line used and on the virulence of mycobacteria. Virulent *M. tuberculosis* is internalized at lower rates by macrophages when comparing to the avirulent counterparts fast growing *M. smegmatis* and slow growing *M. bovis* BCG. Additionally, we identified six vesicular traffic genes, Rab27a, Rab39b, RABEP1 and Stx4, whose knockdown reduced macrophage internalization of virulent *M tuberculosis.* Two other additional genes identified Rab27a and Stx4 were shown to possess a reduced internalization effect on knocked-down macrophages infected with the avirulent *M. smegmatis*.

Results

Quantification of Mycobacteria Internalization by FACS

In order to establish a method based on flow cytometry to assess the rate of mycobacteria internalization by macrophages we first used *Mycobacterium smegmatis* expressing GFP to infect phorbol-esters PMA diferentiated THP-1 cells at different multiplicities of infection (MOI). After a 3 hours pulse the percentage of GFP positive THP-1 cells were quantified by flow cytometry (Figure 4.1). Gated Forward Scatter (FSC) and Side Scatter (SSC) were measured from infected cells samples (Figure 4.1a and 4.1d). The gated population was used to establish a SSC /FL1 ratio allowing to distinguish between THP-1 cells that internalized GFP expressing bacteria (GFP positive) (Figure 4.1e) from uninfected control cells (Figure 4.1b). By

transforming the FL1 data in histograms one can compare the distribution of fluorescent intensity in the GFP positive population (Figure 4.1c). We observed an increased THP-1 fluorescence intensity concomitant with an increase on the MOI. Treatment of THP-1 with 1ug/ml of cytochalasin   D, an inhibitor of actin polymerization and therefore on macrophage internalization [12], for 15 minutes before and during the pulse time, significantly reduced the internalization o GFP mycobacteria in 4 fold change (ANOVA; $p<0,001$; n=3).
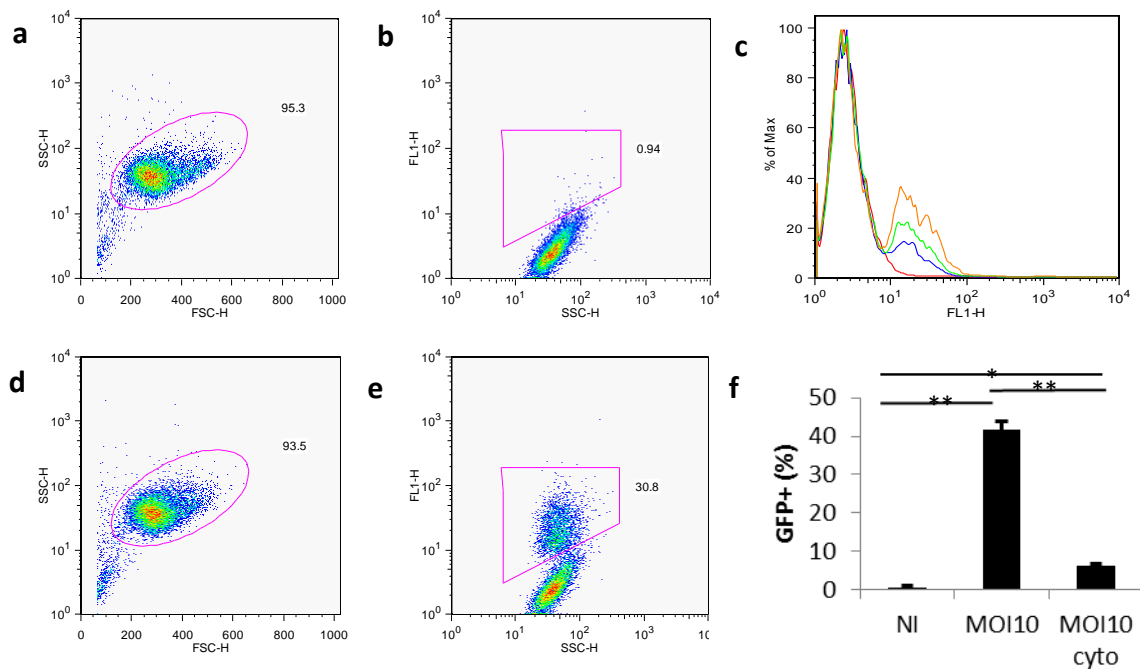
Figure 4.1. Flow cytometry analysis of mycobacteria infected THP-1 cells. (a and c) macrophage sample acquired in the Forward Scater (FSC) and Side Scater (SSC), respectively. (b) The cell population can be subsequently gated and a precise quantification of the macrophages that do not contain GFP-bacteria and (d) those who contain GFP-bacteria, at a MOI of 20. e) Different amounts of bacteria are distinguishable as a function of the fluorescence intensity. GFP-positive cells show higher intensity as the MOI increases from 5 (blue), to10 (green) and to 20 (red). f) Internalization of mycobacteria is inhibited by cytochalasin D (A-NOVA;n=3; *p=0,001; ** $p<0,001$).

These results suggest that increments in GFP positive cells associated with increasing amounts of mycobacteria per macrophage were due to an increase in mycobacteria uptake. To confirm that mycobacteria were internalized by macrophages and not just adherent outside of the membrane we quantified the extracellular mycobacteria directly after the uptake phase (Figure 4.2a), while others were subjected to every step of the post-infection protocol treatment (Figure 4.2b). From a random sampling, we calculated the percentage of macrophages with adjacent extracellular mycobacteria (Figure 4.2c). The treated samples with a protocol described in methods of washing were completely clear of adherent mycobacteria, while 58% of the macrophages in the non-treated samples were not.
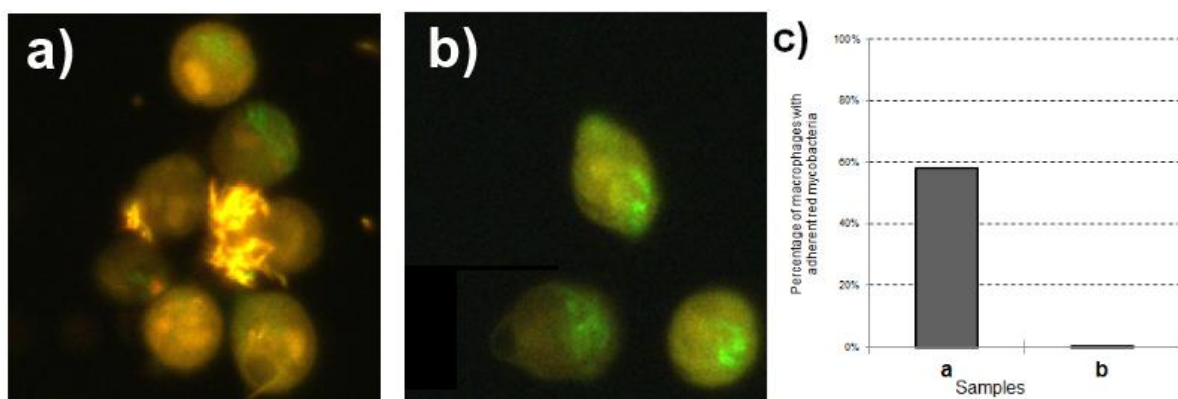
Figure 4.2. Fluorescence microscopy images of macrophage samples infected with Mycobacterium smegmatis. J774 cells were infected at a MOI 100 and analysed 1 hour post infection. In a) the sample was stained with ethidium bromide and immediately observed under a fluorescence microscope. In b) the sample was stained and subjected to the entirety of the post-infection protocol c) Bar plot representing the quantification of adherent extracellular mycobacteria in the original samples from where images a and b were taken. Images captured with a Zeiss Axioskop 40 microscope and its software AxioVision 4 using a FITC filter.

Rates of internalization

Figure 4.3 presents representative histograms of uninfected and infected THP-1 macrophages with a MOI of 1 bacterium per macrophage for 4 hours. In order to optimize the macrophage internalization assay for bacteria we further tested the

influence of macrophage species or of mycobacteria and the minimum time required and multiplicity of infection (MOI) on uptake rate. Figure 4.4 shows the internalization profiles on J774 mouse macrophages. A marked difference between multiplicities of infection is observed, as they maintain some graphical distance, with no overlap. When using a MOI of 100 almost all macrophages were infected by mycobacteria, which is not surprisingly if we consider such a high bacterial burden. Considering the avirulent *M. smegmatis* is not only internalized faster, but also to a greater extent, reaching a higher percentage of infected macrophages than the other mycobacteria (although these differences were non-significant by the Holm-Sidak pairwise comparison, p>0.05). *M. tuberculosis* appears to be internalized at a lower rate than the other mycobacteria during the first hour of contact with macrophages, which is particularly evident in the curve corresponding to a MOI of 1, hardly reaching 20% at the end point.
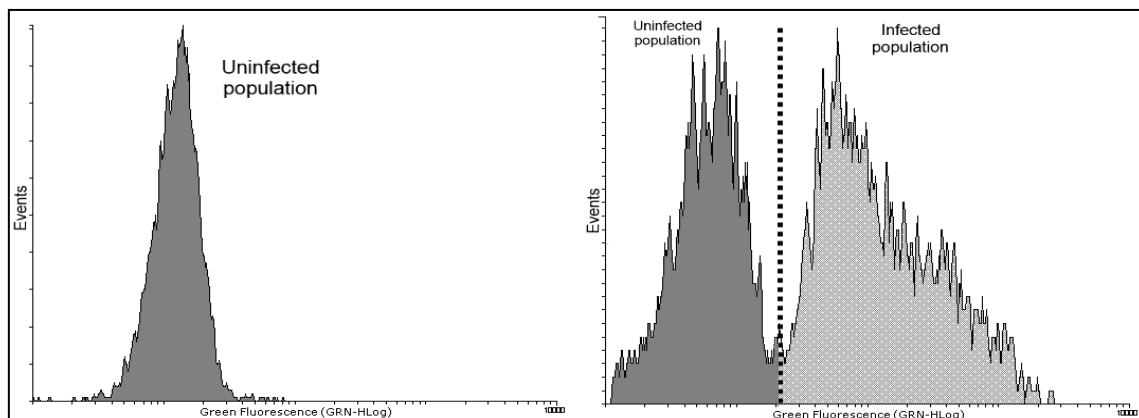
Figure 4.3. Example populations of uninfected and infected macrophages, as obtained by flow cytometry and represented in histograms. Left: Uninfected control sample of THP-1 macrophages. Right: Sample of THP-1 macrophages infected with *Mycobacterium smegmatis* for 4 hours with a multiplicity of infection of 1. X axis represents intensity of green fluorescence in a logarithmic scale. Y axis represents number of events. The two samples are taken from the same experiment. With flow cytometry software we calculated the percentage of total events that are in each population.
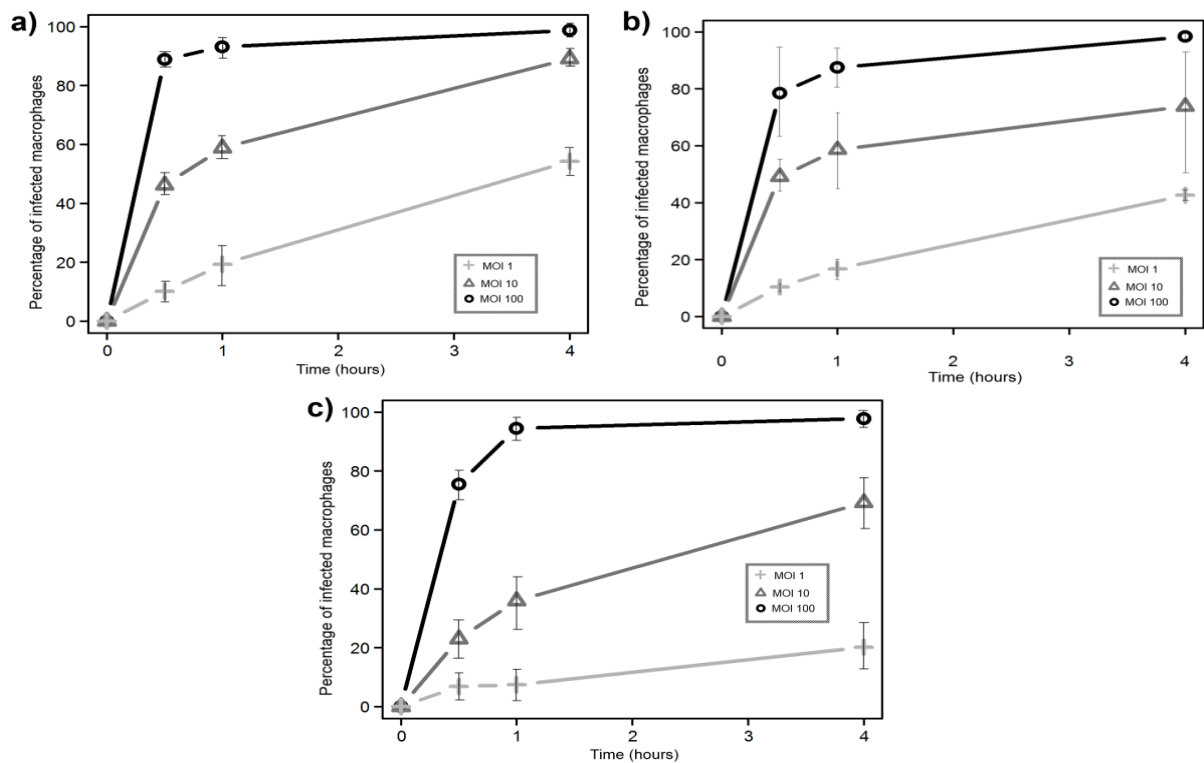
Figure 4.4. Internalization by J774 mouse macrophages of different mycobacteria. a) *M. smegmatis*; b) *M. bovis* BCG; c) *M. tuberculosis*. Each data point includes the average and standard deviation of three replicate experiments.

In Figure 4.5 we can observe the internalization profiles on THP-1 human macrophages. Figure 4.5a confirms that *M. smegmatis* is slightly more internalized than its other counterparts contrary to *M. tuberculosis* that shows a tendency for a slower internalization rate especially at a MOI of 1 or 10, as indicated by a less steep curve. Nonetheless, there is substantial difference in the kinetics of internalization of *M. tuberculosis* compared to other mycobacteria at the early stages. Global differences were evaluated using the Holm-Sidak method, indicating that the differences between *M. tuberculosis* and other mycobacteria were significant ($p < 0.05$). The apparent decline on the 4 hour mark of MOI 100 in Figure 4.5.c is buffered by the standard deviation and is not likely to represent a real decrease in internalization.
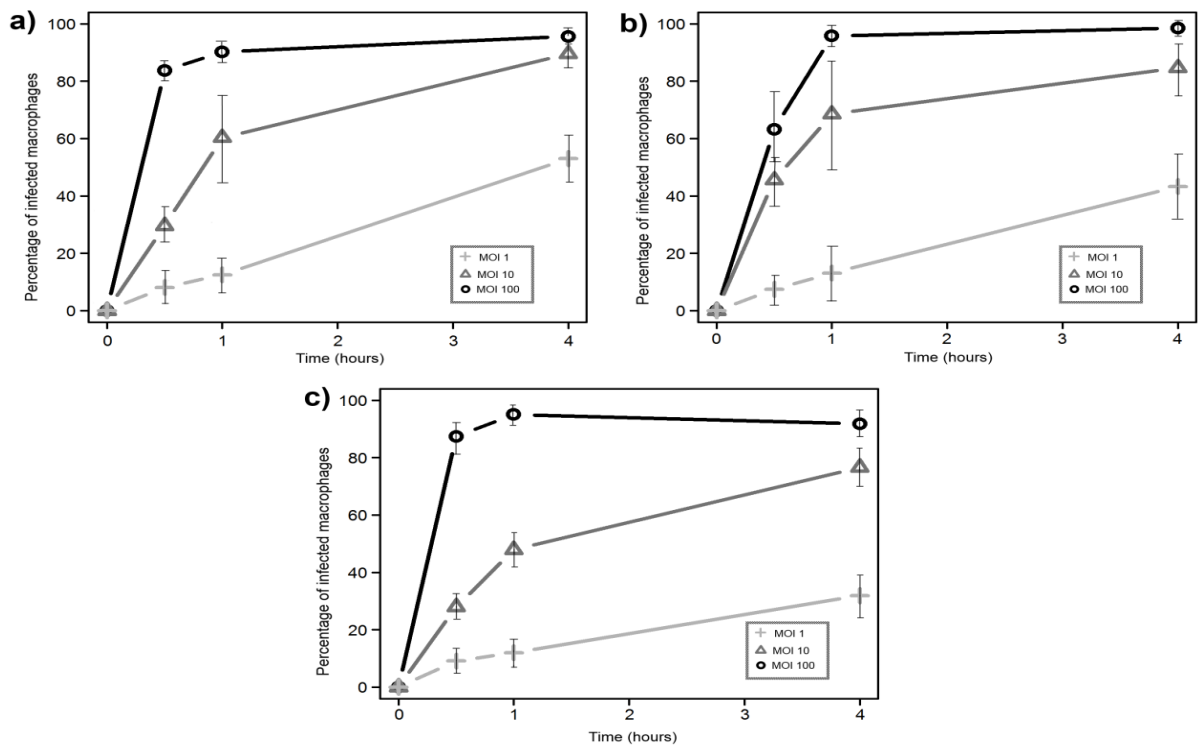
Figure 4.5. Internalization by THP-1 macrophages of different mycobacteria. a) *M. smegmatis*; b) *M. bovis* BCG; c) *M. tuberculosis*. Each data point includes the average and standard deviation of three replicate experiments.

In human monocyte-derived macrophages (HMDM), represented in Figure 4.6, the results shows a reach to the plateau earlier on, as we can see a shorter difference between the time points of 1 hour and 4 hours, which is more evident in the case of *M. tuberculosis*.
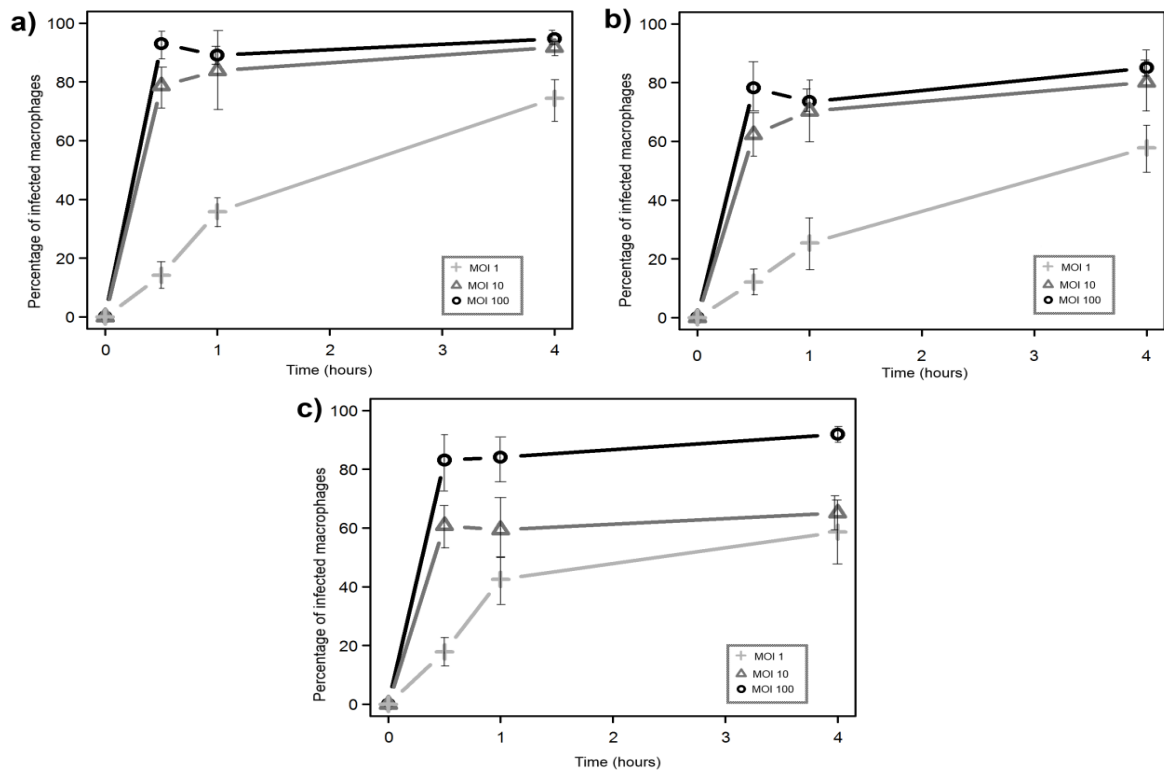
Figure 4.6. Internalization by human monocyte-derived macrophages of different mycobacteria. a) *M. smegmatis*; b) *M. bovis* BCG; c) *M. tuberculosis*. Each data point includes the average and standard deviation of three replicate experiments.

Figure 4.7 represents the results from the previous experiments but with a different graphical arrangement in order to allow a clear analyse of the difference in the uptake rate of the different macrophage species. The results show that human monocyte-derived possess the greatest phagocytic efficiency, largely exceeding its counterparts in the first hour (significant for HMDM *versus* J774, $p < 0.05$), although all reach the peak activity before the fourth hour. No significant differences were observed between J774 and THP-1 cells in these measurements. A relevant observation is that *M. tuberculosis* is shown to be internalized to a lesser extent, although it was present in the same concentrations as the other mycobacteria at the time of infection (significant, $p < 0.05$). Simultaneously there is an inverse correlation between virulence and percentage of internalization; we observe the latter is greater with *M. smegmatis*, lower with BCG and the lowest with *M. tuberculosis*, a pattern easily observed in HMDM.
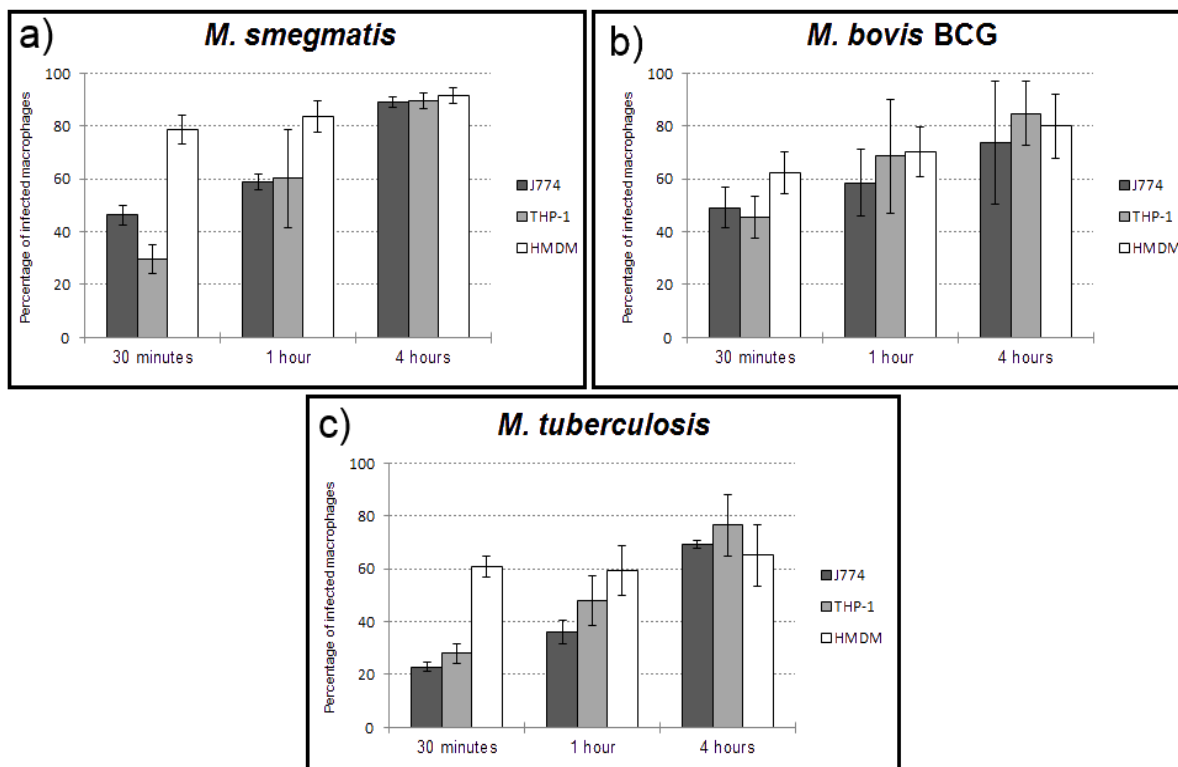
Figure 4.7. Internalization efficiency of different macrophages, sorted by species of mycobacteria. Only the MOI of 10 is represented.

Vesicular traffic genes are positive regulators of mycobacteria internalization

In order to validate the internalization method set up we further determined the role of host vesicular trafficking factors during macrophage internalization of avirulent (*M.* smegmatis) and virulent (*M. tuberculosis*). For this purpose we used mycobacteria expressing GFP to infect THP-1 cells at a MOI 10 after one hour of pulse and measure the percentage of GFP positive THP-1 cells by flow cytometry. Figure 4.8 displays the overall results for internalization of mycobacteria in THP-1 cells knockdown for the candidate genes validated in the genomic screen. Overall most of the knockdowns led to a reduction in the internalization of both mycobacteria species indicating that these proteins are likely positive regulators of internalization. The pattern was rather similar between the two species of mycobacteria, despite the difference in baseline internalization rates between them. The reduction, was

however, slightly higher in *M. tuberculosis* compared to *M. smegmatis*. The internalization rate reduction was almost twofold more substantial with virulent *M. tuberculosis* (23%) than with the avirulent *M. smegmatis* (12%).

The selection of host factors with an effect on internalization was based on the criteria that two or more hairpins silencing each protein had to cause a difference in internalization of at least 2.5 times the standard deviation of the controls and the the hairpins of the same gene have the same tendency (incresing or decreasing macrophage uptake). We found seven macrophages candidate genes for internalization of *M. tuberculosis* and 4 candidate genes for *M.* smegmatis (Figure 4.9).

It is not surprising to realize that proteins mostly associated with vesicular traffic and phagosome maturation exert influence on internalization, which is a vesicular and membrane process [13]. The fact that the silencing of these proteins significantly decreased the efficiency of internalization suggests that some cross-regulation must exist between the chronologically separate systems of internalization and phagosome maturation.
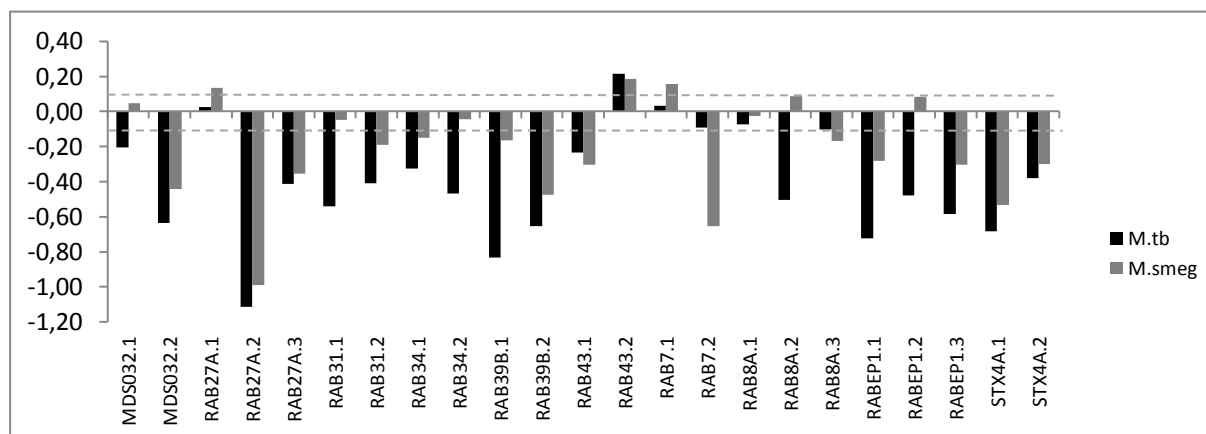
Figure 4.8. Overview of the internalization assay performed on candidate vesicular traffic proteins. The different gene interference hairpins are sorted in the vertical axis for the two strains. The horizontal axis expresses normalize internalization to the control (internalization / control). M.tb: *Mycobacterium tuberculosis;* Msmeg:*Mycobacterium smegmatis*
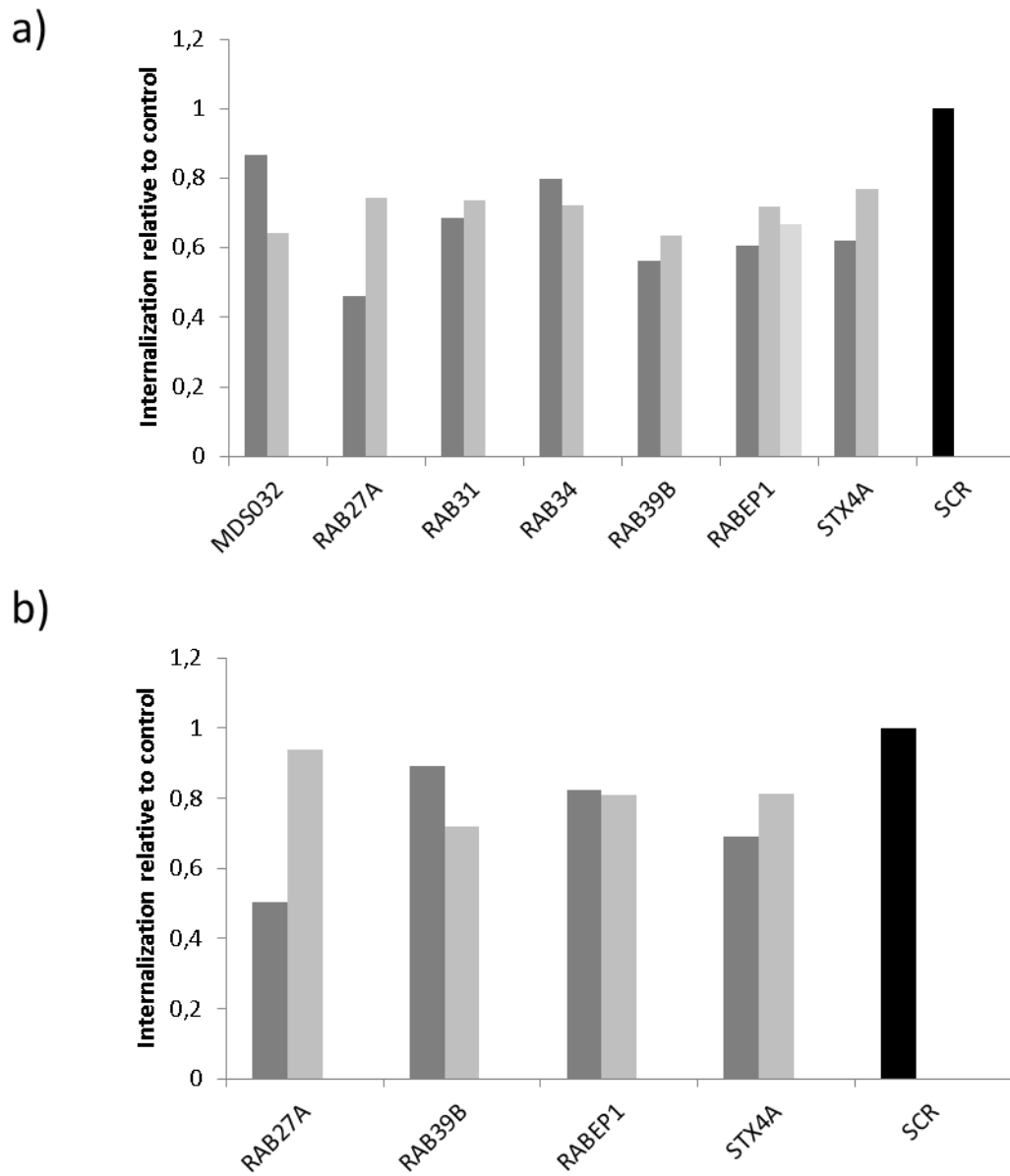
Figure 4.9. Candidate genes with a role in internalization in two species of mycobacteria. a) *Mycobacterium tuberculosis* and b) *Mycobacterium smegmatis*. Different gray tones represent different gene interference hairpins.

Discussion

In the present work flow cytometry was successfully used to assess of mycobacteria uptake by macrophages. The results shown here indicate that internalization of mycobacteria by macrophages is dependent on the multiplicity of infection, on the macrophage type and on mycobacteria species. Indeed we show that mycobacteria uptake by macrophages is a fast phenomenon, as we observed that the majority of mycobacteria are internalized in the first 30 minutes after contact with the macrophages. HMDM were more competent to internalize mycobacteria than THP-1 or J774 macrophages.

The decreasing order of internalization among the tested mycobacterial species is coherent with the growth rate of each one. Faster-growing mycobacteria were internalized at a higher rate and to a higher extent, and the reverse is also true (Figure 4.7). This leads us to raise the supposition that bacterial growth occurred during the experiment, affecting the results. This hypothesis can be dismissed for *M. bovis* BCG and *M. tuberculosis*, for which the doubling time greatly exceeds the 4-hour maximum duration of the experiment. *M. smegmatis*, on the other hand, has a doubling time of approximately 3 hours and could present a liability to the robustness of the method, given that the infection takes place at 37°C. However, when we consider that the bacteria were taken from a culture in exponential phase, thoroughly washed and individualized, significantly diluted and ressuspended in a non-optimal medium, exponential bacterial growth is not expected to take place in these conditions.

The observed relationship between growth rate and internalization are also correlated when analysing virulence. Indeed, *M. tuberculosis*, *M. bovis* BCG and *M. smegmatis* are in a decreasing scale of virulence inversely proportional to the scale observed in internalization (Figure 4.7). It seems that *M. tuberculosis* may be internalized by a different route of *M. smegmatis* or *M. bovis* BCG, or actively inhibits its internalization. Previous work by Stockes and co-workers demonstrated that

glycan-rich outer layer of *M. tuberculosis* is antiphagocytic controlling and limiting the interaction of the bacterium with macrophages [14].

The knockdown of several candidate vesicular traffic genes involved in *M. tuberculosis* macrophage infection interfere with macrophage uptake of *M. smegmatis* and *M. tuberculosis*. In this situation we could observe the same tendency of a lower uptake of *M. tuberculosis*. Based on our criteria we selected four candidate genes that have a potential effect on *M. smegmatis* macrophage uptake and seven for *M. tuberculosis*. For all at least two hairpins induced a reduction in the percentage of macrophages infected with *M. tuberculosis*, suggesting that these proteins might be positive regulators of macrophage uptake. Curiously the proteins whose knockdown led to a reduction in *M. tuberculosis* macrophage internalization also lead to reduced intracellular *M. tuberculosis* burden.

Nevertheless, the involvement of MDS032 in *M. tuberculosis* uptake is an attractive candidate in *M. tuberculosis* macrophage interaction. D12, the mouse homolog of MDS032, is a SNARE from the ER [15]. D12 formed a tight complex with Stx 18 as well as Sec22b and bound to SNAPα, indicating that D12 is a SNARE protein [16]. This complex has been associated with ER involvement of phagocytosis [15]. Analyses of deletion mutants using the opsonized zymosan assay and immunoprecipitation showed that this inhibition is mediated by the interaction with Stx 18 and/or D12 [15]. We do not know if this has a parallel to human macrophages. Although we observe that MDS032 knockdown reduces mycobacteria internalization, we didn't observe influence of Sec22b in *M. tuberculosis* infection in the genomic screen from the previous chapter. Additionally, the involvement of the ER in early time points of *M. tuberculosis* infection could provide a route of pathogen subversion of macrophage antigen presentation [17].

Stx4 is a SNARE present in the cellular membrane of macrophages and is recruited to the nascent phagocytic cup to mediate the membrane fusion events involved in exocytosis necessary for the extra membrane needed for particle uptake [18]. Additionally, Stx4 and Rab27a have been implicated in phagocytosis by macrophages [19,20].

Rab27a was reported to regulate macrophage uptake in complement mediated phagocytosis by prolongation of phagosome F-actin coating by GTP Rab27a and recruitment of Coronin 1A by the GDP form [20]. We observed a reduction in mycobacteria uptake in Rab27a knockdown human macrophages. The association between Coronin 1A and *M. tuberculosis* survival [21] makes this candidate worth of study.

Since the first studies on flow cytometry for quantification of mycobacteria uptake by host cells to the best of our knowledge this is the first to compare *in vitro* different strains and macrophage types. This technique can also be adapted for *in vivo* studies using knockout mice for study of host genes in alveolar macrophage phagocytosis [22].

Materials and Methods

Mycobacteria cultures

Mycobacterium tuberculosis strain H37Rv and *Mycobacterium bovis* BCG were cultured in 7H9 medium supplemented with 10% oleic acid albumin dextrose catalase and 0.05% tyloxapol. All manipulations of *M. tuberculosis* were performed in a Biosafety Level 3 environment.

Mycobacterium smegmatis (mc2 155) was grown in liquid culture medium containing 4,7g/l Middlebrook 7H9 broth and 5g/l Nutrient broth (Difco), supplemented with 0.05% tyloxapol and 0.5% glucose.

Each of these species of mycobacteria harbors a plasmid constitutively expressing Green Fluorescent Protein (GFP) and a hygromicin resistance as a selection marker. The culture medium contained 50 µg/ml hygromycin B (Sigma-Aldrich) in order to maintain selective pressure on the plasmid carriers.

All cultures were kept at 37°C and were subcultured until achieving exponential phase before being used on experiments: 7-10 days beforehand for *M. tuberculosis* and *M. bovis* BCG, but only overnight for the fast-growing *M. smegmatis*.

Cell cultures

The murine macrophage cell line J774A.1 (ATCC TIB-67[TM]), referred to as 'J774', was cultured in Dulbecco's Modified Eagle Medium (DMEM, Gibco) supplemented with 10% (v/v) fetal bovine serum (FBS), 1% (v/v) glutamine and 1% antibiotic – penicillin-streptomycin (v/v).

The human monocyte cell line THP-1 (ATCC TIB-202) was cultured in RPMI 1640 RPMI media 1640 (Gibco) supplemented with 10% (v/v) Foetal Bovine Serum (Gibco), 1% (v/v) Pyruvate (Gibco), 1% (v/v) L-Glutamine (Gibco), 1% (v/v) Non-essential aminoacids (Gibco), 1% (v/v) Hepes buffer (Gibco)..

The formulations described above are also referred to as 'complete' DMEM or RPMI media. If antibiotic is not included, they are referred to as 'infection' media.

Primary human monocyte-derived macrophages were obtained from blood from donors. Monocytes were first isolated according to the protocol from *Miltenyi Biotec*, using the MidiMACS kit and LS columns. For the differentiation of monocytes into macrophages, 300,000 cells were seeded on a 24-well plate with 300 µl RPMI medium per well and allowed to adhere to the plate bottom. After 2 hours, 300 µl of RPMI with 20% (v/v) FBS, 2% (v/v) penicillin-streptomycin, 2% (v/v) sodium pyruvate, 2% (v/v) β-mercaptoethanol and 0.6 µl of macrophage colony stimulating factor (M-CSF 1000x) for a final concentration of 20 ng/ml in each well. After approximately 72 hours 600 µl of complete RPMI containing 20 ng/ml M-CSF were added. At the seventh day the macrophages were collected via resuspension with a trypsin-EDTA solution and were ready to be plated for the infection experiments.

The HEK 293T cell line (ATCC CRL-11268) was used to amplify the viral constructs of the lentiviral knockdown libraries. They were maintained in DMEM supplemented with 10% (v/v) fetal bovine serum and 1% (v/v) antibiotic – penicillin-streptomycin.

All of the above were cultivated at 37°C in an atmosphere containing 5% carbon dioxide.

Infection protocol

Preparation of macrophages

Cells were seeded onto 24 or 12-well plates (approximately 500,000 cells per well) with the appropriate culture medium (complete DMEM or RPMI). THP-1 cells were plated for 24 hours in contact with 20 nM phorbol 12-myristate 13-acetate (PMA, Sigma-Aldrich), which differentiates the monocytes into macrophages, followed by 24 hours of *resting* in complete culture medium without PMA. J774 macrophages were plated 24 hours in advance at half the desired concentration, so that they would multiply to the intended final concentration on the day of the experiment.

Preparation of bacteria

Disassembly of bacterial aggregates is necessary as large clumps may have a strong influence on phagocytosis. The steps involved are: washing with Phosphate Buffered Saline (PBS) at 1x concentration; resuspension in infection medium (DMEM or RPMI medium according to the cells to be infected); passaging several times with a 5ml syringe and a 21 gauge needle; a 5-minute ultrasound bath followed by a short centrifugation at a low force: 1 minute, 300xg to pellet any remaining aggregates. After the last centrifugation, only the supernatant was collected.

By reading the optical density at 600 nanometers, bacterial suspensions were adjusted for concentrations corresponding to multiplicities of infection (MOI) of 1, 10 and 100 bacteria per macrophage. This calculation was based on the standard relationship between optical density (OD) and concentration of bacteria (OD 0.1 <=> $1*10^7$ bacteria/ml)

Infection

The contact between macrophages and bacteria was initiated by removing the cell culture medium and replacing it with the bacterial suspension in infection medium.

To achieve the three different lengths of infection, the samples were infected at different times, so that afterwards they could all be stopped and processed at the same time. Considering the stopping time of the infection as the "time point –zero", samples were infected at –4 hours, –1 hour and –30 minutes. Between manipulations, samples were incubated at 37°C in an atmosphere containing 5% CO_2.

Processing samples after infection

While remaining adhered to the plate, the cells were washed three times with warm PBS, thus removing the mycobacteria. Cells were then dislodged using 400 µl trypsin with a 5-minute incubation at 37°C. Afterwards the cells were resuspended in 1 ml of infection (antibiotic-free) DMEM or RPMI medium to neutralize the proteolytic action of trypsin. This was followed by centrifugation for 10 minutes at 450 *xg*. Fixation was then performed with 4% paraformaldehyde, for 30 minutes at room temperature, and the samples were then finally washed and resuspended twice in PBS with 1% fetal bovine serum and kept at 4°C until they were used for flow cytometry.

Alternate protocol for screening of knockdown cells

The experiments regarding protein knockdown were restricted to the time point of 1 hour and the MOI of 10 mycobacteria per macrophage. This was necessary to accommodate the large number of samples – 181. The values were chosen because they present a more moderate burden on the macrophages and at the same time allow for more expressive differences across all cell types.

The experimental handling itself differs from the previous sections in that it was performed on 96-well microplates in proportionally smaller volumes. The infection and post-infection protocols were otherwise identical to those described before.

Confirming the absence of extracellular bacteria

Extracellular bacteria adherent to the macrophage, but not internalized, can compromise the readings of flow cytometry. To determine whether the post-infection protocol was effective in separating bacteria from the macrophages, a parallel experiment was conducted. Wild-type J774 macrophages were first plated in two different conditions: either onto glass coverslips placed on the plate wells (*group A*) or onto the plate wells' bottom (*group B*). Both samples were infected with *M. smegmatis* with a MOI of 100 for 1 hour. Group B was subjected to the entire post-infection protocol, while group A was not. All samples were stained with 25 µg/ml of ethidium bromide at the end of the infection. Extracellular mycobacteria stained red, while internalized mycobacteria emitted only green fluorescence from GFP.

Samples were placed on microscope slides and observed under a Zeiss Axioskop 40 fluorescence microscope (Göttingen, Germany) using a FITC filter. Besides qualitative observations of the relative abundance of red mycobacteria around the macrophages, quantification was also made: from a random sampling, we determined the percentage of macrophages with neighboring red mycobacteria.

Production of Lentiviral particles

Lentivirus vector library was obtained from the RNAi Consortium in partnership with Professor Luís Moita from the Institute of Molecular Medicine (Lisbon, Portugal), contained hits from a previous screen performed in our laboratory, whereby knockdowns of several membrane-associated proteins were shown to affect intracellular survival of mycobacteria in macrophages (see previous chapter).

Lentiviruses were contained in 96-well microplates with plKO.1 plasmids which coded for a different short specific RNA hairpin, lentiviral proteins and the resistance to puromycin as a selection marker. Each hairpin has a specific target on the host's messenger RNA.

The plasmids contained in the library were transfected into *Escherichia.coli* via electroporation. After overnight growth at 37°C with mixing (220 revolutions per minute), the DNA was extracted, in plasmid form, from the bacteria, using a PureLink Quick Plasmid Miniprep Kit and its respective protocol (Invitrogen).

The DNA was then quantified using picoGreen, a fluorescent nucleic acid stain, and its corresponding protocol (Life Technologies). The plasmids were co-transfected onto HEK 293T cells together with additional lentiviral proteins. These provide the necessary materials for the assembly of mature viral particles. The HEK 293T cells then began producing these particles containing the desired DNA construct, whilst being selected for transfection via the addition of 5 µg/ml puromycin to the growth medium.

After 24 hours, the virus particles were passage into DMEM containing 30% fetal bovine serum and collected 24 hours later. These virus particles were used to infect wild-type THP-1 monocytes, on a 96-well microplate. The monocytes were maintained in culture medium with 5 µg/ml puromycin and passaged or split into new microplates to obtain larger numbers of cells with a stable knockout.

Before infection, THP-1 cells were counted, normalized and plated on a fresh 96-well microplate at a concentration of 375 000 cells/ml.

The negative controls for the protein knockdowns were infected with viruses that contained an RNA hairpin with no target in the human genome, meaning that it would not bind to any messenger RNA of the host cell nor silence protein production. These hairpins contain a scrambled sequence and are called shScramble.

Quantification of internalization by flow cytometry

Samples were read on a Milipore EasyCyte H6 Guava flow cytometer, using its proprietary InCyte software, as well as the freeware Flowing Software (Turku Centre for Biotechnology, Finland). Fluorescence was measured using the excitation and emission wavelengths of 488 and 525 nanometers with a 75 miliwatt blue laser. The macrophage population was gated based on forward and side scatter values, in such a way that extracellular bacteria and debris were excluded from the event count. 5000 events from inside that gate were acquired with an average rate of 260 events per second.

The mycobacteria constitutively expressed Green Fluorescent Protein, while the macrophages did not, and so internalization was measured by quantifying the percentage of total macrophages that emitted intense green fluorescence. Uninfected macrophage samples were used as negative controls to calibrate the readings of green fluorescence intensity for each experiment.

Using the values from different time points, the kinetics of internalization were determined and plotted using a custom function in R software. Data points were connected to create a growth-like profile for the internalization rates, which include the average values as well as the standard deviation for each data point. All experiments were performed in triplicate.

Statistical treatment

The software SigmaPlot 12.0 (*Systat Software Inc.*) was used for statistical analysis. Three-way ANOVAs were performed to evaluate the global differences in internalization between different macrophages and different bacteria by taking into account the variables of time and MOI. Pairwise differences between types of macrophages and types of mycobacteria were evaluated using the Holm-Sidak method. Differences were considered significant for $p < 0.05$.

Labelling hits in the knockdown screen

To evaluate whether the effect of knocking down the selected proteins was relevant for internalization, a criterion had to be fulfilled: two or more hairpins silencing each protein had to cause a difference in internalization of at least 2.5 times the standard deviation of the controls.

References

1. Stuart LM, Ezekowitz RAB. Phagocytosis: elegant complexity. *Immunity*. 2005;22(5):539–50.

2. Pieters J. Mycobacterium tuberculosis and the macrophage: maintaining a balance. *Cell Host Microbe*. 2008;3(6):399–407.

3. Brennan PJ, Nikaido H. The envelope of mycobacteria. *Annu Rev Biochem*. 1995;64:29–63.

4. Ernst JD. Macrophage Receptors for Mycobacterium tuberculosis. *Infect Immun*. 1998;66(4):1277–1281.

5. Schäfer G, Jacobs M, Wilkinson RJ, Brown GD. Non-opsonic recognition of Mycobacterium tuberculosis by phagocytes. *J Innate Immun*. 2009;1(3):231–43.

6. Hackam DJ, Rotstein OD, Sjolin C, Schreiber a D, Trimble WS, Grinstein S. v-SNARE-dependent secretion is required for phagocytosis. *Proc Natl Acad Sci U S A*. 1998;95(20):11691–6.

7. Bajno L, Peng XR, Schreiber a D, Moore HP, Trimble WS, Grinstein S. Focal exocytosis of VAMP3-containing vesicles at sites of phagosome formation. *J Cell Biol*. 2000;149(3):697–706.

8. Rosales C. *Molecular Mechanisms of Phagocytosis*. Boston, MA: Springer; 2005:172.

9. Cox D, Lee DJ, Dale BM, Calafat J, Greenberg S. A Rab11-containing rapidly recycling compartment in macrophages that promotes phagocytosis. *Proc Natl Acad Sci U S A*. 2000;97(2):680–5.

10. Campbell-Valois F-X, Trost M, Chemali M, et al. Quantitative proteomics reveals that only a subset of the endoplasmic reticulum contributes to the phagosome. *Mol Cell Proteomics*. 2012;11(7):M111.016378.

11. Huynh KK, Kay JG, Stow JL, Grinstein S. Fusion, fission, and secretion during phagocytosis. *Physiology (Bethesda)*. 2007;22:366–72.

12. Elliott JA, Winn WC. Treatment of alveolar macrophages with cytochalasin D inhibits uptake and subsequent growth of Legionella pneumophila. *Infect Immun*. 1986;51(1):31–6.

13. Hutagalung AH, Novick PJ. Role of Rab GTPases in Membrane Traffic and Cell Physiology. *Physiol Rev* . 2011;91(1):119–149.

14. Stokes RW, Norris-Jones R, Brooks DE, Beveridge TJ, Doxsee D, Thorson LM. The glycan-rich outer layer of the cell wall of Mycobacterium tuberculosis acts as an antiphagocytic capsule limiting the association of the bacterium with macrophages. *Infect Immun*. 2004;72(10):5676–86.

15. Hatsuzawa K, Hashimoto HH, Arai S, Tamura T, Higa-Nishiyama A, Wada I. Sec22b is a negative regulator of phagocytosis in macrophages. *Mol Biol Cell*. 2009;20(20):4435–43.

16. Okumura AJ, Hatsuzawa K, Tamura T, et al. Involvement of a novel Q-SNARE, D12, in quality control of the endomembrane system. *J Biol Chem*. 2006;281(7):4495–506.

17.   Baena A, Porcelli SA. Evasion and subversion of antigen presentation by Mycobacterium tuberculosis. *Tissue Antigens.* 2009;74(3):189–204.

18.   Kay JG, Murray RZ, Pagan JK, Stow JL. Cytokine secretion via cholesterol-rich lipid raft-associated SNAREs at the phagocytic cup. *J Biol Chem.* 2006;281(17):11949–54.

19.   Murray RZ, Kay JG, Sangermani DG, Stow JL. A role for the phagosome in cytokine secretion. *Science.* 2005;310(5753):1492–5.

20.   Yokoyama K, Kaji H, He J, et al. Rab27a negatively regulates phagocytosis by prolongation of the actin-coating stage around phagosomes. *J Biol Chem.* 2011;286(7):5375–82.

21.   Seto S, Tsujimura K, Koide Y. Coronin-1a inhibits autophagosome formation around Mycobacterium tuberculosis-containing phagosomes and assists mycobacterial survival in macrophages. *Cell Microbiol.* 2012;14(5):710–27.

22.   Pitz AM, Perry GA, Jensen-Smith HC, Gentry-Nielsen MJ. A flow cytometric assay to quantify in vivo bacterial uptake by alveolar macrophages. *J Microbiol Methods.* 2010;81(2):194–6.

Chapter 5

Micro RNA mir-142-3p is modulated by *Mycobacterium tuberculosis* and its partner, N-WASP, is involved in the internalization of the bacilli.

Micro RNA mir-142-3p is modulated by *Mycobacterium tuberculosis* and its partner, N-WASP, is involved in the internalization of the bacilli.

Abstract

Micro RNAs (miRs) are involved in the post-transcriptional repression of the target protein mRNAs. Recently our laboratory has shown that miR-142-3p is induced upon macrophage infection by mycobacteria. A gain-of-function by increase the amount of miR-142-3p led to a reduction in N-Wasp protein and, consequently to a reduced internalization of mycobacteria by murine macrophages. Likewise, virulent *Mycobacterium tuberculosis* induced miR-142-3p expression and decreased N-Wasp in monocyte derived human macrophages (MDHM). In this study we show that miR-142-3p induction and consequent N-Wasp reduction of protein amount in MDHM is specifically induced by virulent *M. tuberculosis* but not by the non-pathogenic species *Mycobacterium smegmatis* or by latex beads. Furthermore, reduction of N-Wasp by RNAi induced a decrease of *M. tuberculosis* internalization in MDHM.

Introduction

Tuberculosis (TB) is still a global public health problem being responsible for more than 1,3 million deaths every year. The success of *Mycobacterium tuberculosis* (*M. tuberculosis*), the etiologic agent of TB, relies on the capacity to replicate within host cells responsible for clearance of invading organisms: the macrophage. In order to establish its intracellular niche *M. tuberculosis* subverts macrophage's microbicidal factors by modulating its route of internalization, inhibiting the phagolysosome formation while keeping the macrophage from displaying a proper inflammatory response[1].

A central feature to *M. tuberculosis* strategy is the manipulation of actin's fate within macrophage such that it favours bacterial survival. *M. tuberculosis* is able to disrupt the macrophage actin network[2]. Actin polymerization has been observed in phagosomes containing latex beads or mycobacteria and facilitates maturing phagosomes with lysosomes leading to the killing of mycobacteria [3–5]. Several signalling lipids, cAMP, extracellular ATP and the P2X7 receptor, were shown to be involved in actin assembly and the killing/survival of pathogenic mycobacteria[6–10]. In addition, actin assembly is involved in the pro-inflammatory response. Disruption of actin cytoskeleton leads to *NF-kB translocation*, a transcription factor involved in the pro-inflammatory response [11]. *Moreover,* some lipid effectors that regulate actin assembly also control NF-κB[12]. Actin may also be involved in cytokine secretion once been observed that TNFα containing vesicles are delivered to the actin-rich phagocytic cup before secretion[13].

MicroRNAs (miRs) are post-transcriptional factors, with 20-22 nucleotides, that regulate translation of the mRNA of determined proteins. After being released to the cytoplasm, these molecules can bind to complementary proteins mRNA inducing their silencing by inhibiting ribosomal translation or by mRNA destruction, reducing protein genetic expression and thereby their function. A growing body of evidence suggest a broad involvement of miRs in *M. tuberculosis* infection and highlighted their potential in diagnosis, treatment and understanding TB[14–16].

In order to identify potential miRs involved in mycobacteria infection, our laboratory performed a global transcriptomic analysis to assess the modulation of miRs upon *M. smegmatis* infection of the murine macrophage cell line, J774A.1. This approach identified miR-142-3p as a potential candidate being modulated during *M. smegmatis* infection. Expression of miR-142-3p was up regulated in murine macrophages upon mycobacteria infection. Moreover, it was found that N-Wasp mRNA, was targeted by miR-142-3p leading to a decrease in N-Wasp protein in macrophage s. N-Wasp is involved in signal transduction from receptors on the cell surface, leading to the promotion of F-actin polymerization, via the Arp2/3 complex and is involved in macrophage phagocytosis [17]. In this work we further analyse the expression of miR-142-3p and N-Wasp regulation by *M. tuberculosis* in monocyte derived human macrophages (MDHM). Our results confirms that in MDHM as well in the murine

model, a decrease in N-Wasp modulated by miR-142-3p leads to a specific reduction in *M. tuberculosis* internalization. However, in MDHM both miR-142-3p induction and internalization reduction were specifically induced by pathogenic *M. tuberculosis* but not by avirulent mycobacteria or latex beads.

Results

M. tuberculosis modulates miR-142-3p expression levels in human macrophages

Human macrophages were exposed to latex beads as an inert stimulus, since they can be internalized by these cells without subverting the phagocytic pathway. In parallel and addiction they were challenged with either *M. smegmatis* or *M. tuberculosis*. The miR-142-3p expression was quantified by qPCR analysis in all conditions tested. Our results indicate that while *M. tuberculosis* infection of human macrophages specifically induces the expression of miR-142-3p in the first hour of infection, the challenge with *M. smegmatis* or with latex beads failed to do so (Figure 5.1a).

Our results show that pathogenic *M. tuberculosis* modulation of miR-142-3p in human macrophages modulates its internalization when compared to latex beads or avirulent *M. smegmatis.* MiR-142-3p is highly conserved across species[18]. Our findings in the murine model suggest that *M. tuberculosis* induces the timely expression of miR-142-3p in order to down-modulate the function of N-Wasp protein, and therefore, modulate the uptake by phagocytic cells. Given the *M. tuberculosis* is the etiological agent of TB in humans, and that human macrophages are the main reservoir for this intracellular pathogen, here we used primary human monocyte-derived macrophages in order to investigate whether the expression of miR-142-3p leads to a subsequent reduction of N-Wasp and alter the rates of phagocytosis.

Next, we measured whether the difference in miR-142-3p expression obtained from the challenge with each mycobacterial species at 1 hpi is sustained throughout infection. Indeed, we observed that it became more pronounced at 4 hpi, with an eventual decline at 24 hpi, but remaining always above the expression level of non-infected cells (Figure 5.1b).
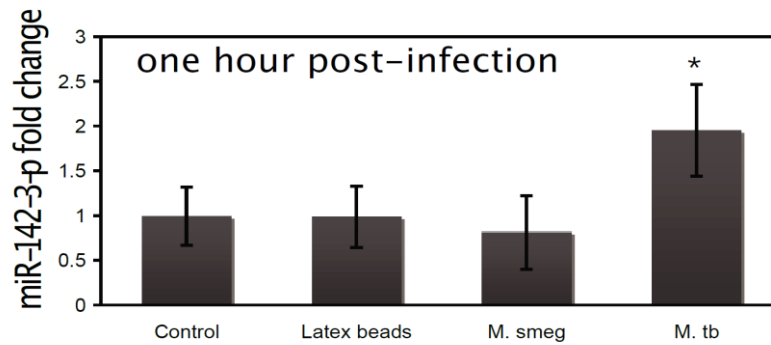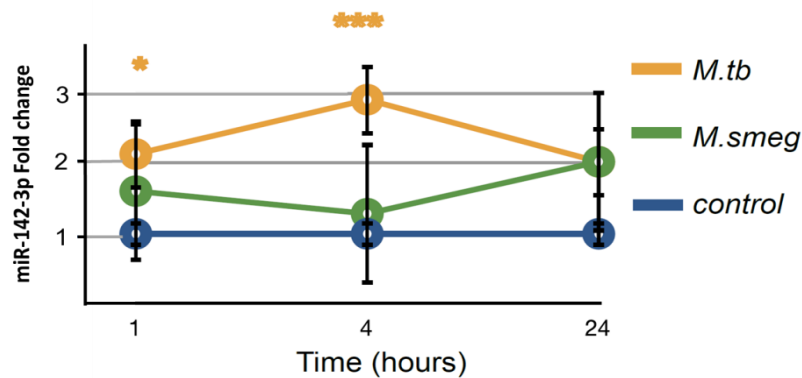
Figure 5.1. Relative expression of miR-142-3p in MDHM. a) Under *M. smegmatis*, *M. tuberculosis* or latex beads, exposure (1 h) of macrophages, as measured by qPCR analysis. b) Relative expression of miR-142-3p in human macrophages infected with *M.smegmatis* or *M. tuberculosis* as the indicated time points, as measured by EXIQON (DK) microRNA qPCR services. The data are representative of two independent experiments done in triplicates ± SD (*P = 0.05; ***P = 0.01).

M. tuberculosis modulates N-Wasp expression levels in human macrophages

Coincidently, the protein levels of N-Wasp were slightly, but significantly reduced (~20%) at both 1 and 4 h upon *M. tuberculosis* infection, while remaining unaffected by the challenge with *M. smegmatis* or exposure to latex beads (Figure 5.2). These results, along with previous findings in the mouse model, prompted us to examine whether the decrease in N-Wasp expression had any functional consequence for the phagocytosis process of *M. tuberculosis*. N-Wasp is involved in transduction of signals from receptors on the cell surface to the actin cytoskeleton and is involved in macrophage phagocytosis. In order to identify the potential role of N-Wasp we hypothesised whether N-Wasp was involved in the internalization of *M. tuberculosis* by MDHM.
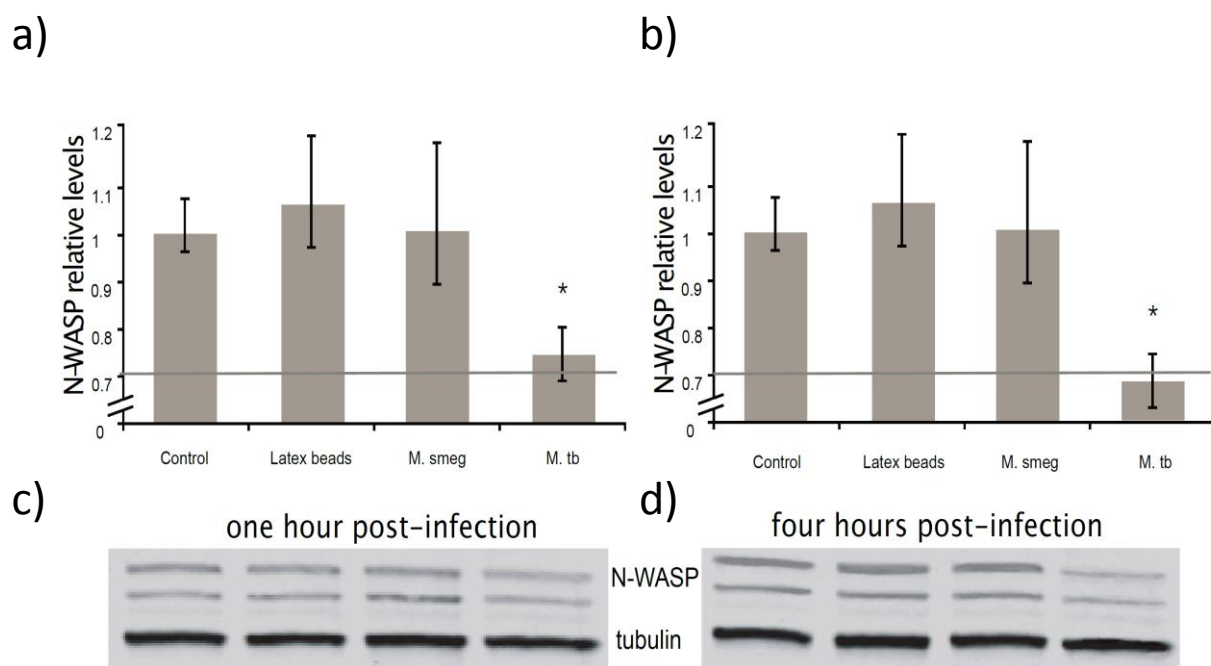
Figure 5.2. N-WASP is downregulated in *M. tuberculosis* infected primary human macrophages. Relative protein levels by western blot analysis. N-Wasp levels relative to β-Tubulin either at 1 h post-infection with 20% reduction (a) or 4 h post-infection with 40% reduction (b). A representative blot (c and d) from three independent experiments is shown with densitometry quantification for each time point; data are represented as the mean fold change per sample ± SD (∗P = 0.05).
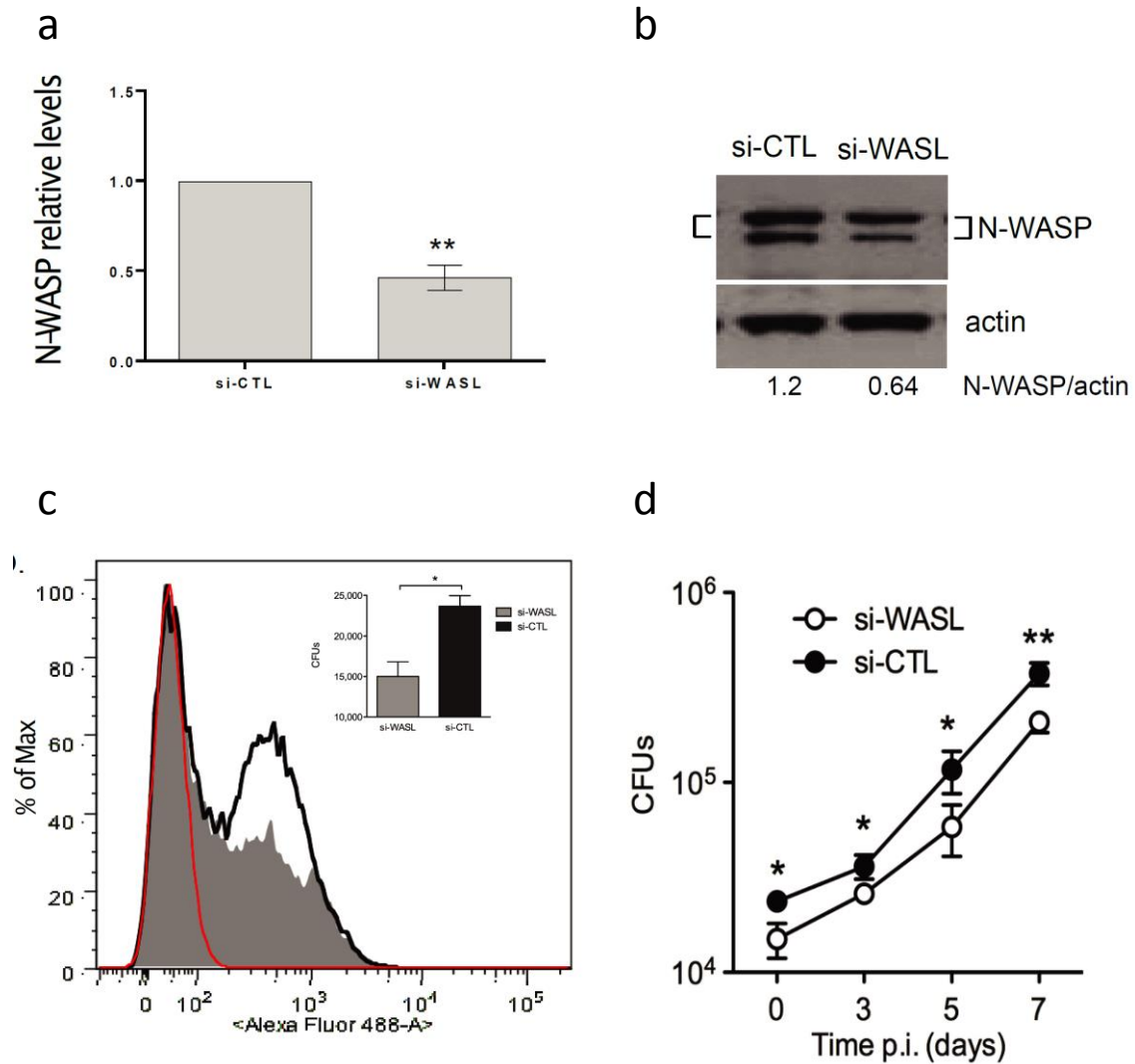
Figure 5.3. N-Wasp knockdown reduces *M. tuberculosis* internalization in human primary macrophages. siRNA-mediated inactivation of N-Wasp (WASL) was performed as described in materials and methods. Transfection of the siRNA SMARTpool targeting N-Wasp (si-WASL) resulted in an average of about 54% reduction of the protein level relative to that of the transfection with a non-targeting control siRNA pool (si-CTL; a). A representative western blot analysis (b) illustrates the gene inactivation obtained from four independent experiments (c); data are represented as the mean fold change relative to control sample (set arbitrarily at 1) ± SD (**P ≤ 0.01). phagocytosis of H37Rv-eGFP by human macrophages either inactivated for N-Wasp (si-WASL, gray) or transfected with the non-targeting siRNA pool (si-CLT, black), was analysed either by flow cytometry (histogram) analysis at MOI 10 (c), or by CFU (inlet) assay at MOI 0.1, after 4 h of infection (d). Red indicates the fluorescence background of non-infected macrophages. The median fluorescence intensities (MFI) are as follow: 36 (non-infected), 117 (si-WASL) and 189 (si-CTL). Right: H37Rv-eGFP proliferation as measured by CFU analysis for different time points (days) for the same cellular conditions and donor as described for left panel. The data are representative of two independent experiments done in triplicates ± SD (*P = 0.05; **P = 0.01).

To accomplish this, we used a siRNA-based protocol that we have adapted and improved to effectively inactivate the gene expression in MDHM[19]. Using this protocol, we obtained a significant reduction (on average ~54%) of N-Wasp protein levels in human macrophages (Figure 5.3 a and b). This partial reduction of N-Wasp protein resulted in a decrease of *M. tuberculosis* uptake as measured either by flow cytometry (Figure 5.3b), or by CFU assays at 4 hpi (Figure 5.3c,); this pattern continued over a time course of 1 week (Figure 30d). Altogether, these results suggest that the modulation of N-Wasp function via miR-142-3p might contribute to the phagocytosis process of *M. tuberculosis* in human cells.

Discussion

The regulation of N-Wasp activity is important for host-pathogen interactions, since this protein is known to be involved in actin dynamics required during the invasion of host cells by several pathogens. For instance, salmonella induces actin assembly via N-Wasp and therefore bacteria uptake by non-professional phagocytes through a type III secretion system [20]. Additional examples include the actin filament assembly and regulation associated with the establishment of actin pedestals during enteropathogenic *E. coli* EPEC [21] and Vaccinia virus invasion [22], and the actin tail-propulsion based invasion of host cells by shigella [23] and listeria [24]. More relevant for our study, actin tail based movement dependent on N-Wasp during mycobacteria infection was also described for *Mycobacterium marinum*, a close relative of *M. tuberculosis* [25,26]. Finally, knock-out of N-Wasp was associated with a defective immune response to *M. bovis* BCG [27]. Our findings strongly suggest that effective modulation of N-Wasp activity via miR-142-3p can influence the rate of bacterial intake by macrophages, and to our knowledge, this is the first description of a microbial strategy employing the use of miRs to regulate actin-mediated events that potentially leads to phagolysosome biogenesis. The central role of N-Wasp in this process is indeed supported by the case of *Yersinia pseudotuberculosis*, which modulates the activity of N-Wasp to control its internalization in host cells [28].

The present study proposes a novel but general strategy in the context of mycobacteria infection is the role of miRs in modulating mycobacterial uptake by phagocytic cells, revealed by the partial and temporal inhibition of N-Wasp activity via miR-142-3p. Collectively, throughout this project we demonstrated that: (1) mycobacteria infection of macrophages results in a short-lived induction of miR-142-3p, and in the case of *M. tuberculosis*, accompanied by a partial decrease of N-Wasp protein levels (2) N-Wasp mRNA (Wasl) is a direct target for miR-142-3p, (3) miR-142-3p leads to a significant decrease of intracellular mycobacteria intake by macrophages, and (4) the siRNA-mediated inactivation of N-Wasp in human Mφs affects the initial rate of phagocytosis of *M. tuberculosis*.

Moreover, recent reports show a broader implication of miR-142-3p in mycobacterial infection. Xu and co-workers shown that during infection *of* murine macrophage by *Bacillus Calmette-Guérin* (*BCG*), miR-142-3p is also down regulated. They demonstrate that miR-142-3p post-transcriptionally down-regulation of IRAK-1 protein expression. This reduction leads to a decrease in pro-inflammatory mediators nuclear factor kappa-light-chain-enhancer of activated B cells (NF-κB), tumour necrosis factor alpha (TNF-α) and interleukin (IL)-6 in macrophages. These findings show the ability of mycobacteria in the reduction of macrophage pro-inflammatory response through miR-142-3p [29]. Furthermore, TB patients with active disease show a decrease expression of miR-142-3p in CD4+ cells as well as in blood cells of children with both active and latent TB infection, which may represent that *M. tuberculosis* miR-142-3p subversion to be systematic in TB and not just in the macrophage. The decreased expression of miR-142-3p in latent TB infection highlights this miR as a potential candidate for diagnose latent TB.

Material and Methods

Cell preparation, cell lines and bacterial culture conditions

The human monocyte derived macrophages were obtained from healthy blood donors (Instituto Português do Sangue, Lisbon, Portugal), and differentiated following a previously published procedure[30]. A protocol of collaboration was established between Drs. Anes and Castro (the head of the Portuguese Institute for Blood in 2007), in order to have access to buffy coats from blood donors for scientific research. Alternatively, monocytes were obtained from healthy blood donors Etablissement Français du Sang (EFS) in Toulouse, France. Written informed consents were obtained from the donors under EFS contract n°21/PVNT/TOU/IPBS01/2009-0052. Following articles L1243-4 and R1243-61 of the French Public Health Code, the contract was approved by the French Ministry of Science and Technology (agreement nuAC 2009-921). The monocytes were differentiated into Mφs following a previously published protocol [31].

The strain *Mycobacterium smegmatis* mc^{2}155, containing a p19 (long lived) EGFP plasmid was kindly provided by Dr. Douglas Young (London School of Hygiene and Tropical Medicine, London, UK), and the green fluorescent protein (GFP)-expressing strain of *M. tuberculosis* (H37Rv-pEGFP) plasmid was a kind gift from G. R. Stewart (University of Surrey, United Kingdom). *Msmeg* was grown in medium containing Middlebrook's 7H9 broth Medium (Difco, USA), Nutrient broth (Difco, USA) supplemented with 0.5% glucose and 0.05% Tween 80 at 37°C on a shaker at 200 r.p.m.[3]. Bacteria were sub-cultured every day in fresh medium before use. *M. tuberculosis* H37Rv was grown in Middlebrook's 7H9 medium (Difco) and supplemented with 10% OADC Enrichment (Oleic acid; Albumin Factor V, Bovine; Dextrose; Catalase Powder; Sodium Chloride) (Difco, USA) [3]. All manipulations of *M. tuberculosis* were performed in a Biosafety Level 3 environment.

MicroRNA expression

Total RNA was isolated using TRIzol reagent (Invitrogen, Paisley, Scotland) according to the manufacturer's instructions. RNA quality was controlled using the RNA 6000 Pico LabChip kit (Agilent, Waldbronn, Germany) and quantified with a NanoDrop ND-1000 Spectrophotometer (Nanodrop Technologies, Wilmington, DE, USA). Microarray results were submitted to GEO repository with the GEO accession number GSE23429.

RT-qPCR

Messenger RNA relative quantification started with 1 μg of total RNA that was used for random hexamer primed cDNA synthesis (SuperscriptTM II reverse transcriptase, Invitrogen) according to the manufacturer protocol. Amplification was detected using SYBR Green PCR master mix (Applied Biosystems) and different sets of primers (MWG) at a final concentration of 0.5 μM. The PCR settings used: 1 cycle of 95°C for 10 min, followed by 40 cycles of 95°C for 15 s, 60°C for 30 s, and 72°C for 30 s. The mRNA expression profiles were normalized with respect to GAPDH (Glyceraldehyde 3-phosphate dehydrogenase). The qPCR was performed using an ABI 7500 Real Time PCR System (Applied Biosystems) and data was collected at the amplification step and analysed with SDS v1.2. Software. Fold increase of each gene was calculated using the $-2^{-\Delta\Delta Ct}$ method.

The specific relattive quantification of miR-142-3p in total RNA samples was based on TaqMan MicroRNA Assays from Applied Biosystems (ABI) in our laboratory or by final report analysis provided by EXIQON (DK) microRNA qPCR services. Briefly, 10 ng of total RNA were used for cDNA synthesis, according to the manufacturer protocol. The qPCR was run with the following steps: 1 cycle of 95°C for 10 min, followed by 40 cycles of 95°C for 15 s, and 60°C for 15 s, without dissociation stage. The miR expression profiles were normalized either to reference gene U6 (snRNA) or to the average obtained between miR-23a, miR-23b, and miR-24, whose

expression levels are suitable under the experimental conditions applied in this study. The mean and standard deviation over all the median normalized intensity data obtained from the microarray was calculated. The data was filtered so that the mean expression of the median normalized intensity value is high (higher than 10), and that the standard deviation is low (15 % of the mean).

Western blot

Cells plated in 24-well plates, under different conditions, were washed twice with PBS, and harvested in 250 µl of ice-cold, non-denaturating lysis buffer (TRIS 50 mM, NaCl 150 mM, Triton 1%, EDTA 1 mM, Protease Inhibitor Cocktail Tablets from Roche, Mannheim, Germany). Lysates were collected after 30 min of incubation and spun down for 5 min at 12000 xg, to remove debris of broken cells. The supernatant was collected and the protein concentration was measured using Bradford method. Approximately 20 µg of protein extracts were subjected to electrophoresis in 10% SDS-PAGE gels, transferred to a nitrocellulose membrane and blocked with 0.1% Tween20, 5% of low fat milk Tris Buffered Saline (TBS). For the confirmation of siRNA-mediated inactivation of N-Wasp, total protein lysates were extracted in the same manner as above. Proteins were separated with 4–12% Bis-Tris Gel (Invitrogen), transferred onto nitrocellulose membranes and incubated with anti-N-WASP (H100, Santa Cruz Biotechnology, 1/200), anti-actin (A5060, Sigma-Aldrich, 1/10000) overnight at 4°C. All membranes were washed and incubated with secondary HRP-conjugated antibodies. The bands were visualized with a chemiluminiscence reagent (Amersham Biosciences, UK) and quantified using Adobe Photoshop CS3 software.

SiRNA-mediated gene silencing

Human Mφs were transfected with the siRNA (final concentration of 133 nM) using the Hiperfect transfection reagent according to the protocol we have developed and optimized[19]. This siRNA targeted the following human genes (all SMARTpool from Dharmacon): WASL and a non-targeting/scramble. This protocol resulted in a transfection efficiency of nearly 100% and a survival rate ranging no less than 85%, as determined by flow cytometry of cell transfected with siGLO RISC-free siRNA (Dharmacon) and the Anexin-V kit (Miltenyi Biotec). Upon 6 h of transfection with these siRNAs, the reaction was stop by adding medium with the presence of MCSF (10 ng/ml) (Miltenyi Biotec). After 96 h, MDMs were used for experiments. The gene silencing effect lasted up to 7 days with no significant toxicity to MDMs. Functional gene silencing was verified by western blot analysis as described above.

Statistical analysis

Data are presented as mean either ± SD or ± SEM of at least three independent experiments; p-values (Student's T-Test) are relative to the control. Statistical significance was assumed when $P < 0.05$.

References

1. Pieters J. Mycobacterium tuberculosis and the macrophage: maintaining a balance. *Cell Host Microbe.* 2008;3(6):399–407.

2. Castandet J, Prost J-F, Peyron P, et al. Tyrosine phosphatase MptpA of Mycobacterium tuberculosis inhibits phagocytosis and increases actin polymerization in macrophages. *Res. Microbiol.* 2005;156(10):1005–13.

3. Anes E, Kühnel MP, Bos E, Moniz-Pereira J, Habermann A, Griffiths G. Selected lipids activate phagosome actin assembly and maturation resulting in killing of pathogenic mycobacteria. *Nat. Cell Biol.* 2003;5(9):793–802.

4. Kjeken R, Egeberg M, Habermann A, et al. Fusion between phagosomes, early and late endosomes: a role for actin in fusion between late, but not early endocytic organelles. *Mol. Biol. Cell.* 2004;15(1):345–58.

5. Marion S, Hoffmann E, Holzer D, et al. Ezrin promotes actin assembly at the phagosome membrane and regulates phago-lysosomal fusion. *Traffic.* 2011;12(4):421–37.

6. Kalamidas SA, Kuehnel MP, Peyron P, et al. cAMP synthesis and degradation by phagosomes regulate actin assembly and fusion events: consequences for mycobacteria. *J. Cell Sci.* 2006;119(Pt 17):3686–94.

7. Treede I, Braun A, Sparla R, et al. Anti-inflammatory effects of phosphatidylcholine. *J. Biol. Chem.* 2007;282(37):27155–64.

8. Jordao L, Bleck CKE, Mayorga L, Griffiths G, Anes E. On the killing of mycobacteria by macrophages. *Cell. Microbiol.* 2008;10(2):529–48.

9. Jordao L, Lengeling A, Bordat Y, et al. Effects of omega-3 and -6 fatty acids on Mycobacterium tuberculosis in macrophages and in mice. *Microbes Infect.* 2008;10(12-13):1379–86.

10. Kuehnel MP, Rybin V, Anand PK, Anes E, Griffiths G. Lipids regulate P2X7-receptor-dependent actin assembly by phagosomes via ADP translocation and ATP synthesis in the phagosome lumen. *J. Cell Sci.* 2009;122(Pt 4):499–504.

11. Kustermans G, El Benna J, Piette J, Legrand-Poels S. Perturbation of actin dynamics induces NF-kappaB activation in myelomonocytic cells through an NADPH oxidase-dependent pathway. Biochem J. 2005;387(Pt 2):531-40.

12. Gutierrez MG, Gonzalez AP, Anes E, Griffiths G. Role of lipids in killing mycobacteria by macrophages: evidence for NF-kappaB-dependent and -independent killing induced by different lipids. *Cell. Microbiol.* 2009;11(3):406–20.

13. Murray RZ, Kay JG, Sangermani DG, Stow JL. A role for the phagosome in cytokine secretion. *Science.* 2005;310(5753):1492–5.

14. Harapan H, Fitra F, Ichsan I, et al. The roles of microRNAs on tuberculosis infection: Meaning or myth? *Tuberculosis (Edinb).* 2013;93(6):596–605.

15. Chen M, Gan H, Remold HG. A mechanism of virulence: virulent Mycobacterium tuberculosis strain H37Rv, but not attenuated H37Ra, causes significant mitochondrial inner membrane disruption in macrophages leading to necrosis. *J. Immunol.* 2006;176(6):3707–16.

16. Singh PK, Singh AV, Chauhan DS. Current understanding on micro RNAs and its regulation in response to Mycobacterial infections. *J. Biomed. Sci.* 2013;20:14.

17. Park H, Cox D. Cdc42 regulates Fc gamma receptor-mediated phagocytosis through the activation and phosphorylation of Wiskott-Aldrich syndrome protein (WASP) and neural-WASP. *Mol. Biol. Cell.* 2009;20(21):4500–8.

18. Kozomara A, Griffiths-Jones S. miRBase: integrating microRNA annotation and deep-sequencing data. *Nucleic Acids Res.* 2011;39(Database issue):D152–7.

19. Lefèvre L, Lugo-Villarino G, Meunier E, et al. The C-type lectin receptors dectin-1, MR, and SIGNR3 contribute both positively and negatively to the macrophage response to Leishmania infantum. *Immunity.* 2013;38(5):1038–49.

20. Unsworth KE, Way M, McNiven M, Machesky L, Holden DW. Analysis of the mechanisms of Salmonella-induced actin assembly during invasion of host cells and intracellular replication. *Cell. Microbiol.* 2004;6(11):1041–55.

21. Kalman D, Weiner OD, Goosney DL, et al. Enteropathogenic E. coli acts through WASP and Arp2/3 complex to form actin pedestals. *Nat. Cell Biol.* 1999;1(6):389–91.

22. Frischknecht F, Moreau V, Röttger S, et al. Actin-based motility of vaccinia virus mimics receptor tyrosine kinase signalling. *Nature.* 1999;401(6756):926–9.

23. Suzuki T, Miki H, Takenawa T, Sasakawa C. Neural Wiskott-Aldrich syndrome protein is implicated in the actin-based motility of Shigella flexneri. *EMBO J.* 1998;17(10):2767–76.

24. Gouin E, Gantelet H, Egile C, et al. A comparative study of the actin-based motilities of the pathogenic bacteria Listeria monocytogenes, Shigella flexneri and Rickettsia conorii. *J. Cell Sci.* 1999;112 (Pt 1:1697–708.

25. Stamm LM, Morisaki JH, Gao L-Y, et al. Mycobacterium marinum escapes from phagosomes and is propelled by actin-based motility. *J. Exp. Med.* 2003;198(9):1361–8.

26. Stamm LM, Pak MA, Morisaki JH, et al. Role of the WASP family proteins for Mycobacterium marinum actin tail formation. *Proc. Natl. Acad. Sci. U. S. A.* 2005;102(41):14837–42.

27. Andreansky S, Liu H, Turner S, et al. WASP- mice exhibit defective immune responses to influenza A virus, Streptococcus pneumoniae, and Mycobacterium bovis BCG. *Exp. Hematol.* 2005;33(4):443–51.

28. McGee K, Zettl M, Way M, Fällman M. A role for N-WASP in invasin-promoted internalisation. *FEBS Lett.* 2001;509(1):59–65.

29. Xu G, Zhang Z, Wei J, et al. microR-142-3p down-regulates IRAK-1 in response to Mycobacterium bovis BCG infection in macrophages. *Tuberculosis.* 2013;93(6):606–611.

30. Wang C, Peyron P, Mestre O, et al. Innate immune response to Mycobacterium tuberculosis Beijing and other genotypes. *PLoS One.* 2010;5(10):e13594.

31. Tailleux L, Neyrolles O, Honoré-Bouakline S, et al. Constrained intracellular survival of Mycobacterium tuberculosis in human dendritic cells. *J. Immunol.* 2003;170(4):1939–48.

Chapter 6

The role of Rab GTPases in exosome secretion

The role of Rab GTPases in exosome secretion

Abstract

Exosomes are secreted membrane vesicles that share structural and biochemical characteristics with intraluminal vesicles of multivesicular endosomes (MVEs). Exosomes are secreted by several cell types and could be involved in intercellular communication and in the pathogenesis of infectious and degenerative diseases. The molecular mechanisms of exosome biogenesis and secretion are, however, poorly understood. Using a genomic screen RNA interference screen, we identified 5 small GTPases of the Rab family that promote exosome secretion in HeLa cells, including Rab27a and Rab27b.

Introduction

Exosome are small membrane vesicles (50-100nm) secreted by most types of cells[1]. Although, exosomes display a common protein composition, mostly including proteins from the endocytic system, the plasma membrane and cytosol, specific cells have a specific set of proteins[2].

Exosomes are secreted by most cell types and have been implicated in cell-to-cell communication[3] . They have been implicated in important immune responses[4]. For example, exosomes secreted by antigen presenting cells bears MHC class I and II, which can be directly recognized by activated CD4+ and CD8+ T cells. Exosomes from mice or cultured macrophages infected with mycobacteria contain several host proteins and pathogen antigens that induce a pro-inflammatory response in naïve macrophages and activate antigen-specific CD4^{+} and CD8^{+} T Cells *in vitro* and *in vivo*[5–7].

Evidence collected during the last 20 years suggests that in most cell types, exosomes correspond to secreted intraluminal vesicles (ILVs) of MVEs[8]. ILVs are formed by inward budding of the limiting membrane of MVEs into the lumen of these endosomes[9]. The observation by electron microscopy (EM) of fusion profiles between MVEs and the plasma membrane, with the consequent release of ILVs as exosomes, has been to date the strongest evidence of the endosomal origin of exosomes[10–12]. Nevertheless, in some cell types, such as T-lymphocytes, exosomes bud at the plasma-membrane from endosome-like domains[13]. Therefore, identification of the molecular machinery responsible for the control of the intracellular trafficking of MVEs and their fusion with the plasma membrane is of crucial importance for understanding key aspects of exosome secretion.

Since members of the Rab family of GTPases functionally participate in different steps of intracellular membrane trafficking, both along the endocytic and the secretory pathways, we analysed here the roles that the different Rab proteins could specifically play in exosome production or secretion, using the human HeLa cell line. To this end, a shRNA-based screen targeting human Rabs was performed. We observed that knocking-down five Rab proteins (Rab2b, Rab9a, Rab5a, Rab27a and Rab27b) inhibited exosome secretion without major modifications in the secretion of soluble proteins through the regular secretory pathway.

Results

Semiquantitative detection of exosomes in cell culture supernatants

To allow large-scale screening of molecules specifically involved in exosome secretion, we developed a quantitative FACS-based assay allowing simultaneous detection of exosomes and of proteins secreted through the classical secretory pathway, in small volumes of cell culture supernatants. The HeLa B6H4 tumour cell line, which stably expresses the transactivator CIITA (which drives expression of all genes of the MHC class II family, including HLA-DR) and a secreted form of chicken ovalbumin (OVA), was used for this assay. These cells secrete soluble OVA through the classical secretory pathway, and HLA-DR-positive exosomes: these two molecules can thus be used as reporters of alterations of either type of secretion.

Briefly, exosomes present in cleared cell culture supernatants were captured onto latex beads coated with antibodies to CD63, a tetraspanin strongly enriched in late endosomes and exosomes. Exosome-bearing beads were analysed by FACS after staining with either anti-HLA-DR and anti-CD81 fluorescent antibodies (CD81 is another tetraspanin abundant on exosomes)[11,14], or Annexin V (which binds to the phosphatidyl-serine (PS) present at the surface of exosomes)[15](Figure 6.1A). Membrane vesicles with a diameter ranging from 50 to 100 nm and with the typical cup-shaped morphology of exosomes were detected by electron microscopy (EM) on the surface of the beads (Figure 6.1B). As expected, exosome detection was dependent on the number of exosome-secreting cells present in the wells (Figure 6.1C, D), with a threshold of sensitivity of 75,000 cells/well. To assess the specificity of this assay for exosomes, as opposed to other secreted membrane vesicles originating from the plasma membrane, supernatants from apoptotic cells (which are known to secrete abundant apoptotic blebs) were tested. The FACS signals obtained with these supernatants were significantly lower than those obtained using supernatants from living cells (Figure 6.1E). We conclude that this assay allows the specific detection of a population of CD63/HLA-DR/PS-positive membrane vesicles produced by living cells, corresponding to exosomes.

A PE-conjugated antibodies
CD81 — HLA-DR
CD63 — Annexin V-APC
Anti-CD63-coated latex bead

B
250 nm

C

Number of secreting cells

| Unconditioned culture medium | 72000 | 120000 | 177000 |

HLA-DR/CD81

0.59   3.11   11.6   29.3

Forward Scatter

AnnexinV

0.3   1.3   3.75   12.6

Forward Scatter

Beads   Beads   Beads   Beads

D

HLA-DR/ CD81 (AU) vs Cell number (x10³)

Annexin V (AU) vs Cell number (x10⁻³)

E

HLA-DR/CD81   Annexin V
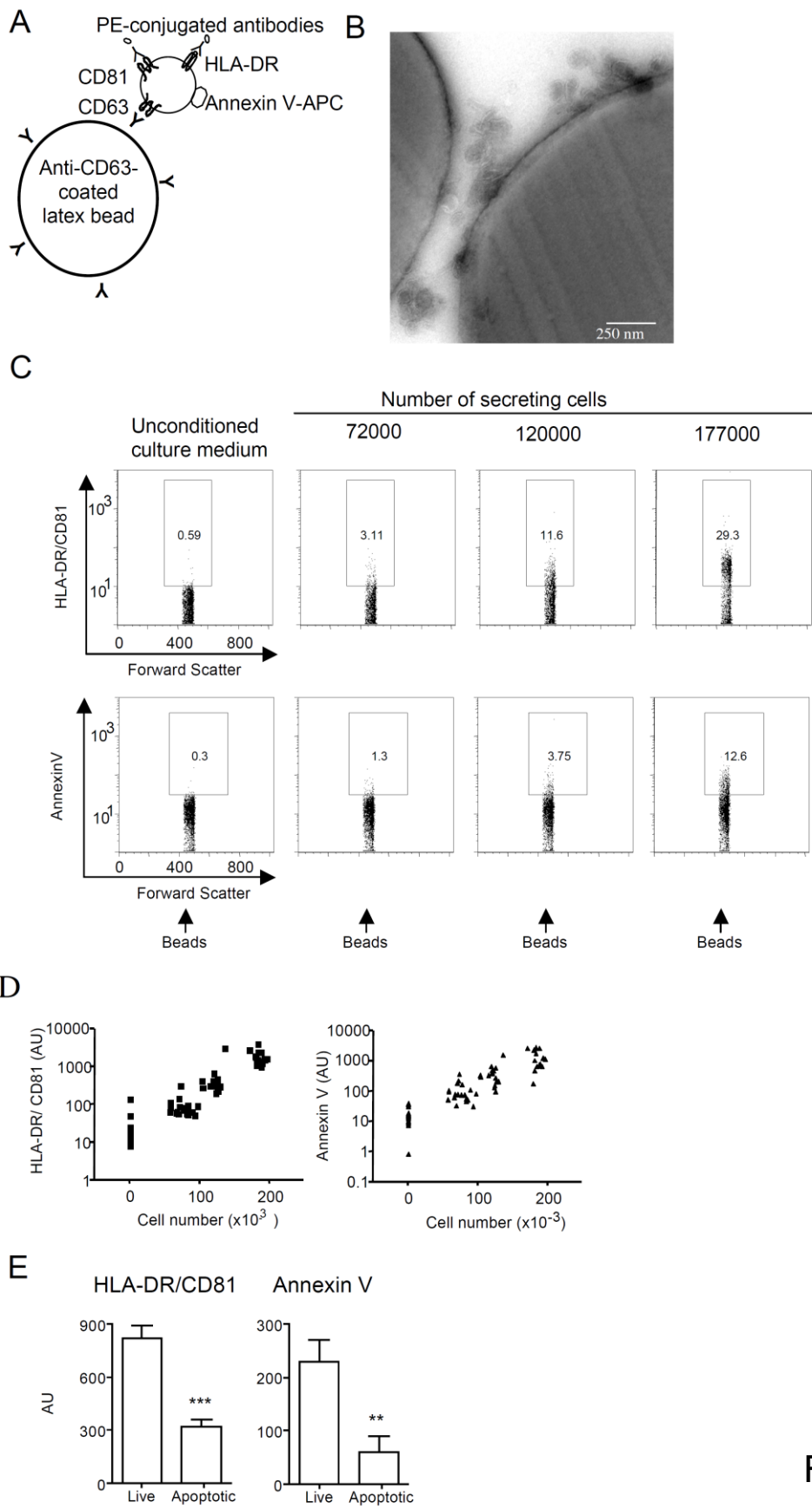
AU — Live / Apoptotic ***

Live / Apoptotic **

Figure 6.1.

158

Figure 6.1. Semi-quantitative detection of exosomes in cell culture supernatants. (continued). (A) Schematic drawing of the technical approach used to selectively capture and stain exosomes present in cell culture supernatants by using anti-CD63-coated beads and FACS detection. (B) EM image of exosomes present on the surface of anti-CD63-coated beads after incubation with supernatant from B6H4 cells. (C) Representative flow cytometry dot-plots showing HLA-DR/CD81 (top) and Annexin V (bottom) stainings of exosomes captured by beads incubated with supernatants from increasing numbers of cultured cells. Percent of positive beads are indicated inside the positive region. (D) Dose-response curve of HLADR/CD81 (left) and Annexin V (right) staining of exosomes captured by beads incubated with 66 different supernatants. (E) Specific detection of exosomes secreted by live cells, as compared to membranes secreted by apoptotic cells. A total of 50,000 cells either UVirradiated or untreated were seeded in a 96-wells plate. After 12h incubation, exosome depleted-medium was added and 24h later supernatants were incubated with anti-CD63-coated beads and analysed by FACS.

Soluble OVA in cell culture supernatants was detected using beads coated with anti-OVA antibodies and subsequently stained with a secondary anti-OVA fluorescent antibody (data not shown). This methodology allowed the quantitative detection of OVA, with a sensitivity of 30,000 cells/well. The detection of OVA in the supernatants of cells in which apoptosis was induced by UV-irradiation was significantly lower, as compared to live cells. Altogether, these assays allow the simultaneous quantification of both exosomes and OVA in very small volumes of culture supernatants collected from 96-well plates.

Role played by members of the Rab GTPase family in exosome secretion

In order to identify proteins involved in exosome secretion, a lentiviral shRNA library targeting 59 members of the Rab GTPase family was screened using the methodology described above as readout. Variability of the signals for exosome and OVA secretion obtained in control cells expressing a scrambled shRNA were below 20%, as shown in Figure 6.2A. Candidate genes that induced a significant modification in the secretion of exosomes but not in the secretion of OVA were selected if at least two different shRNAs (out of the three to five that target each individual gene) induced a similar phenotype.

Some examples of Rab proteins that were not considered as hits in the screen because did not fulfil the selection criteria are shown in Figure 6.2B. For instance, silencing of a Rab associated with the secretory pathway, Rab6a (Golgi) inhibited the secretion of OVA but did not affect exosome secretion. In contrast, inhibition of two

endocytic Rabs, Rab7 (late endosome) or Rab11a (recycling endosome), modified neither exosome nor OVA secretion significantly. Following the primary screen, 19Rab proteins that modified exosome production were selected. These candidates were re-evaluated in a second round of the screen performed in independent triplicate plates. The Rab proteins that yielded consistent results between replicates and between the two independent screens were chosen for a final confirmation step.
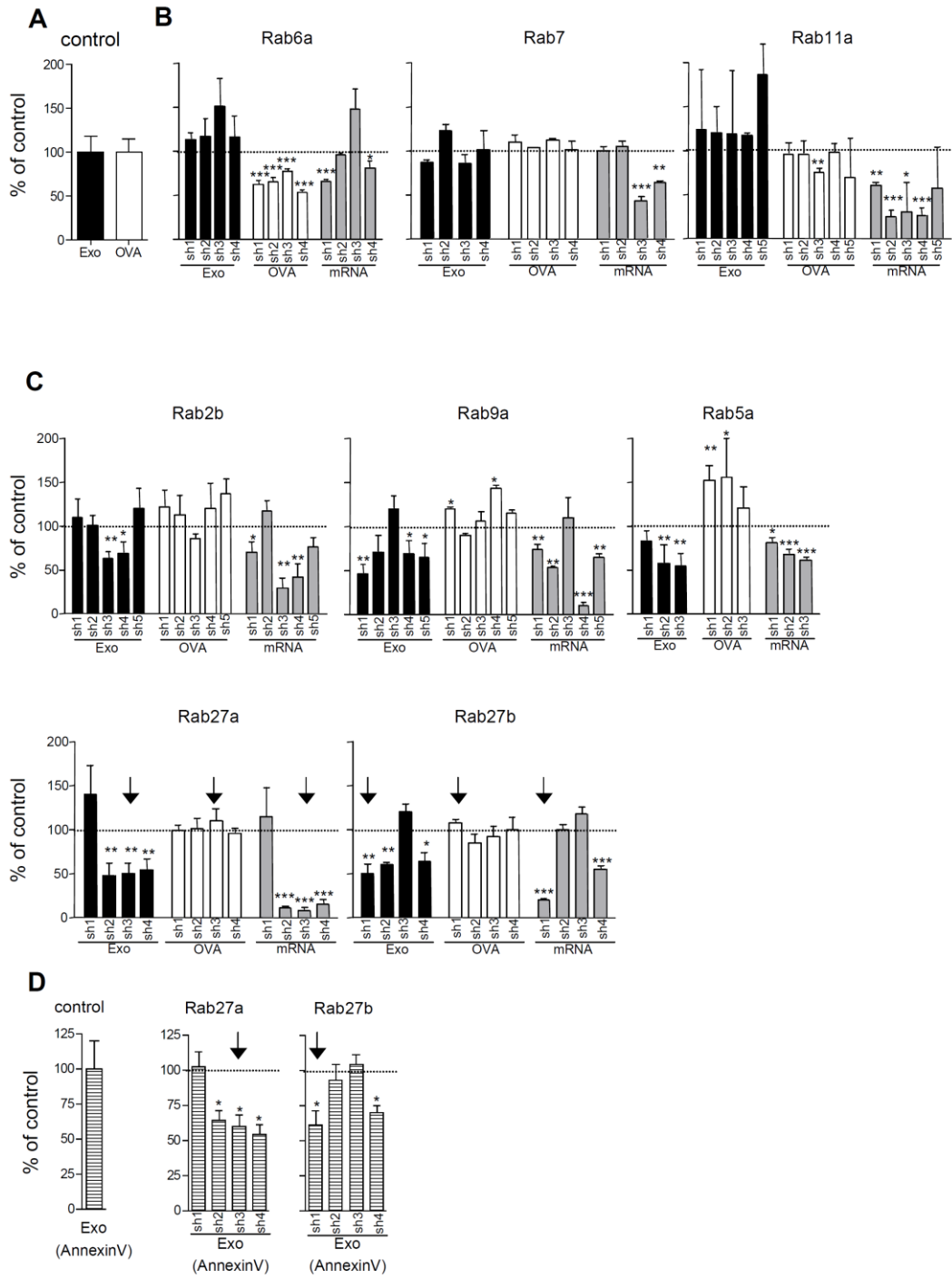
Figure 6.2.

Figure 6.2. Modulation of exosome and OVA secretion by members of the Rab family.
(continued). (A) Exosome secretion measured as HLA-DR/CD81 staining (Exo, black bars) and OVA secretion (white bars) by cells transduced with a control shRNA. Mean±sd of 3 experiments (in each experiment, 100% = mean of 3 independent control wells). (B) Exosome and OVA secretion and specific mRNA levels of cells transduced with different shRNAs (each bar represents a different shRNA) targeting Rab proteins that were not selected as hits in the screen, either because neither exosome nor OVA secretion were modified (Rab7, Rab11a) or because only OVA secretion was inhibited (Rab6a). Pooled results from duplicate plates in one experiment are shown. (C) Exosome and OVA secretion, and specific mRNA levels in cells transduced with shRNAs targeting Rab family members that were selected as candidate hits because at least 2 shRNAs significantly affected exosome without affecting OVA secretion. Pooled results from duplicate experiments (2-3 plates / experiment) are shown. (D) Exosome secretion by control and by either Rab27a or Rab27b-KD cells was also evaluated by detection of exposed PS with Annexin V. Arrows indicate the shRNAs that were chosen for further characterization. Stars indicate statistically significant differences with control.

Discussion

Two major results are presented here. First, we have set up an assay allowing medium-scale screens of the molecular machinery specifically involved in exosome secretion. Second, using this assay, we identified a few Rab family members, including Rab27a and Rab27b that play a role in exosome secretion.

Several other Rabs, in addition to Rab27, were identified in this study as being potentially involved in exosome secretion. Most of them are known to participate in trafficking in the endocytic pathway [19,20], thus supporting the endosomal origin of exosomes: Rab9 associates with late endosomes and orchestrates retrograde trafficking to the TGN, Rab5 functions at the level of early endosomes. Finally, Rab2 is generally described in association with the intermediate compartment between endoplasmic reticulum and Golgi apparatus, but in phylogenetic trees, it is closer to Rab4, Rab11 and Rab14[17], i.e. Rabs associated with the endocytic pathway. On the other hand, other Rabs associated with the endocytic system, such as Rab7 or Rab11, did not modify exosome secretion in HeLa cells. These observations suggest that a specific subset of the endocytic system participates in the generation of exosomes.

Material and Methods

Cells and reagents

HeLa-CIITA cells49 were stably transfected with pcDNA3 encoding the OVA cDNA fused to the signal peptide of lactadherin[21], and a subclone named HeLa B6H4 was selected. These cells were cultured in DMEM containing 4.5 g glucose/l (Invitrogen, Paisley, Scotland) supplemented with 10% fetal calf serum (Abcys), 2 mM glutamine, penicillin/streptomycin (100 IU/ml and 100 µg/ml, respectively), 300 µg/ml hygromycin B (Calbiochem, La Jolla, CA) and 500 µg/ml of geneticin (Gibco-Invitrogen). For exosome production, cells were cultured in "exosome-depleted medium", i.e. complete medium depleted of FCS-derived exosomes by overnight centrifugation at 100,000 g[22]. Lentiviruses expressing shRNA specific for the choosen genes were obtained from the RNAi consortium (TRC) and produced as previously described[23]. Antibodies: for FACS analysis : mouse anti-human CD63 (FC-5.01, Zymed) and goat anti- OVA (ICN) for coupling to aldehyde sulfate latex 4 µm beads (Invitrogen), PE-conjugated mouse anti- HLA-DR (L243, BD), anti-CD81 (BD), rabbit anti-OVA (Sigma-Aldrich) coupled to FITC according to manufacturer instruction (Pierce), mouse anti-CD63 followed by Alexa488-coupled goat anti-mouse (Molecular Probes).

Immunoadsorbtion and detection of exosomes by FACS

Anti-human CD63 or anti-OVA antibodies were coupled to 4 µm beads following the manufacturer instructions. Briefly, 35 µg of antibody were coupled to 1×10^{8} beads in MES buffer overnight at room temperature. Remaining free activated groups were blocked with PBS-4% BSA (30 min RT) and beads were stored in PBS with 0.1 % glycine and 0.1% sodium azide.

Cell culture supernatants were cleared from cell debris by successive centrifugations at 1,200 rpm for 5 min and 4,000 rpm for 20 min. Hundred µl of cleared supernatants

were incubated with 20,000 anti-CD63 and 20,000 anti-OVA coupled beads overnight at room temperature (with shaking at 6,500 rpm). Beads were washed twice in PBS 2% BSA and incubated with PE-conjugated anti HLA-DR and anti-CD81 and FITC-coupled anti-OVA (all at 1:100 dilution) for 30 min on ice. Beads were washed twice in annexin V buffer (BD Biosciences) and incubated with APC-conjugated annexin V (1/10) for 10 minutes. Stained beads were acquired on a FACSCalibur (BD Biosciences) and data were analysed with FlowJo software (Tree Star, Ashland, OR). Threshold of negative staining was obtained with beads incubated with unconditioned medium, and for each culture condition, arbitrary units (A.U.) of exosome or OVA secretion were calculated as % of positive beads x MFI of positive beads.

Lentiviral infection and screening procedure

HeLa B6H4 cells were plated in 96 well round-bottom plates at 2,500 cells per well with 10µl of virus plus 8 µg/ml polybrene and the plates were centrifuged at 2,250 rpm for 90 minutes. Infection medium was replaced with fresh complete medium. Puromycin was added at a final concentration of 5 µg/ml at day 2. Medium was replaced with exosome-depleted medium at day 4. Supernatants were collected 48 h later for OVA and exosome quantification, and the amount of live cells in each well was determined using the Cell titer blue reagent viability assay (Promega). Both OVA and exosome secretions were normalized to the number of viable cells present in the wells, and only wells with a minimal cell number of 75,000 cells/well were analysed. In each experiment, the basal level of exosome or OVA secretion (= control) was calculated as either A.U. of cells transduced with control scrambled shRNA, or mean of A.U. of one entire plate. A candidate gene was defined as a hit if two or more shRNAs modified A. U. of exosome secretion, in duplicate, by more than one standard deviation from the control. Results are presented as percent of A.U. of control.

Quantitative RT-PCR

RNAs were isolated from each well at day 5 after lentiviral infection with the Qiagen RNeasy Mini Kit and 200 ng were reverse transcribed with SuperScript II (Invitrogen) according to the manufacturer's directions. 1/10th of cDNA was used for each PCR reaction, performed in absolute QPCR ROX MIX (Abgene) on iCycler (BioRad). Primers used for GAPDH amplification were: GAPDH_F: GAG TCA ACG GAT TTG GTC GT and GAPDH_R: TTGATT TTG GAG GGA TCT CG. Primer sequences for each gene were either retrieved from Primer Bank (http://pga.mgh.harvard.edu/primerbank/) or designed using Primer3 (http://frodo.wi.mit.edu/cgi-bin/primer3/primer3_www.cgi). Cycle thresholds (Ct) were normalized to Ct of GAPDH and fold enrichments were calculated as compared to the control shRNA-transduced cells values.

Statistical analyses

Student's t-test was used for statistical analyses of the shRNA screen (exosome secretion, OVA secretion, mRNA level). Values are given as mean ± S.D.. *= $p<0.05$, **= $p<0.01$, ***=$p<0.001$

References

1. Raposo G, Stoorvogel W. Extracellular vesicles: exosomes, microvesicles, and friends. *J. Cell Biol.* 2013;200(4):373–83.

2. Mathivanan S, Simpson RJ. ExoCarta: A compendium of exosomal proteins and RNA. *Proteomics.* 2009;9(21):4997–5000.

3. Camussi G, Deregibus MC, Bruno S, Cantaluppi V, Biancone L. Exosomes/microvesicles as a mechanism of cell-to-cell communication. *Kidney Int.* 2010;78(9):838–48.

4. Bobrie A, Colombo M, Raposo G, Théry C. Exosome secretion: molecular mechanisms and roles in immune responses. *Traffic.* 2011;12(12):1659–68.

5. Anand PK, Anand E, Bleck CKE, Anes E, Griffiths G. Exosomal Hsp70 induces a pro-inflammatory response to foreign particles including mycobacteria. *PLoS One.* 2010;5(4):e10136.

6. O'Neill HC, Quah BJC. Exosomes secreted by bacterially infected macrophages are proinflammatory. *Sci. Signal.* 2008;1(6):pe8.

7. Giri PK, Schorey JS. Exosomes derived from M. Bovis BCG infected macrophages activate antigen-specific CD4+ and CD8+ T cells in vitro and in vivo. *PLoS One.* 2008;3(6):e2461.

8. Lakkaraju A, Rodriguez-Boulan E. Itinerant exosomes: emerging roles in cell and tissue polarity. *Trends Cell Biol.* 2008;18(5):199–209.

9. Futter CE, Collinson LM, Backer JM, Hopkins CR. Human VPS34 is required for internal vesicle formation within multivesicular endosomes. *J. Cell Biol.* 2001;155(7):1251–64.

10. Pan BT, Teng K, Wu C, Adam M, Johnstone RM. Electron microscopic evidence for externalization of the transferrin receptor in vesicular form in sheep reticulocytes. *J. Cell Biol.* 1985;101(3):942–8.

11. Raposo G, Nijman HW, Stoorvogel W, et al. B lymphocytes secrete antigen-presenting vesicles. *J. Exp. Med.* 1996;183(3):1161–72.

12. Zitvogel L, Regnault A, Lozier A, et al. Eradication of established murine tumors using a novel cell-free vaccine: dendritic cell-derived exosomes. *Nat. Med.* 1998;4(5):594–600.

13. Booth AM, Fang Y, Fallon JK, Yang J-M, Hildreth JEK, Gould SJ. Exosomes and HIV Gag bud from endosome-like domains of the T cell plasma membrane. *J. Cell Biol.* 2006;172(6):923–35.

166

14. Escola JM, Kleijmeer MJ, Stoorvogel W, Griffith JM, Yoshie O, Geuze HJ. Selective enrichment of tetraspan proteins on the internal vesicles of multivesicular endosomes and on exosomes secreted by human B-lymphocytes. *J. Biol. Chem.* 1998;273(32):20121–7.

15. Morelli AE, Larregina AT, Shufesky WJ, et al. Endocytosis, intracellular sorting, and processing of exosomes by dendritic cells. *Blood.* 2004;104(10):3257–66.

16. Tisdale EJ, Bourne JR, Khosravi-Far R, Der CJ, Balch WE. GTP-binding mutants of rab1 and rab2 are potent inhibitors of vesicular transport from the endoplasmic reticulum to the Golgi complex. *J. Cell Biol.* 1992;119(4):749–61.

17. Pereira-Leal JB, Seabra MC. Evolution of the Rab family of small GTP-binding proteins. *J. Mol. Biol.* 2001;313(4):889–901.

18. Ramalho JS, Tolmachova T, Hume AN, et al. Chromosomal mapping, gene structure and characterization of the human and murine RAB27B gene. *BMC Genet.* 2001;2:2.

19. Zerial M, McBride H. Rab proteins as membrane organizers. *Nat. Rev. Mol. Cell Biol.* 2001;2(2):107–17.

20. Béraud-Dufour S, Balch W. A journey through the exocytic pathway. *J. Cell Sci.* 2002;115(Pt 9):1779–80.

21. Zeelenberg IS, Ostrowski M, Krumeich S, et al. Targeting tumor antigens to secreted membrane vesicles in vivo induces efficient antitumor immune responses. *Cancer Res.* 2008;68(4):1228–35.

22. Théry C, Amigorena S, Raposo G, Clayton A. Isolation and characterization of exosomes from cell culture supernatants and biological fluids. *Curr. Protoc. Cell Biol.* 2006;Chapter 3:Unit 3.22.

23. Moffat J, Grueneberg DA, Yang X, et al. A lentiviral RNAi library for human and mouse genes applied to an arrayed viral high-content screen. *Cell.* 2006;124(6):1283–98.

Chapter 7

Concluding Remarks

Concluding Remarks

Macrophages are an important part of host defence, playing a critical role in innate immune responses against pathogens and in the initiation of adaptive immunity. One of the main characteristics of these cells is their ability to recognize and internalize invading microorganisms into a phagosome. The internalized microbe is rapidly delivered into a mature phagolysosome where it is killed and degraded. However, *M. tuberculosis*, have evolved complex mechanisms to manipulate these intracellular organelles to establish its survival niche. Vesicular traffic genes such as Rab GTPases and SNAREs have been associated with *M. tuberculosis* phagolysosome biogenesis inhibition. Micro RNAs by its turn have been associated with immune response to Tuberculosis. In the present thesis we aimed to study the effect of several human factors in phagocytosis and their effect in the survival/persistence of *M. tuberculosis*. To achieve this we developed and optimized several methodologies to quantify the role of several host factors in macrophage *M. tuberculosis* infection, macrophage uptake of mycobacteria and exosome secretion.

To achieve this, we took advantage of the fluorescent proteins properties and used two different fluorescent reporters for assessment of macrophage and mycobacteria viability during infection. This methodology might be applied to test intracellular survival of mutant mycobacteria within macrophages and, can be used in other host-pathogen studies. Additionally, the study of anti-mycobacterial effect of pyrazinoic acid esters in GFP expressing mycobacteria broth cultures highlighted the importance of intracellular environment in the assessment of the biological activity of candidate drugs against *M. tuberculosis*. To the best of our knowledge this is the first non-invasive, long-term and live methodology that can help to study both host and pathogen during infection.

Subsequently, we applied the dual fluorescence reporter technic combined with lentivirus-delivered stable gene silencing by RNAi in human macrophage cell line

and made a genomic screen to knockdown 120 genes associated with human vesicular traffic (mainly Rab GTPases and SNAREs proteins). After infection with *M. tuberculosis* we found 10 candidate genes whose knockdown affected the survival/persistence of intracellular mycobacteria. From these candidates, 9 were recently described in phagosomes and 5 have been already associated with mycobacterium containing phagosomes. We further observe that the results of the dual fluorescence assay for the candidates could be corroborated by CFU for Rab7, Rab 34, Rab14 and Stx4 proteins either when testing virulent or avirulent *M. tuberculosis*.

To further characterise the candidate genes, we optimized a macrophage uptake assay based in flow cytometry in order to define if the results obtained from the genomic screen could, in part, be justified by macrophage defects in *M. tuberculosis* uptake. We first compared several mycobacterial strains and macrophage types and observed that the internalization of mycobacteria by macrophages is a fast phenomenon and that virulent *M. tuberculosis* rate of uptake is slower than avirulent *M. smegmatis* and BCG independently of the macrophage type. Indeed this was observed even after knockdown of candidate genes: knockdown of candidate genes that led to a reduction in intracellular *M. tuberculosis* burden also induced a reduction in *M. tuberculosis* macrophage uptake. We couldn´t however dismiss a potential role of this genes in phagosome maturation. Indeed confirmation by alternative methods should be used to further confirm the role of identified candidates in *M. tuberculosis* infection and also identify the mechanisms underlying their interference in infection of both virulent and avirulent *M. tuberculosis*.

In sum, the candidate genes identified were found to be specific of several different organelles suggesting that phagosome maturation and in particular the maintenance of mycobacteria containing phagosomes may be regulated by other pathways than the endosomal pathway alone. In particular, the possible association between the ER and the mycobacteria containing phagosome might explain the reduced antigen presentation of infected macrophages via MHCII. Additionally, the reduction in the rate of virulent *M. tuberculosis* uptake led us to conclude that this strain probably invades macrophages by a different route than that one of avirulent mycobacteria.

Undeniably, we were able to demonstrate a mechanism by which virulent *M. tuberculosis* controls its uptake by macrophages. We found that virulent *M. tuberculosis*, but not avirulent *M. smegmatis* or latex beads, induce the expression of macrophage miR-142-3p during the initial stages of infection. The miR-142-3p reduction leads to the reduction of N-Wasp, a miR-142-3p partner, involved in signal transduction of surface phagocytic receptors. Reduction of N-wasp by miR-142-3p expression or by RNAi of Wasl, the N-Wasp gene, leads to a reduction in *M. tuberculosis* macrophage uptake. We have shown a probable mechanism by which virulent *M. tuberculosis* modulate macrophage infection in order to maintain low levels of immune activation.

In order to dissect the role of Rab GTPases in exosome secretion we performed a genomic screen to knockdown 57 Rab family members. In this screen we identified 5 small GTPases of the Rab family that promote exosome secretion in HeLa cells, including Rab27a and Rab27b. This approach led to the demonstration that exosomes are secreted from multivesicular bodies. However it was not possible to apply this methodology to our infection model in order to determine the role of vesicular traffic genes in exosome secretion in the context of *M. tuberculosis* macrophage infection.

In conclusion, in this thesis we developed, optimized and applied several tools for the study of macrophage phagocytosis and its subversion by *M. tuberculosis* that can help future identification of new host and pathogen factors involved in tuberculosis infection. We highlighted the importance of drug screening using models with intracellular *M. tuberculosis,* the relevance of the of virulent strains other than surrogate strains to study *M. tuberculosis*-human interactions and the importance determination of viable intracellular mycobacteria when defining the importance of an host factor in *M. tuberculosis* infection. We unveil the impact of several host factors involved in macrophage phagocytosis and *M. tuberculosis* infection. Both Rab GTPases and microRNAs are targeted host factors for new treatment strategies and differentially expressed in *M. tuberculosis* infected individuals highlighting the importance of these host factors in tuberculosis. The study and identification of members from these groups of host factors implicated in *M. tuberculosis* infection will

allow identifying new targets for the development of new diagnosis markers and host-targeted drugs to control one of the most ancient diseases that still takes a big toll to mankind: tuberculosis.